CHARACTERISING THE ACID MINE DRAINAGE POTENTIAL OF FINE COAL WASTES

Research Candidate:

Lerato Olga Kotelo

Student No:

KTLLER001

August 2013

Dissertation is submitted in fulfilment of,

Master of Science in Engineering degree,

Minerals to Metals Initiative,

Department of Chemical Engineering,

University of Cape Town

minerals to metals

DEPARTMENT OF CHEMICAL ENGINEERING

I know the meaning of plagiarism and declare that all the work in this document, save for that which is properly acknowledged, is my own. This has not been submitted for any degree or examination at any other university

Signed_____ August 2013

(Lerato Olga Kotelo)

SYNOPSIS

Acid mine drainage (AMD) is one of the major environmental challenges facing the South African mining sector. Acid mine drainage has received significant public attention in recent years. South Africa's long mining history has led to a growing concern that coal-related AMD from these mines (both operational and defunct) will continue for centuries to come. Pyrite bearing fine waste, generated during coal preparation and beneficiation, is thought to carry a significant amount of AMD pollution risk. Coal-related AMD generation has not been afforded the same exposure as AMD generation from high sulphide minerals such as gold and copper ores. This is exacerbated by the growing concern over water quality degradation in the Mpumalanga region of South Africa. The development of integrated solutions to address the management of coal-related AMD requires an understanding of the principle causes behind coal-related AMD. To date, most of the prediction methods described in literature have been derived for the prediction of AMD in metal bearing ores. Furthermore, some of these methods are based on assumptions and do not take into consideration the various sulphur species present. Additionally, some of these methods have limited applicability to coal due to the high total organic carbon content (TOC) of the material.

This research project attempts to address these short comings and uncertainties by developing a systematic and meaningful framework for the characterisation of South African coal and coal waste. The research project contributes to the knowledge of coal-related AMD with particular emphasis on the characterisation methods responsible for sulphur speciation and mineralogy for coal. The approach entails carrying out a case study assessment aimed at empirically assessing a coal tailings sample according to: particle size distribution, textural reference, mineralogical characteristics, and how the aforementioned factors influence the acid potential in coal. The approach intends to address key factors which include: identifying the sulphur bearing organic and inorganic constituents related AMD generation in coal, assessing how the mineralogy, texture and particle size distribution contribute to AMD potential in coal tailings, and then identifying suitable analytical techniques and test methods which can provide data. The combination of these key outcomes will seek to provide a systematic and meaningful framework for the characterisation of coal and coal waste streams.

The characterisation methods used in this case study outlined a framework focusing on four main areas of acid mine drainage characterisation for coal wastes, these included: chemical characterisation, mineralogical characterisation, sulphur speciation and AMD prediction. This comprehensive approach employed a suite of techniques, including: petrography, quantitative x-ray diffraction (QXRD) and quantitative evaluation of minerals by scanning electron spectrometry (QEMSCAN).

SYNOPSIS

The case study was carried out on a fresh sample collected from a thickener underflow waste stream with typical tailings characteristics. The sample was assessed across a particle size distribution of 5 size classes (-75µm, +75-106µm, +106-180µm, +180-212µm, +212-355µm). The initial petrography assessment found the coal tailings sample to be of a slightly weathered nature, indicating the onset of mineral oxidation. Mineralogy characterisation found the presence of acid forming pyrite to be most prominent in the smaller size fractions (-75, +75-106µm), with the pyrite presenting as finely disseminated grains within the matrix of the coal. Sulphur chemistry was determined through two sulphur speciation procedures, the standard ISO 157:1996 procedure and the method developed by the Australian Coal Industry's Research Program (ACARP). The sulphur speciation tests confirmed that pyritic sulphur contributes the highest proportion of sulphur, between 50 – 67%, to the total sulphur presence in the sized samples. The fine grain texture of pyrite and the higher concentrations of pyritic sulphur in the smaller size samples suggest that the propensity for coal related AMD increases with a reduction in grain size. This was confirmed through AMD prediction tests, which included static acid base accounting (ABA) tests and net acid generating tests (NAG), where a net acid producing potential (NAPP) of 31.75 kg H_2SO_4/tonne was determined for the -75µm sample.

Biokinetic AMD prediction tests were performed and provided information on the relative rates of the acid producing and acid consuming reactions in a microbially enhanced environment. The biokinetic tests were operated under two conditions, namely batch and semi-batch. The leachability of the pyrite was tested under two pH conditions pH 2 (acidic) and pH 6 (circum-neutral). Findings showed that acid consuming reactions dominated the first 2-3 days of the bioleaching investigations. The inoculated systems showed signs of bacterial activity with increases in the redox potentials and ferric iron (Fe^{3+}) concentrations, whilst the abiotic systems remained unchanged. These findings suggest that microbial activity is likely to contribute and possibly exacerbate coal related AMD.

This case study has aided in identifying the strengths and limitations of AMD characterisation techniques and their applicability to coal. A number of recommendations in terms of optimising and further developing these techniques have been made on the basis of this understanding. In particular, it is recommended that further work is done to develop the ACARP sulphur speciation testwork with the aim of producing a comparative assessment against the standard ISO 157:1996 method. Further refinement of the biokinetic tests is also considered necessary to attain a standardised approach to different ore types and testing routines. The case study also highlighted the uncertainties brought about by inadequate sample preparation in QEMSCAN resulting in biased data sets. This will ultimately provide scope for the development of an AMD characterisation protocol based on suitably selected techniques which should maximise characterisation efficiency.

ABBREVIATIONS AND NOMENCLATURE

ACARP	Australian coal association research program
AMD	Acid mine drainage
ARD	Acid rock drainage
ABS	Autotrophic basalt salt solution
BSE	Back scattered electron
Cl	Chlorine
CP	Cleaner production
CSIR	Council for scientific and industrial research
CRS	Chromium reducible sulphur
DME	Department of Minerals and Energy
DMS	Dense medium separation
DWAF	Department of Water Affairs and Forestry
EPS	Extracellular Polymeric Substances
H_2SO_4	Sulphuric Acid
ISO	International Standards Organization
PM	Particulate matter
QEMSCAN	Quantitative evaluation of minerals by scanning electron microscopy
ROM	Run-of-Mine
S	Sulphur
$S_{(total)}$	Total sulphur
SANS	South African National Standard
SD	Sustainable development
TOC	Total organic carbon

TERMINOLOGY

Acidification	A process commonly associated with atmospheric pollution whereby nutrient bases (calcium, magnesium and potassium) are replaced with acidic elements such as hydrogen and aluminium.
Acid neutralising minerals	Alkaline carbonate minerals which raise pH conditions when reacted with an acid.
Acid forming minerals	Sulphide bearing minerals which react to form acidic conditions under suitable biological and environmental conditions.
Acid rock drainage	The term acid rock drainage, or ARD, indicates acidic drainage originating from sources other than mines.
Ash	A common by-product of the combustion of coal comprising of residual mineral matter.
Biokinetic shake flask tests	Microbiological semi-continuous tests used to determine the acid potential within an ore type as a result of both acid generating reactions and acid neutralising reactions under microbiological conditions.
Biomass	Biological material derived from plants life providing a source of organic material for the geological formation of coal.
Beneficiation	Metallurgical processes whereby extracted ore from mining is separated into mineral and gangue materials.
By-pass fraction	Describes the amount of coal which does not undergo classification during separation - using defined as the ultra-fine material entrained within the liquid phase.
Colliery	A coal mine and its structures including processing plant and outbuildings.
Discard/s	Coal resulting from beneficiation practices which may have been deemed poor quality or too expensive to apply further beneficiation.
Disseminated	Refers to the scattered nature of the occurrence of pyrite within coal.
Effluent	Liquid waste containing dissolved mineral resulting from mining and/or beneficiation processes.
Fossil fuels	Fuels such as coal which have been formed through the decomposition of organic materials such as plant life and other living organisms.
Froth flotation	Process that utilizes the difference in surface characteristics between coal and gangue material to separate the materials from one another.
Gangue	Describes the unwanted material that is closely mixed with the coal

TERMINOLOGY

	when mined.
Leachability	Describes the ease with which a mineral is dissolved to the liquid phase.
Liberation	Describes the extent of released pyrite away from the associated gangue and coal material.
Macerals	Refers to the organic remains from the peatification process resulting in the formation of the combustible organic phase of coal, often designated by the suffix "inite".
Microlithotypes	Refers to the designation of thin rock type bands within coal which are on a microscopic scale and are defined by the maceral percentage.
Middlings	Middlings refers to the extent of pyrite liberation expressed as a percentage of the total perimeter surface area.
Mining fragments	Refers to any undesirable iron based material, commonly referred to as tramp iron.
Particle size distribution	Describes the proportions of coal within various size ranges.
Peatification	Describes the geological formation of coal through the several cycles and influencing factors including: the deposition of plant material (biomass), bacterial life, oxygen, temperature and the acidity of the peat formed during the geological stages.
Spontaneous combustion	A type of combustion that occurs as a result of self heating due to exothermic reactions.
Tailings	Describes poor quality coal within the -106μm size range often discarded due to the cost factors involved with the beneficiation thereof.
Texture	Describes the crystallographic orientations of a mineral such as pyrite giving rise the mineral's crystalline properties and strength
Top size	The largest aperture size through which the largest particle within a sample would pass through.
Thickener underflow	The agglomerated ultra fine coal particles resulting from the settling process in a thickening tank.
Weathering	The breaking down of mineral matter and organic matter as a result of exposure to harsh environmental conditions.

ACKNOWLEDGEMENTS

I would like to extend my sincerest gratitude to those who contributed to the fulfilment of this dissertation. It is through your guidance, patience, understanding, criticisms and continued support that I am able to present this completed work.

- I would like to first make mention that it is through the difficulties of this dissertation that I have grown to find love for my GOD, so for that I am entirely and eternally grateful.
- I would never have reached this point or any point better if it were not for my Supervisor , Dr Jenny L. Broadhurst her perseverance and patience have not only led me be in a position where I may present this dissertation but I have also grown to admire how strong of a woman and academic she is. My co-supervisors, Dr M. Becker, Prof S.T.L Harrison and Dr J-P Franzidis, who have provided me with their input and guidance, are equally greatly appreciated. A big thank you is also extended to Dr C. Bryan who provided much needed guidance and support.
- A huge thank you is extended to the Centre for Bioprocess Engineering Research (CeBER) staff. Frances Pocock and Emmanuel Ngoma, whose management of the labs ensured the labs were always a pleasure to work in. The Minerals to Metals research initiative for their support of the project through group discussions, seminars and student days.
- To the Centre of Minerals Research (CMR), Kirsten for her assistance with QXRD measurements and refinements and Jenny Weise and her colleagues for their assistance in the labs.
- Helen Divey and her team for the assistance in the analytical labs. Dr C. Van Alphen at the Eskom Research and Innovation Centre (ERIC) for providing me with assistance on the QEMSCAN analysis.
- Thank you to the Minerals to Metals initiative and the Department of Chemical Engineering at UCT as well as the National Research Foundation for their financial support.
- A very big thank you to the friends I have gained for their support , Gracia, Tapiwa, Porogo, Mussa, J-P, Hartmut, Maureen, Ziningi, Mpho and Nomsa.
- Finally, a very special thank you to my family and my dearest Bruh Terfie, whose unrelenting support, words of encouragement, prayers and love have kept me motivated.

LIST OF TABLES AND FIGURES

LIST OF TABLES AND FIGURES

LIST OF TABLES AND FIGURES

LIST OF TABLES AND FIGURES

LIST OF TABLES AND FIGURES

LIST OF TABLES AND FIGURES

CHAPTER 1

INTRODUCTION

South Africa relies heavily on its coal deposits as a source for both local energy generation and export. A number of environmental impacts are however associated with coal production and utilisation, many of which can be attributed to the presence of sulphur in coal. One such critical impact is acid mine drainage (AMD). The reappraisal of the risks attributable to AMD formation in South Africa has become increasingly necessary in view of the looming crisis in the mining basins of the Witwatersrand region (Inter-ministerial committee, 2010). The implementation of interventions to mitigate long-term AMD risks in vulnerable areas, such as the Mpumalanga coal fields, requires a quantitative understanding of the sulphur characteristics and related acid generating potentials of coal and coal wastes. The focus of this particular project is on the characterisation of sulphur and other mineral matter and the associated acid generating potential of coal beneficiation wastes, in the fine to ultra-fine particle size range.

1.1. Background - South African coal industry

South Africa has a generous yet limited supply of readily extractable coal in widely separated coal provinces as indicated in Figure 1. These coal provinces are themselves divided into distinct coalfields namely: Waterberg, Highveld, Witbank, Ermelo, Utretcht and Klip River coalfields (Jeffrey, 2005; Keaton Energy Holdings, 2009). Most of this commercially mineable resource is contained in the Permian-aged Vryheid formations of the Ecca Group which have been found to be rich in both inertinite and vitrinite (Snyman and Botha, 1993; Hutton and Mandile, 1996). South African coals are generally regarded as low in sulphur (S), the sulphur content of raw coals can range anywhere between 1% and 4% (Jeffrey, 2005). Ash content is another criteria for the determination of coal quality. South African's average coal ash content varies, but has been found to be as high as 65% (Eberhard, 2011). Coal obtained directly from mining operations is called Run-of-Mine (ROM) coal. ROM often contains gangue minerals, impurities and unwanted mining fragments, in order to meet buyer quality specifications the ROM is often subjected to various beneficiation processes.

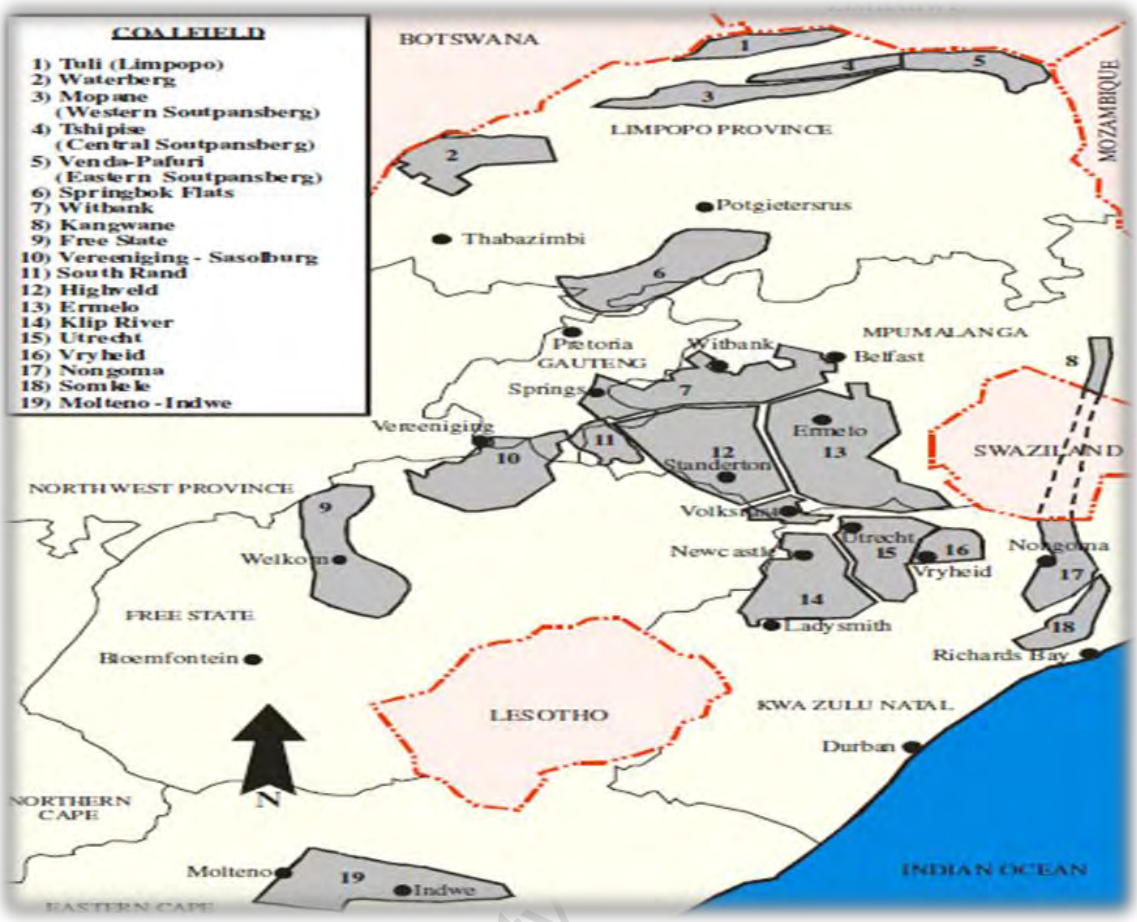

Figure 1: Indication of geographical orientation of coal fields in South Africa (Eberhard, 2011)

South Africa mines and produces both export quality metallurgical coal and thermal grade coal (Snyman and Botha, 1993; DME, 2010). Eskom, South Africa's national energy producer utilises a third lower grade coal, frequently termed middlings, for the purpose of electricity generation (Keaton Energy Holdings, 2009; DME, 2010). The resource remains the most commercially viable energy source for the country, with 96% of the country's electricity derived from coal-fired power stations (Eberhard, 2011; DME, 2010). Eberhard (2011) indicated that alternative energy sources such as wind energy have not been explored on a large scale in South Africa. This, coupled with insufficient natural gas and hydro capacities, has resulted in South Africa being heavily reliant on its coal reserves. The primary challenges with the continuing usage of coal as a chief energy source are the associated environmental concerns. Coal mining, preparation and utilisation require large amounts of land, which results in the first significant impact on the environment, land disturbance.

CHAPTER 1 INTRODUCTION

As with many other industrialised processes, coal mining and preparation is associated with a variety of waste types:

- Overburden, which refers to vast amounts of stripped away rock and unwanted material.
- Coal discard, which refers to undesirable material including stones, rock, wood and ash-forming minerals (clays, carbonates, quartz and pyrite).
- Coal tailings, which refers to undesirable coal in the fine to ultra-fine size range, due to quality control requirements.

In 2001, a Department of Minerals and Energy national inventory report indicated that 53.8 million tonnes of coal reported as waste in that year (DME, 2001). In 2007, that figure rose to 63 million tonnes (Prevost, 2010). Large amounts of waste, in the form of ash are also produced during subsequent combustion of coal in power stations. Land disposal of these wastes can result in the degradation of local water resources and air quality, ultimately impacting on local eco-systems and the health of surrounding communities (Geldenhuis and Bell, 1998; Asokan *et al.*, 2005). Furthermore, coal utilisation by way of coal fired power stations contributes to 38% of the carbon dioxide (CO_2) generated from the burning of fossil fuels, whilst the sulphur dioxide (SO_2) output has a 40% conversion rate to sulphuric acid (H_2SO_4).

1.2. Sulphur-related impacts associated with coal preparation and utilisation in South Africa.

Various studies have shown that the environmental risks associated with coal preparation and utilisation can largely be attributed to the presence of sulphur in coal (Bell *et al.,* 2001; Guma and Sofute; 2006). The various forms of sulphur found in coal contribute to a range of impacts, some of these include but are not limited to: spontaneous combustion, salinisation, acidification and acid mine drainage (AMD). Figure 2 illustrates the system with which each risk is associated and the output stream from which it originates.

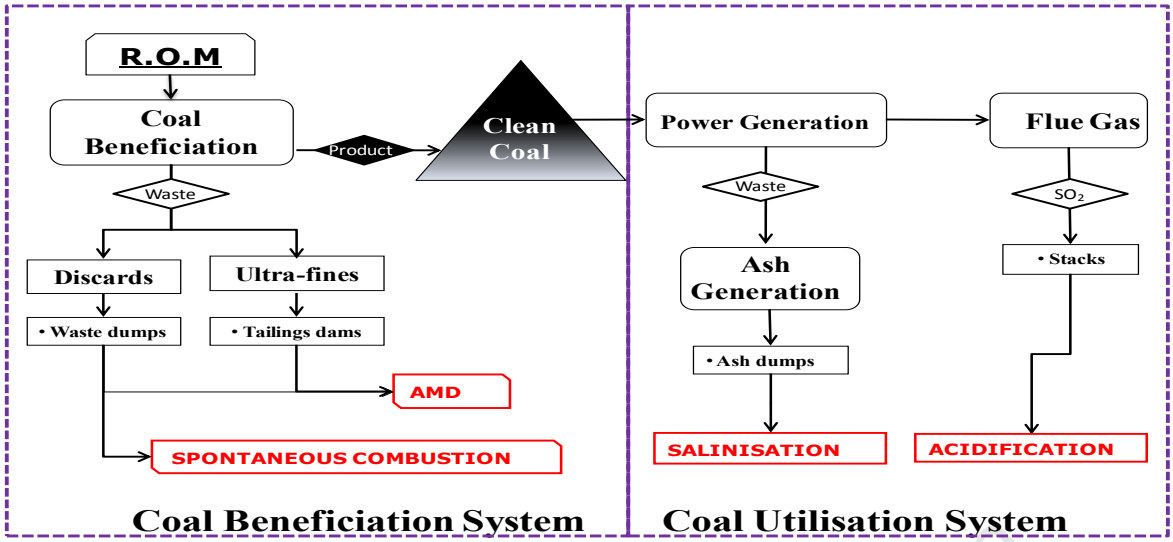

Figure 2: Sulphur-related impacts arising from coal preparation and power generation

Spontaneous combustion

The phenomenon of spontaneous combustion occurs through the oxidation of coal (Bell *et al.*, 2001). Heating is initiated by the circulation of oxygen through joints in the coal waste dumps and stockpiles. Once conditions become favourable (i.e. moisture content and oxygen content are sufficient) the oxidation reaction can easily become catalysed (Kaymakci and Didari 2002). Factors which affect the susceptibility of coal to self-heating and spontaneous combustion can be defined under two primary categories namely: intrinsic factors, these refer the natural state of coal and extrinsic factors, these refer to the external atmospheric, geological or mining conditions surrounding the coal. Table 1 summarizes the factors affecting spontaneous combustion.

Table 1: Factors affecting spontaneous combustion of coal (Guney, 1968)

Intrinsic factors	Extrinsic factors
Pyrite	Temperature, moisture, barometric pressure, oxygen concentration
Inherent moisture	Bacteria
Particle size and surface area	Coal seam and surrounding strata, method of working
Rank and petrographic constituents	Ventilation and/or air flow rate
Mineral matter	Timbering, roadways

The rate of self-heating increases as temperature within a dump or coal body increases, and thus the additional energy required for spontaneous combustion and self-sustained burning is reduced. According to Michalski *et al.* (1990), the tendency for coal to self-heat increases with lower rank coals. It is understood that lower rank coals have an increased moisture content, oxygen content and

internal surface area making low ranked coal susceptible to the permeation and liberation of heat throughout the coal body (Bell *et al.,* 2001). Furthermore, the oxidation of pyrite is conducive to the occurrence of spontaneous combustion by means of the heat generated through the exothermic nature of the reaction (Stracher and Taylor, 2004; Bell *et al*., 2001). According to Kaymakci and Didari (2002), ash content is also known to have an effect on the propensity of coal to spontaneously heat. Certain constituents such as: lime ($CaCO_3$), soda (Na_2CO_3) and iron (Fe), may promote the spontaneous combustion, while alumina (Al_2O_3) and silica (SiO_2) produce a retarding effect. Mineralogical analyses conducted on condensed particle matter (PM), from the by-products of spontaneous combustion, showed these to contain large proportions of solid sulphur compounds (Pone *et al*., 2007; Kuenzer *et al*., 2007). The solid sulphur compounds released as PM into the atmosphere may subsequently dissolve (at least partly) into natural water systems, contributing to the formation of acid (Pone *et al*., 2007; Kuenzer *et al*., 2007). The gases released during the spontaneous combustion of waste dumps in the Witbank coalfields have also been found to contain carbon monoxide (CO), benzene, toluene and xylene in toxic concentrations (Pone *et al*., 2007).

Salinisation

A common by-product from the combustion of coal is solid waste known as ash. Ash is generally stored in landfills or combined with coal wastes as backfill in mines. Landfills which impound solid waste are lined with seals or underground leachate collection systems (Keating *et al*., 2001). These innovations should impede any leachate generated by the fill. However, over the longer term, leachate from ash piles can infiltrate to water ways and aquifers causing an increase in the concentration of dissolved metals and salts in ground water sources (Sheps-Pelleg and Cohen 1999). The most common and leachable of elements are sulphur (S), chlorine (Cl) and molybdenum (Mo) (Álvarez-Ayuso, *et al*., 2006). These elements can cause an increase in its salinity when leached into groundwater.

Hansen *et al*., (2002) examined the leachate generated from a typical South African power station's ash dams. They noted that the groundwater in the local region had a pollution potential due to the presence of ash dams and the stockpiling of coal. Leachability tests were conducted on ash samples collected at the power station. Table 2 shows how the concentration of sulphates assessed by the tests is significantly higher the Department of Water Affairs and Forestry (DWAF) guidelines.

Table 2: Leachability results of ash from a typical South African power station, Source: Hansen *et al*., 2002; Guma and Sofute (2007)

Species	Average (mg/L)	DWAF guidelines (mg/L)
Sulphates	257	20
Calcium	122	150
Magnesium	0.9	70
Iron	0.024	0.1
Manganese	0.0014	0.05
Aluminium	2.93	0.15
pH	8	6.0 – 9.0

Acidification

The combustion of fossil fuels for the generation of electricity results in the emissions of harmful pollutants. Particulate matter (PM), carbon dioxide (CO_2) and sulphur dioxide (SO_2) are amongst some of these harmful pollutants. Electrostatic precipitators are used for particulate matter control to remove the fly ash from flue gasses (Gaffney and Marley, 2009). However, even with efficiencies as high as 99%, due to the large amount of coal required for electricity generation large amounts of PM are still emitted. The emission of SO_2 is of particular concern as it reacts with water in the atmosphere to produce sulphuric acid (Kaymakçi and Dıdarı, 2002; Kuenzer *et al*., 2007; Pone *et al.,* 2007). Flue gas desulphurization (FGD) refers to a set of technologies used for the removal of SO_2 gas from coal-fired power stations. FGD technology is currently not in use at the coal-fired power stations in South Africa. According to Reid (2007), the combined average SO_2 emissions from all Eskom's power stations for a 10 year period between 1996 to 2006 was approximately 1,600,000 tonnes. Furthermore, SO_2 has been known to have an average conversion factor to sulphuric acid (H_2SO_4) of 40% (Gaffney and Marley, 2009). This translates to an average generation of 640 000 tonnes of sulphuric acid over 10 years. The generated sulphuric acid, coupled with the generation of strong nitrogen based acids from the emissions of NO_x gases, results in an increase in the acidity of rain water or "Acid Rain". Acid rain is known to change the chemistry of soils and water (Alewell *et al.,* 1992). This occurs through the imbalance which is created between the natural internal hydrogen ions (H^+) sources and the H^+ from acid rain (Alewell *et al.,* 1992). The ecosystem relies on the natural uptake and turnover of H^+. However, acid rain can cause the eventual net accumulation of these cations, which then facilitates the propagation of acidification.

AMD

Acid mine drainage is the chemical process in which sulphide-bearing minerals are oxidised to produce acidic conditions in effluents (Johnson and Hallberg, 2005). The mineralogy of the mineral matter in coal, the surrounding atmospheric environment and local microbial activity all influence

the potential for sulphur species mobilisation and AMD formation. The reddish colour characterised by AMD effluent results from the generation of ferric hydroxide ($Fe(OH)_3$) although the most relevant effects of AMD formation from an environmental perspective are the associated low pH values and elevated concentrations of salts and heavy metals. In view of the deteriorating water qualities at the Loskop dam and Olifants river catchment, AMD resulting from coal mining has now become accepted as a major contributing factor to the degradation of the natural resources in South Africa (Van der Scholtz and Trautmann, 2007; Inter-ministerial committee, 2010; Karadad-Nelson, 2010; Sonjica, 2010). Although much of the AMD originates from the flooding of defunct mine shafts, coal stockpiles and waste dumps also carry a significant AMD pollution risk (Bell *et al*., 2001; Akcil and Koldas, 2006). More recently Sonjica (2010) indicated that the presence of fine coal contained in waste dumps is commonly thought to have a significant influence on local ground and surface water environments due to the correlation between the particle breakdown and the rate of oxidation of sulphide within this size range (Devasahayam, 2007; Reddick *et al*., 2007). In accordance with data provided by Reddick *et al*. (2007), over 10 million tonnes of waste in the ultra-fine particle size range is disposed of annually in South Africa.

Despite the risks associated with coal processing wastes, they are poorly characterised particularly in terms of their potential to generate AMD over the long-term. There are several techniques used to characterise the AMD generating potential of coal wastes however, there is little consistency in how and when these methods are used. Few attempts have been made to link the AMD generating potential of coal wastes to the mineralogy of the coal wastes, particularly with regards to the forms of sulphur occurring in coal. The result of this is either an under- or over-estimation of the AMD risks, these are often interpreted from data where results are based on assumptions and not quantitative data. This in turn results in uncertainties with respect to the actual environmental impacts associated with the land disposal of coal wastes, particularly over the long-term.

1.3. Problem statement

AMD and the mitigation thereof is critically important to South Africa. Coal beneficiation wastes and in particular, tailings slurries, are a large contributing factor to AMD generation. The characterisation of the acid generating properties of coal wastes is fraught with uncertainty and the influence of the speciation and deportment of sulphur and other inorganic minerals (such as carbonates) goes largely unexplored. These uncertainties and deficiencies create difficulties in evaluating and selecting suitable interventions for mitigating associated AMD risks in line with cleaner production (CP) and sustainable development (SD) principles.

1.4. Research objectives

The primary objective of this dissertation is to develop a quantitative understanding of the various sulphur species and other inorganic minerals within the tailings waste stream of a typical South African coal beneficiation circuit. Furthermore, the development of a quantitative understanding of the acid generating potential of such a stream is also important. On the basis of this understanding, the outcome would be the recommendation of a reliable generic framework for the systematic characterisation of sulphur and AMD potential of coal and coal wastes.

The aim of this investigation will seek to address the following key research questions:

i. In which minerals and macerals are the various forms of sulphur and acid neutralising constituents distributed through the coal tailings?
ii. How does the mineralogy, texture and particle size distribution of the coal tailings influence their acid generating potential?
iii. What analytical techniques and test methods are suitable for the accurate and reliable characterisation of the sulphur chemistry and acid generating potential of coal tailings?
iv. How can the methods and techniques in (iii) be combined in the form of a systematic and meaningful framework for the characterisation of coal and coal waste streams?

1.5. Dissertation structure

Chapter 1 comprises of an introductory background to the problem statement, providing contextual understanding of the status quo. Research objectives and pertinent key research questions are also included in this chapter. Chapter 2 draws on relevant literature pertaining to the project, highlighting key aspects of the current knowledge base, with specific emphasis on pyrite contribution to the generation of AMD and static AMD characterisation techniques. Chapter 3 provides the methodological approach of the project, highlighting the experimental scope and design, and describing the materials and characterisation methods used. The results of the selected case study are presented in Chapter 4, and their relevance discussed in detail in Chapter 5. Chapter 6 concludes the study, highlighting the study's significance and limitations as well as the recommendations it holds. Figure 3 outlines the schematic structure of the dissertation.

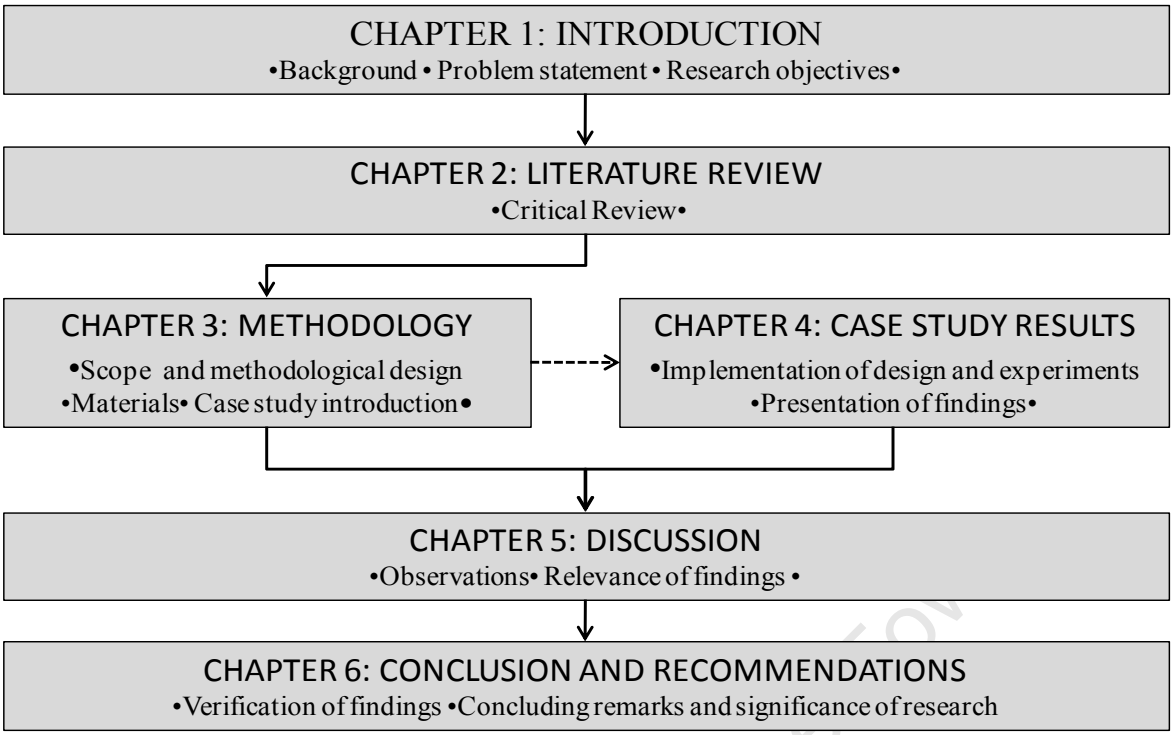

Figure 3: Schematic representation of dissertation structure

CHAPTER 2

LITERATURE REVIEW

This section comprises of a review and assessment of the generation, characteristics and environmental implications of coal processing wastes in South Africa, with specific emphasis on acid mine drainage (AMD). Existing tools and techniques which may be used to classify coal wastes according to their AMD generating potential and risks are also discussed.

2.1. South African coal and its preparation

As indicated in the previous section, the coal industry sector is likely to continue being of strategic socio-economic and local importance. This sub-section of the dissertation provides an overview of the characteristics, processing and uses of coal in South Africa.

2.1.1. Coal characteristics and uses

Coal is a solid, but brittle combustible carbonaceous rock, formed over an extensive period of time through the decomposition of biomass (Speight, 2005). As a result coal is made up largely of organic material with a proportion of inorganic matter which can vary from 5% to 38% in South African coals (Snyman and Botha, 1993). The environment under which coal geologically ages strongly influences the type, grade and rank of the coal formed, these terms respectively relating to the organic composition (maceral group), mineral matter composition and maturity of the coal (Speight, 2005). South African coal falls under the classification of Gondwana coals (this refers to the geological time and region in which the coal was formed) and is generally considered to be relatively low in sulphur (S < 2 %) and high in ash-forming minerals i.e. mineral matter remaining after combustion (ESKOM, 2007).

Mineral matter characteristics

South African coal has been reported to be considerably high in clay minerals and aluminosilicates (Snyman and Botha, 1993; Pinetown *et al.,* 2007). Various studies have reported on the quantitative presence of the different mineral phases in South African coals (Falcon, 1988; Snyman and Botha, 1993; Pinetown *et al.,* 2007). Pinetown *et al.*, (2007) commissioned a study to quantitatively evaluate the minerals in the coal deposits of the Witbank and Highveld Coalfields with the aim of improving the understanding of the mineralogy and geochemistry of these coals deposits. Table 3 presents the quantitative distribution of minerals in South African coals.

Table 3: Typical composition of mineral matter in coal (Snyman and Botha, 1993; Pinetown *et al*., 2007)

Mineral Group	Composition	Content (% of mineral matter)
Clay		
Kaolinite	$Al_4Si_4O_{10}(OH)_2 \cdot H_2O$	20 – 70
Illite	$KAl_2(AlSi_3O_{10})(OH)_2$	< 16
Sulphide		
Pyrite	FeS_2	1 – 6
Marcasite	FeS_2	Trace
Carbonates		
Calcite	$CaCO_3$	< 2
Dolomite	$CaMg(CO_3)_2$	< 2
Siderite	$FeCO_3$	< 3
Oxides		
Quartz	SiO_2	20 – 30
Hematite	Fe_2O_3	Trace
Sulphates		
Jarosite	$KFe_3^{3+}(OH)_6(SO_4)_2$	Trace
Alunite	$KAl_3(SO_4)_2(OH)_6$	Trace
Phosphates		
Apatite	$Ca_5(PO4)_3(F,Cl,OH)$	Trace
Others		
Rutile	TiO_2	Trace

Table 3 indicates that the mineral matter in South African coal is predominantly composed of clays with a significant presence of silicates in the form of quartz (SiO_2). Carbonate minerals typically make up less than 7 percent of the total mineral phase with the remainder of the mineral phase consisting of pyrite (1 – 6%) and trace amounts of sulphates and phosphates. Pyrite and marcasite and have been identified by several authors as the primary sulphur bearing minerals responsible for AMD formation in coal, while sulphates such as jarosite ($KFe_3(OH)_6(SO_4)_2$) and alunite ($KAl_3(SO_4)_2(OH)_6$) are prevalent in weathered or oxidised coal and therefore play a secondary role in AMD formation (Gluskoter 1975; Skousen *et al*., 1998, Naicker *et al*., 2002, Johnson and Hallberg 2005, Bryan, 2006). The occurrence of pyrite and other sulphide minerals in coal has been the focus of many studies (Rao and Gluskoter, 1973; Harvey and Ruch, 1986; Querol *et al*., 1988; Ward, 2002). Pyrite can occur as framboids which are small spherically shaped polycrystalline aggregates, euhedral crystals or larger pyrite accumulations within the maceral (organic phase). The origin and formation of pyrite is considered to be the result of decaying organisms converted together with sulphates in seawater by sulphur reducing bacteria producing hydrogen sulphide (Koper, 2004). The combination of the hydrogen sulphide with iron oxides from sediments resulted in the precipitation of the iron sulphide compound (Ward, 2002; Koper, 2004). Epigenetic pyrite is

formed within the coal seam and deposited as cleats along vertical fractures during the first coalification stages (Gluskoter 1975). The cleats of pyrite occur as discrete pyrite crystals of a euhedral crystallography approximately 10 - 20μm in size (Demchuk, 1992).

The occurrence of sulphates in coal is generally an artefact of pyrite oxidation therefore, trace indications of sulphate minerals are generally reflective of fresh coal. Traces of phosphates and rutile have also been identified in South African coal. Many authors have examined the linkage between trace element concentrations and the minerals in coal (Swaine 1990; Spears and Zheng 1999; Ward *et al*., 1999). The knowledge gained from these studies is of particular importance with respect to assessing the likelihood of the release of any toxic elements during the mining and preparation of coal.

Organic composition

The fundamental composition of coal includes organic matter which consists of fragmented and partially decomposed organic remains known as macerals. Macerals can be combined into three primary groups namely: vitrinite, liptinite and inertinite (Falcon 1988). South African coal is considered to be poor in liptinite and rich in inertinite with a varying composition of vitrinite (Snyman and Botha, 1993). Roberts (1988) showed that the organic sulphur in coal varies in sympathy with the vitrinite content. Organic sulphur in coal is usually distributed in a uniform manner throughout the matrix of the coal deposit making it very difficult to remove (Koper, 2004). The organic sulphur species associated with coals are mainly thiols, sulfides, disulfides, and thiophenes and their derivatives (Chou, 1990). Chou (2004) showed that the thiophene fraction of organic sulphur increases with the carbon content of coal and since the carbon content of coal is a measure of coal rank, generally, the higher the coal rank, the greater the propensity for organic sulphur. Koper (2004) showed that the organic sulphur content of four South African colliers varied between 0.24% and 0.31% on a dry air basis.

Uses for coal in South Africa

The composition and mineralogy of coal determines the characteristics therein, and ultimately governs the manner in which the material can be used. South African coals are generally described as unpredictable due to the gradual transition of maturity from eastern to the western coalfields resulting in the variability of rank and organic composition (Falcon and Ham, 1988). The multiplicity of the coal types means there are a vast number of end-uses for coal including: metallurgical coal used as a carbon source in the production of steel, synfuel coal used in the production of synthetic fuels (liquid fuels) and thermal coal (both export and Eskom grade) used in the production of electricity. Table 4 summarises the uses and related coal characteristics.

Table 4: Coal characteristics for a selected number of coal uses (Koper, 2004; de Korte, 2007, Eskom, 2010, Eberhart, 2011).

	Metallurgical coal	Export coal	Synfuel coal	Thermal coal
Sulphur (%)	0.5-1.2	0.6-0.7	1-2	0.7-2
Calorific value (MJ/kg)	n/a	25-27	< 21	19-23
Ash (%)	5.5-13	< 15	20-35	30-35

Of significance for steam coals (coal used for power generation) is the calorific value, which is a measure of the heating capacity of coal. Calorific values typically vary between 25 and 27 MJ/kg for export quality steam coal, and can be as low as 19MJ/kg for local thermal coal. Other criteria of key importance in terms of coal use are sulphur and ash content.

2.1.2. Coal processing

ROM received directly from mining sites contains certain proportions of impurities such as rock (non-combustible materials), ash forming minerals and mining fragments. These undesirable materials not only reduce the heating capacity of coal but the mining fragments commonly referred to as tramp iron, also pose the potential for expansive damage to processing machinery. Therefore, coal processing plants are equipped with various types of magnetic separators for the removal of unwanted iron based materials, at the ROM stage. Coal preparation is an upgrading process which typically involves 3 primary processing stages namely: crushing, screening and washing, with the aim of removing the unwanted materials and producing a uniform commercially saleable product, as indicated in Figure 4. ROM is first crushed to reduce the plant feed top size, this is followed by the screening stage which separates the coal into various size fractions which can be treated in subsequent processing stages. Based on market requirements and coal qualities, the unwashed sized coal can be sold directly to the respective markets or it can undergo further processing to improve the overall quality. The final stage of processing is the washing stage which is typically referred to as coal beneficiation and improves the grade or quality of the coal. Particle size distribution determines the processing route of the beneficiation/washing stage. The various coal size fractions are typically treated within their respective size classes by different beneficiation techniques as shown by the generic flowsheet of a South African coal washing plant in Figure 4.

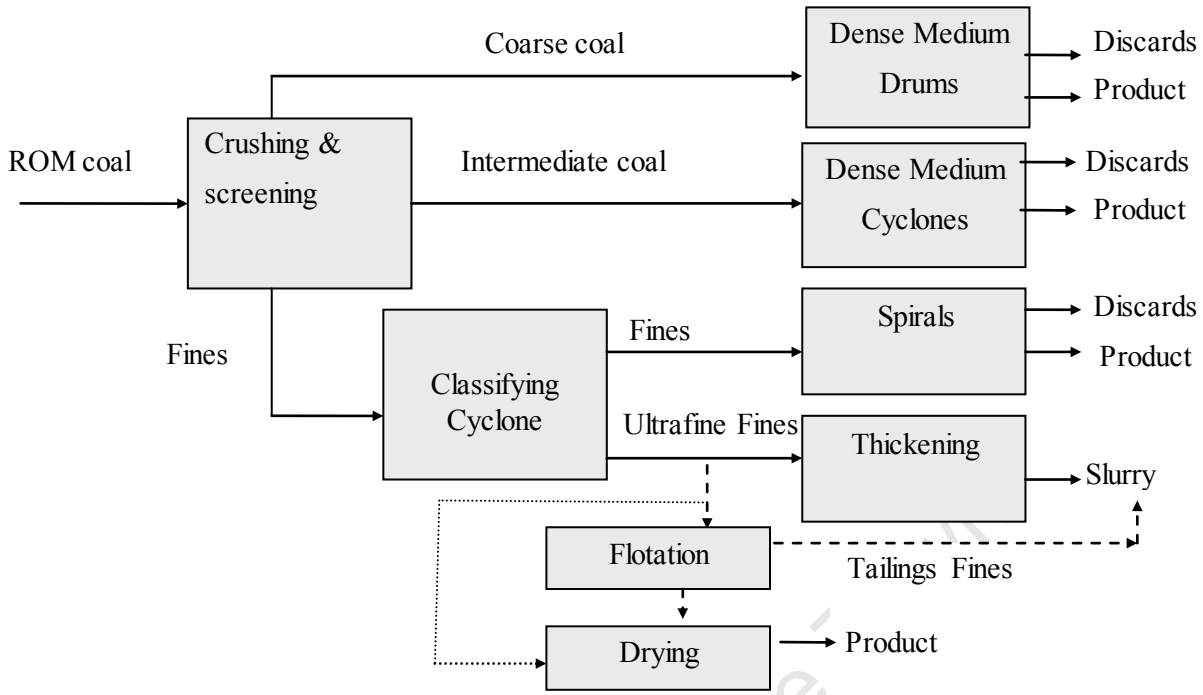

Figure 4: Generic flow diagram of a typical South African coal washing plant (adapted from Reddick, 2006 and Harrison *et al*., 2009)

- *Coarse coal (+6 mm) washing*

The coarse size range is washed in DMS baths typically, Drewboy separators or Wemco drums. Although jigs are cheaper separation units, the near-density nature of South African coal requires an improved sharpness of separation. This sharpness can only be achieved through the use of dense medium separation (Horsfall, 1980).

Intermediate coal (-15 mm + 0.5 mm) washing

Intermediate coal is treated in DMS cyclones which rely on centrifugal forces and dense medium (magnetite) to separate coal from gangue material (Horsfall, 1980; de Korte and Bosman, 2007).

Fine coal (-0.5 mm + 0.15 mm) washing

The beneficiation of fine coal material is largely dependent on its economic feasibility. Fines are classified further into fines and ultra-fines. The fine coal is typically de-slimed (removal of -45µm size material), by way of classification cyclones, prior to entering the spirals circuit, this dewatering process not only reduces moisture content it also removes some ultra-fine material.

Ultra-fine coal (-0.15 mm) washing

Ultra-fines typically report to the by-pass fraction in beneficiation circuits where filtration methods may be used if the ultra-fine material is of a low ash quality. The high costs associated with filtration typically render the recovery of high ash ultra-fines uneconomical. However, in

exceptional cases such as the coking coal market further beneficiation by means of 'froth flotation' may be required. This surface phenomenon process takes advantage of the difference in surface behavioural properties of coal over gangue material. This phenomenon results in separation of coal by adhering to the froth created in the reaction vessel which is then skimmed off the top and recovered as higher grade/quality coal (de Korte and Bosman, 2007). Although froth flotation is a well-known and accepted technique for the treatment of ultra-fine coal, it is not widely practiced in South Africa.

According to Prevost (2010) in 2007 approximately 60% of the 312 Mt (312 000 000) of raw coal mined in South Africa was beneficiated by means of coal washing practices. The resulting conversion of ROM coal to washed saleable coal was found to be 41%. Figure 5 shows the direction of movement of ROM coal and the relative proportions of ROM coal which report as waste and product materials.

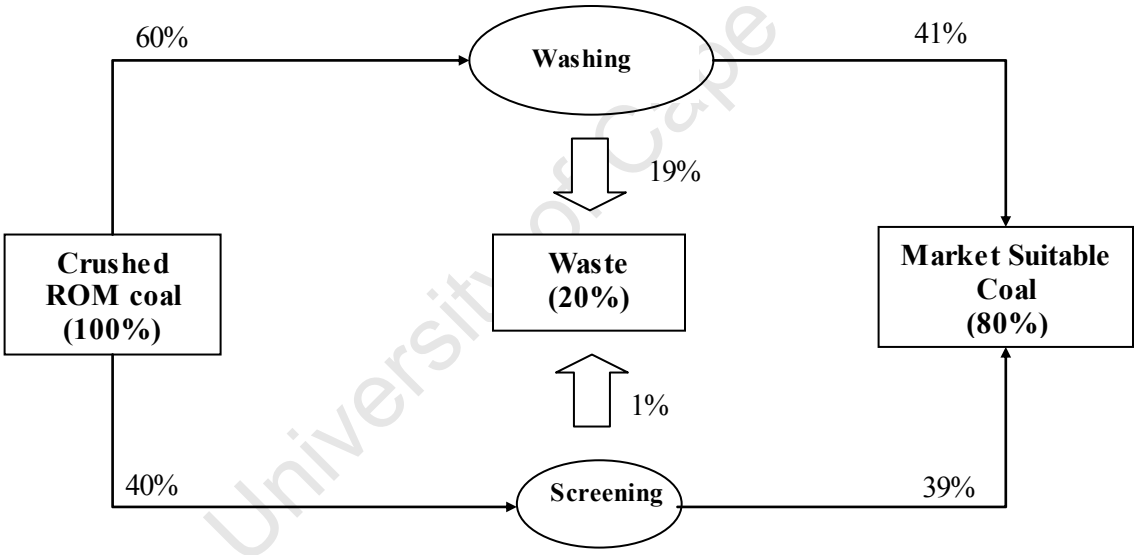

Figure 5: ROM processing routes in order to attain saleable quality coal (Adapted from Prevost, 2010)

2.2. Coal processing wastes

Based on an overall conversion of ROM coal to market suitable coal of approximately 80%, roughly 63 Mt (63 000 000) of material reported as waste in 2007 (Prevost, 2010). This waste occurs in two main forms namely: discards from the coarse, intermediate and fine coal washing circuits and "tailings" which refers to ultra-fine slurry streams (see Figure 4). The term "discard" is also frequently used to describe a combination of these two forms of waste. A Department of Minerals and Energy (DME) inventory commissioned in 2001 determined the qualities of discards and ultra-fine slurry tailings generated in South African collieries, these are summarized in Table 5.

Table 5: Typical characteristics of coal discard and tailings, reported on an as-received basis (DME, 2001)

	Discards	Ultra-fine slurry tailings
Calorific value (MJ/kg)	11 - 14	20 - 27
Ash (%)	30 - 60	10 - 50
Sulphur (%)	1 - 5	< 2
Volatiles (%)	16 - 24	17 - 27
Fixed carbon (%)	18 - 24	41 - 56

In reference to Table 4, the slurry qualities presented in Table 5 are very similar to those of the thermal and export coal products. Additionally, the calorific value of ultra-fine slurry material has been found to be higher than coarser discard material as such studies have sought out ways to reduce the moisture content of ultra-fine waste streams with the aim of directly agglomerating the ultra-fine material with product from collieries (de Korte, 2005; de Korte, 2008). Furthermore, in light of the waste qualities presented in Table 5 and the heightened consciousness of the environmental impact of coal waste, there is greater movement towards re-treating discard streams to produce an acceptable middlings product which is suitable for thermal coal usage and the generation of synthetic fuels (Lloyd, 2000; DME, 2001; Manenga and de Korte, unpublished).

Historically, coal waste has either been tipped over the sides of discard dumps or pumped into slurry ponds, depending on the top size of the waste (DME, 2001). However, with the growing understanding of the environmental implications of this "free-tipping" exercise at discard dumps, the material is now being spread and compacted over the dump to eliminate the ingress of air and reduce some of the previously associated environmental risks such as spontaneous combustion. The improved management of discard dumps is such that dumps are currently being constructed with run-off paddocks to control the potentially harmful run-off. Furthermore, seepage from dumps into ground water systems is becoming more strictly controlled through collection paddocks where it is either re-used in the processing plant or gravitated to evaporation dams (DME, 2001). Nevertheless, these measures are not extensively practiced across the entire coal industry spectrum and poor historical practices are said to have a continued long term effect on the environment (Manders *et al.*, 2009). The disposal of ultra-fine coal waste in the form of slurries has also considerably changed in recent years (DME, 2001). The co-disposal of these slurries with discard material into dumps is becoming increasingly popular.

The risks associated with coal waste generation have the potential to pose significant health problems on local communities (Geldenhuis and Bell, 1998; Harrison *et al.*, 2009). Furthermore, it is well understood that the effect of historical dumping on the generation of AMD will continue to

be felt for years to come. It is for this reason that coal related AMD formation and the conditions under which the process occurs in coal waste systems needs to be properly understood.

2.3. Coal-related Acid Mine Drainage

As discussed in previous sections, the generation of acid mine water relating to coal processing is a growing concern. According to the CSIR (Council for Scientific and Industrial Research), the threat of AMD on the environment is likely to persist for centuries to come and the major point of concern is the absence of a national view on the development of optimal integrated solutions to the management of AMD (Manders *et al*., 2009). This section examines the factors which influence the generation of coal-related AMD including the various sulphur components commonly associated with acid mine drainage.

2.3.1. The geochemistry of coal-related AMD generation

Acid mine drainage generation is a function of the relative kinetic rates of both acid forming and acid neutralising reactions (Singer and Stumm, 1968; Singer and Stumm, 1970; Sobek *et al*., 1978; Skousen *et al*., 1997). The process of AMD generation is catalysed when sulphide-bearing minerals such as pyrite (FeS_2) are exposed to moisture and air in a microbial environment causing them to become oxidised and produce acidic conditions (Johnson and Hallberg 2005; Akcil and Koldas, 2006; Hesketh *et al*., 2010).

AMD formation

Pyrite (FeS_2) is the most abundant sulphide mineral on earth (Bryan, 2006). Thus it is chiefly responsible for the formation of coal-related AMD. When pyrite (FeS_2), is exposed to a suitably oxidising environment the mineral undergoes oxidation according to the reactions outlined in Reactions (1) – (4) (Parker and Robertson, 1999; Akcil and Koldas, 2006; Lefebvre *et al*., 2011).

$$4FeS_2 + \frac{7}{2}O_2 + H_2O \Leftrightarrow Fe^{2+} + 2SO_4^{2-} + 2H^+ \qquad \text{Reaction (1)}$$

Reaction (1) describes the oxidation of pyrite into ferrous iron (Fe^{2+}), sulphate (SO_4^{2-}) and acid (H^+). Reaction (2) indicates the generation of ferric iron (Fe^{3+}) ions which act as leaching agents during further oxidation of pyrite (Reaction 3). Alternatively, Fe^{3+} ions can also precipitate according to Reaction (4) to form ferric hydroxide ($Fe(OH)_3$) when the pH levels of the effluent are slightly elevated (Wilkin, 2007) .

$$Fe^{2+} + \frac{1}{4}O_2 + H^+ \Leftrightarrow Fe^{3+} + \frac{1}{2}H_2O \qquad \text{Reaction (2)}$$

$$4FeS_2 + 14Fe^{3+} + 8H_2O \Leftrightarrow 15Fe^{2+} + 2SO_4^{2-} + 16H^+ \qquad \text{Reaction (3)}$$

$$Fe^{3+} + 3H_2O \Leftrightarrow Fe(OH)_{3(s)} + 3H^+$$ Reaction (4)

Coal-related AMD is largely dependent on the distribution of reactive sulphide minerals in the mineralogical structure of coal. This mainly refers to the distribution of FeS_2, however to a lesser extent other mineral sulphides such as: marcasite (FeS_2), galena (PbS), sphalerite (ZnS) and chalcocite (Cu_2S) are also known to occur in coal (Akcil and Koldas, 2006). Organic sulphur is considered a low risk sulphur contributor of AMD formation.

Organic sulphur is regarded as a low risk AMD contributor, though it is known to form sulphates when oxidized (Koper, 2004). Several authors have concluded that the majority of organically bound sulphur is found in aromatic structures, most of which are thiophenes (Gorbaty and Kelemen 2001; Ross *et al*., 2001; Gryglewicz *et al*., 2002; Jorjani *et al*., 2006; Stefanova *et al*., 2005).

Secondary mineral formation and behaviour

As discussed previously, the primary sulphide oxidation and acid neutralisation reactions result in the release of iron, sulphates, acidity and other metals into solution. These can react to form secondary minerals under sufficiently oxidising conditions i.e: sufficiently moist and aerated conditions and in the presence of a suitably oxidising bacterial environment. Wagner (2008) describes minerals such as pyrite and carbonates present in "fresh coal" as a precursor for secondary mineral formations in oxidised or weathered coal. Reactions (5) and (6) show typical secondary mineral formations expected in coal reflecting the formations of jarosite ($KFe_3(OH)_6(SO_4)_2$) and alunite ($KAl_3(OH)_6(SO_4)_2$) respectively.

$$3Fe(OH)_3 + K^+ + 2SO_4^{2-} + 3H^+ \Leftrightarrow KFe_3(OH)_6(SO_4)_2 + 3H_2O$$ Reaction (5)

$$3Al(OH)_3 + K^+ + 2SO_4^{2-} + 3H^+ \Leftrightarrow KAl_3(OH)_6(SO_4)_2 + 3H_2O$$ Reaction (6)

These secondary minerals play an important role in attenuating or amplifying trace contaminants from mine effluent (Wilkin, 2007). Hydroxide (OH^-), hydroxysulphates (HSO_4) and sulphates (SO_4^{2-}) precipitate at various pH levels, these secondary precipitates can potentially remove contaminants such as: lead (Pb), arsenic (As), zinc (Zn), copper (Cu) and nickel (Ni) out of solution. In as much as secondary precipitates may remove inorganic contaminants from solution, the geochemistry of the effluent may result in the remobilization of the contaminants depending on the pH (acidification) levels of the effluent. Therefore, removal of the contaminants is reversible and as such, the environmental risks associated with AMD effluents may become amplified by the dissolution of these contaminants at a later stage. Table 6 shows the most common secondary minerals associated with weathering in coal waste deposits and their typical pH range of formation and contaminant associations.

Table 6: Secondary mineral formed through AMD and their associated contaminants (Adapted from Wilkin, 2007)

Mineral Phase	Formula	Typical pH of formation	Contaminant associations
Hydroxides			
Gibbsite	$Al(OH)_3$	>5-6	Sorption in the general order of Pb>Cu>Zn>Ni with increasing pH
Hydroxysulphates			
Jarosite	$KFe_3(OH)_6(SO_4)_2$	2-5	Co-precipitation with As(V) replacing sulphate in the jarosite
Alunite	$KAl_3(OH)_6(SO_4)_2$	4-6	Precipitation of Al
Sulphates			
Gypsum	$CaSO_4 \cdot 2H_2SO_4$	>3	"Hardpan" precipitation
Melanterite	$FeSO_4 \cdot 7H_2O$	<2	Co-precipitation with Zn and Cu, temporary metal removal in a highly soluble phase

The precipitation of secondary minerals occurs with an increase in pH indicated by the pH ranges of formation in Table 6. The onset of this is brought about by the neutralisation provided by carbonate minerals in coal (calcite and dolomite). During this time aqueous metal species such as lead (Pb), zinc (Zn) and others, may adsorb on the surfaces of the newly formed secondary minerals (Wilkin, 2007). When high volumes of these minerals are precipitated, subsequent leaching of the secondary minerals poses a potential environment risk (Jambor *et al.*, 2000). The stability of the formed minerals is largely dependent on maintaining the pH levels of the above the typical formation range. Conditions under which a decrease in pH may occur include: the depletion of the neutralising capacity and/or the cessation of neutralisation and the continued dissolution of pyrite. In the context of mining sites in a coal waste disposal scenario the mass flow of acid effluent could act as a potential source for subsequent leaching. As such cognisance must be taken with regards to the long-term potential for acid formation and dissolved toxin transfer by the leaching of the secondary minerals.

AMD neutralisation

Mineral dissolution in coal is not just isolated to acid forming minerals. Carbonate minerals such as calcite ($CaCO_3$), dolomite [$CaMg(CO_3)_2$] and to a lesser extend ankerite [$Ca(Fe,Mg,Mn)(CO_3)_2$] provide a source of stored alkalinity which aids in acid neutralisation. The dissolution rates of highly soluble and highly insoluble minerals react at different rates respectively (Brantley, 2008). According to Brantley (2008), the activation energy (Ea – kcal/mol) required for the dissolution of calcite in water at ambient temperature is 8 times lower than the energy required for the dissociation of clays and oxides such as kaolinite ($Al_2Si_2O_5(OH)_4$) and quartz (SiO_2). The activation energy

required for these reactions influences the rate at which they occur. Table 7 shows the mean lifetime for complete dissolution of a 1mm crystal at 25ºC in a pH 5 solution.

Table 7: Mineral lifetime at ambient temperature and pH = 5 (Adapted from Lasaga, 2000)

Mineral	Lifetime (years)
Calcite	0
Kaolinite	6 000 000
Quartz	34 000 000

The buffering contribution provided by silicate minerals is minimal on a short term basis however, they can provide an additional long-term buffering capacity to coal wastes containing sulphide minerals Reactions 7.1. – 7.3 describe how the dissolution of a carbonate mineral such as calcite is dependent presence of H^+ ions to initiate the formation of the stored alkalinity.

$$CaCO_3 + H^+ \Leftrightarrow Ca^{2+} + HCO_3^- \quad \text{Reaction (7.1)}$$

$$CaCO_3 + H_2CO_3 \Leftrightarrow Ca^{2+} + 2HCO_3^- \quad \text{Reaction (7.2)}$$

$$CaCO_3 + H_2O \Leftrightarrow Ca^{2+} + HCO_3^- + OH^- \quad \text{Reaction (7.3)}$$

Reaction (7.1) describes how the dissolution of calcite is dependent on pH due to the required presence of H^+ ions. If the amount of these minerals in the rock is sufficient enough to offset the acid producing potential of the material, acid drainage will not eventuate. However, this requires for the respective reaction rates of the acid production and acid neutralising reactions to be similar or for acid neutralisation to occur at a faster rate. Furthermore, these minerals would inhibit pyrite oxidation by buffering the pH at a level where ferric iron may precipitates as ferric hydroxide (see Reaction 4) rather than oxidising additional pyrite. There are several factors which may exacerbate coal related AMD, these are discussed in the following sections.

2.3.2. Factors influencing AMD generation in coal

According to literature, the following chemical, physical and biological factors all contribute to the rate and occurrence of coal-related AMD formation (Johnson and Hallberg 2005; Akcil and Koldas 2006; Wilkin, 2007).

- Microbial activity
- Environmental conditions – pH, availability of dissolved oxygen, moisture content
- Mineralogy of ore – grain size distribution, grain morphology
- Geochemistry – extent of weathering, and secondary minerals

Microbial activity and the required environmental conditions

The chemical oxidation of mineral sulphides such as pyrite occurs at a slow rate however, in the presence of various groups of acidophilic micro-organisms, AMD generation is significantly accelerated (Loos *et al.*, 2000; Bryan, 2006; Hesketh, 2010). Micro-organisms which are capable of oxidising ferrous iron (Fe^{2+}) into ferric iron (Fe^{3+}) are responsible for the indirect oxidation of pyrite by Reaction (4). The indirect oxidation of pyrite is aided by planktonic micro-organisms or non-contact organisms (Loos *et al.*, 2000). There are two mechanisms by which pyrite oxidation occurs under microbial influence: indirect oxidation and direct oxidation (or the contact method). Indirect oxidation involves the conversion of ferrous iron (Fe^{2+}) to ferric iron (Fe^{3+}) and thereby the oxidation of pyrite by means of Reaction (3). Whereas, during the contact/direct mechanism sessile micro-organisms attach themselves to the mineral surface via extracellular polymeric substances (EPS) which act as reaction surfaces resulting in the direct oxidation of pyrite (Loos *et al.*, 2002, 2000; Bryan, 2006). Microbial activity is not isolated to just iron oxidising micro-organisms, sulphur oxidisers such as *Acidithiobacillus thiooxidans* and certain pseudonymous strains are for the oxidation of S^{2-} and organic sulphur. Sulphur oxidisers are responsible for the conversion of intermediate sulphur compounds to sulphate (SO_4^{2-}) ions which are paramount in the production of sulphur acid (H_2SO_4). Figure 6 illustrates the two mechanisms by which microbial activity contributes to AMD.

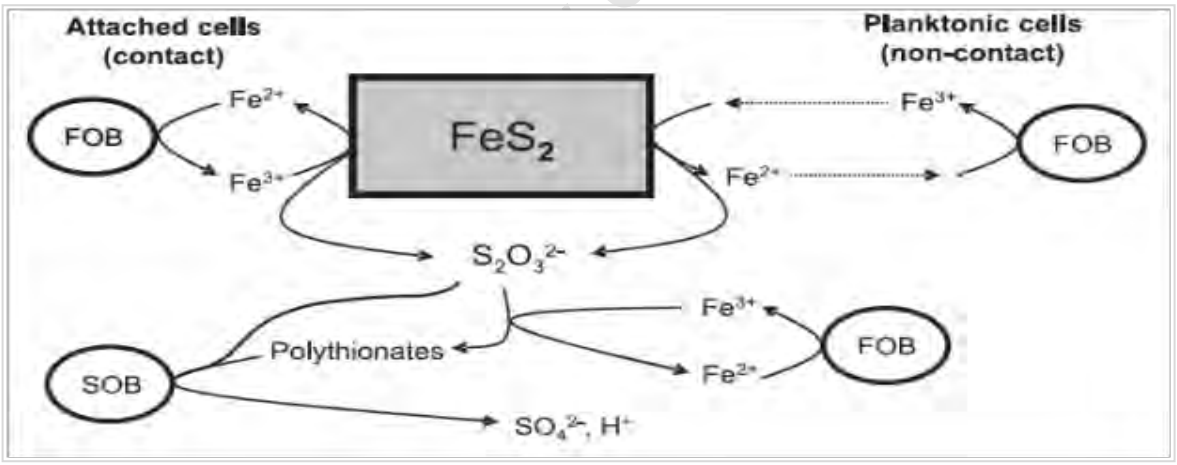

Figure 6: Schematic representation of the two mechanisms responsible for the AMD formation by acidophilic bacterium. FOB: ferrous oxidising bacteria, SOB: sulphur oxidising bacteria (Bryan, 2006).

Common iron oxidising micro-organisms found in coal waste deposits include *Acidithiobacillus ferrooxidans* and *Acidithiobacillus caldus* (Swaine and Goodarzi, 1995). The influence of microbial activity is highly dependent on environmental conditions, i.e. Acidithiobacillus ferrooxidans (ATF) are active in effluents where the pH is less than 3.5 and temperature are slightly elevated (± 35 ºC).

Therefore, if conditions are not favourable, microbial influence on acid generation will be minimal (Akcil and Koldas, 2006).

Availability of oxygen

The process of oxidation, whether chemical or biological, requires oxygen. Chemical oxidation can only occur if a suitably oxidising environment is achieved as indicated by Reaction (1) and (2). Furthermore, microbial activity relies on the transportation of oxygen and carbon dioxide to sustain population growth (Loos *et al.,* 2001; Bryan, 2006). Therefore the movement of oxygen and the presence of oxygen at a sufficient level is essential for the occurrence of AMD.

Moisture content

AMD formation requires the presence of water in order to not only facilitate a medium within which the oxidation reactions can occur but also acts as a transportation vehicle for the ingress of AMD effluent. Water also facilitates a habitat for biological activity and assists in carrying dissolved oxygen required for sustained population growth. Garcia *et al*. (2005) extensively examined the influence of moisture content on the AMD producing potential of mineral sulphide wastes and confirmed, that the presence of water plays an important role in the generation of AMD.

Mineralogy and texture

As indicated earlier, pyrite is the most abundant metal sulphide found on earth. Pyrite is therefore the dominant metal sulphide occurring in coal. However, marcasite has also been found in many coals (Gluskoter, 1975). Marcasite has an identical chemical composition to that of pyrite, though it differs with regards to its crystalline form, pyrite is cubic whilst marcasite occurs as an orthorhombic structure. There are conflicting reports on the effect of the crystallographic structure of iron sulphides (FeS_2) on the rate of bioleaching in coal. Authors such as Swaine and Goodarzi (1995) and Wang *et al*. (2007) agreed that rate of bioleaching of marcasite in coal was higher than that of isometric pyrite, Wang *et al*. (2007) expanded further and determined that marcasite was more chemically reactive than pyrite. This difference in oxidation is presumed to be attributed to the corresponding crystal structures and thermodynamic properties between the two iron sulphide forms. However, Nowaczyk and Domka (2000) determined that the rate of bio-oxidation was greater for pyrite than marcasite whilst Garcia *et al*. (2007) did not find consistent difference between the oxidation rates. Wang *et al*. (2007) ascribes such differences in literature to the variability in sample characteristics (i.e. purity of sample), inocula or the properties of the test cultures used. Moreover, these inconsistencies emphasis the necessity for further study of the mineralogical characteristics responsible for AMD generation in coal. A textural reference with regards to acid generation can be related to the morphological texture or form of pyrite in coal.

Weber *et al*. (2004) reported that framboidal pyrite (a morphological form of pyrite which is formed as small spherical or irregular microcrystals approximately 0.1-10μm in size) undergoes rapid oxidation when compared to euhedral crystalline pyrite. The number of reactive micro-surfaces associated with framboidal pyrite facilitates for an overall larger reactive surface area (Jambor and Blowes, 1998; Weber *et al.*, 2004).

Mineral liberation, liberation size and grain size distribution

The liberation of minerals can be described by liberation size or mineral liberation. The liberation size is the size to which an ore must be crushed or ground to produce separate particles of either value mineral or gangue mineral (Napier-Munn and Wills, 2006). Crushing practices are employed on collieries with the aim of reducing material size to improve handling and mineral liberation. However, the adverse effect is that acid forming sulphides associated with the gangue material also become liberated resulting in the exposure of reactive sulphide surfaces. The concept of mineral liberation with regards to AMD formation refers to the amount of exposed surface of a mineral sulphide surrounded by a non-sulphide mineral or body (Enviromine, 2012). Figure 7 shows four possible scenarios for pyrite or metallic sulphide liberation from non-sulphide minerals such as silicates, oxides and carbonates.

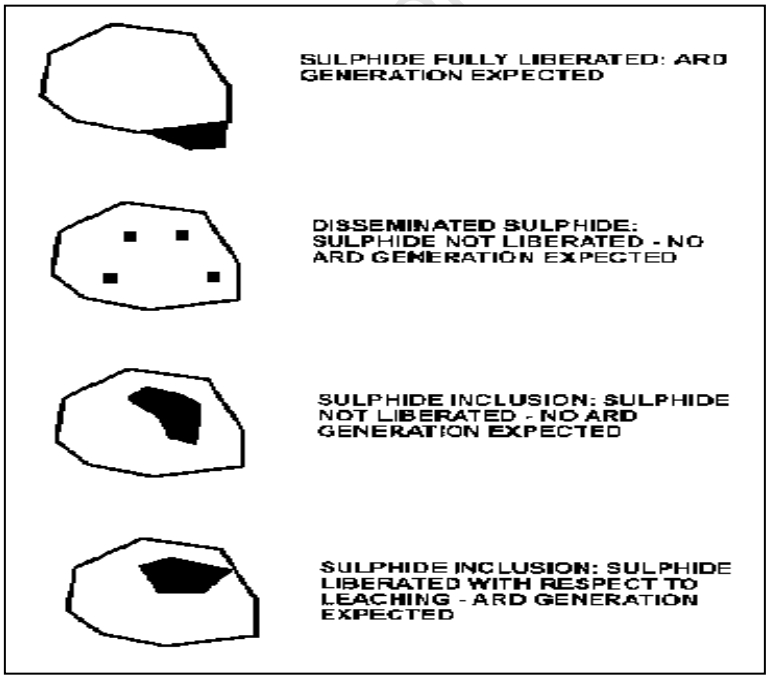

Figure 7: Potential ARD/AMD generating scenarios based on the extent of sulphide minerals liberation. (Napier-Munn and Wills, 2006; Enviromine, 2012)

Therefore atmospheric AMD generation can be expected when a metal sulphide such as pyrite is liberated to some extent. Another contributing factor to coal related AMD is the grain size

distribution of the mineral sulphide (Devasahayam, 2007). Finer particles provide a larger reaction surface area which can increase the overall potential of AMD. Grain size distribution is generally dependant on the geological formation and peatification of coal. The nucleation process of mineral sulphide grains determines the overall size, shape and texture of the grain. According to Harvey and Ruch (1986) minerals in coal occur as discrete grains or flakes in one or more of these five modes: (1) disseminated, (2) layers, (3) nodes, (4) fissures and (5) rock fragments. Any one or more of the five physical modes that provide the greatest surface area would influence the potential for AMD formation. For example, finely disseminated grains of pyrite provide the potential for a larger reactive surface area. However, the extent of liberation of such grains may not be as significant as nodes or layers of pyrite as indicated diagrammatically in Figure 7.

2.4. Characterising the acid generating potential of coal wastes

There are many ways to characterise coal, the methods discussed within this section are of relevance in terms of understanding the AMD generating potential. The following section will cover the most common mineralogical characterisation techniques employed to assess coal, chemical analytical methods that measure elemental concentrations in the coal, determine mineralogical components and their elemental modes.

2.4.1. Mineralogical characterisation techniques

The generation of acid from fine coal wastes is largely dependent on the distribution of acid forming minerals in the deposit. In order to understand and therefore determine the acid generating potential of a deposit, it is vital to establish the mineralogy of that deposit. A mineralogical assessment of the waste is necessary to identify and quantify the various sulphur species present in the coal which could lead to AMD. As outlined in Section 2.3.2, texture (including grain size and shape), liberation and weathering are all pertinent factors which are vital for the comprehensive characterisation of coal. Therefore, in addition to considering potentially acid forming and acid neutralising minerals within a coal sample, their mineralogical occurrence also requires consideration.

Petrography

Petrography is a routine microscopy tool used to qualitatively identify and characterise the various organic and inorganic constituents of a coal sample with the aim of assigning a coal rank and maceral group. Petrography is an ideal method for coal analysis since it enables the investigation of coal macerals (vitrinite, liptinite, and inertinite), their textures and relationship to the minerals as well as the determination of coal rank based on the reflectance of vitrinite. Coal petrography can also quantify and major mineral groups and mineral size (ICCP, 2011). A study conducted by

Roberts (1988) found that both pyritic and organic sulphur varied in accordance with the vitrinite content of South African coals. Therefore, petrography can be used as a screening tool to determine the likelihood for the presence of organic sulphur based on the evaluation of vitrinite content in a sample. Extensive petrographic analyses are also capable of providing insight on the general condition of coal samples specifically, weathering, extent of disintegration, oxidation of pyrite and alterations to the organic material structure can all be reported on (Wagner, 2008; du Cann, 2011). Studies such as those conducted by Wagner (2007) and Wagner (2008) successfully examined the microlithotype features of coal wastes. The greatest advantage of coal petrography is that individual particles can be examined and the data produced is not a bulk average.

Quantitative X-Ray Diffraction (QXRD)

X-Ray Diffraction (XRD) is a method used for the identification of various mineral phases based on their crystallography (Hutton and Mandile 1996; Ward, 2002; Vassilev and Tascon 2003). QXRD is an established technique which provides good reproducibility and has the advantage of producing an average analysis of properties over an entire sample. Organic matter present in coal appears as an amorphous peak on a standard XRD. However, the Rietveld XRD method can be used to assess the weight of the organic lump which can then be used as input data to for the Rietveld method to calculate the mineral contents (Hutton and Mandile, 1996). Figure 8 shows the diffractogram for a sample of coal flyash with peaks: Q – quartz, M-mullite, H – haematite, C – calcium oxide, are shown. The measured intensity is related back to a percentage (%) of the mineral contained in the sample based on the intensity of the x-rays which are reflected by the crystalline form of the mineral.

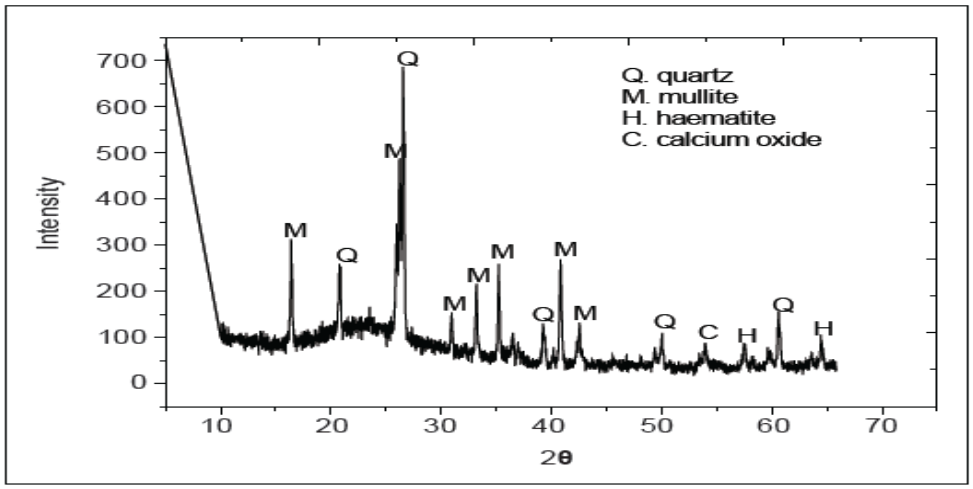

FIGURE 1
The X-ray diffraction profile (diffractogram) of coal fly ash

Figure 8: Diffraction profile (diffractogram) of coal fly ash with peaks indicating, various minerals (Musapatika, *et al*., 2010).

QXRD analysis can be conducted on both coal samples and low-temperature ash (LTA). Ashing is conducted as a pre-treatment to overcome detection limits associated with whole coal analysis. One of the drawbacks to LTA analysis is the transformation of minerals. This often occurs during ashing. XRD patterns from coal reflect both the crystalline components and amorphous carbon forms and the determination of mineral matter from these patterns can be associated with higher errors due to the weaker diffraction peak intensities (Huggins *et al.*, 2002).

The XRD detection limits (± 2 wt%) often preclude the use of this technique for the identification of minor phases i.e. pyrite. However, QXRD can be employed to provide both a qualitative and semi-quantitative understanding of the major mineral phases present in a sample.

Quantitative evaluation of minerals by scanning electron microscopy (QEMSCAN)

The QEMSCAN technique is an automated mineralogical analysis system capable of quantitatively determining the relative abundance of various mineral phases and their textural relationships. The technology is based on the integration of the back scattered electron (BSE) and energy dispersive x-ray (EDX) signals generated by the interaction of the electron beam with the sample (Huggins, 2002). This information is used to identify the phase of interest through a predefined user SIP (species identification protocol) file (Liu *et al.*, 2005a). QEMSCAN has successfully been used in various coal applications (Van Alphen, 2007; Moitsheki *et al.*, 2010). QEMSCAN enables one to quantitatively evaluate the presence of chemically reactive constituents which could potentially produce acid. The comprehensive data which QEMSCAN provides is useful for the qualitative and quantitative prediction of AMD formation in waste deposits. The technique can also provide an understanding of mineral-organic associations which will better aid the predictability of AMD formation (Liu *et al.,* 2005a). As discussed in Section 2.3.2, the liberation of potentially acid forming minerals can influence the overall AMD potential of a sample, i.e. a grain of pyrite which is locked within a grain of quartz or dolomite provides little or no reaction surface for oxidation to occur. Mineral liberation analysis is another evaluation technique which can aid in the characterisation of coal waste according to AMD potential, allowing for a user to pre-define the extent of liberation according to the percentage (%) of exposed surface area of a mineral. The resulting output is a reporting indicating the extent of mineral liberation according to the user-input.

As with any mineralogical analysis technique, sample preparation can have a profound effect on the reliability of results. The development of sample preparation for QEMSCAN has resulted in the use of carnauba wax for mounting media rather than epoxy resin. Liu *et al.* (2005b) explain that this is because the average atomic number of carnauba wax is 5.46 and coal materials have an atomic number ranging from 6.27 to 7.28, thus providing the necessary strong contrast between the

mounting media and coal material under the backscattered electron image. Other cases where sample preparation has shown significant importance involve heavy particle segregation. In cases where certain minerals may have a significantly higher density than others, such as in the case of pyrite (S.G 5.02) and coal (S.G 1.55), segregation of the heavier particles from the lighter can occur (Goodall and Scales, 2007). The consequence of the disparity between settling rates during preparation will result in a biased distribution. Furthermore, kaolinite has shown to have the poorest reproducibility during QEMSCAN analysis due to its low backscattering electron intensity (BSI). In addition to the low BSI of kaolinite the mineral typically occurs as finely disseminated particles occluded in the coal structure. According to Van Alphen (2007) these attributes make it very difficult to accurately detect and quantify kaolinite in coal.

Integrated quantitative coal characterisation methods

While optical imaging analysis such as petrography provides comprehensive information on the organic components in coal (maceral quantities, coal rank and maceral abundance) the samples are generally prepared using an epoxy resin. Epoxy resin does not provide adequate discrimination between the organic coal particle and the mounting resin when using QEMSCAN analysis. Therefore, carnauba wax is generally used for QEMSCAN analysis. However, according to O'Brien *et al*. (2011) samples prepared with carnauba wax are difficult to polish flat and can contain significant topography which precludes accurate reflectance measurements of maceral groups and as such coal rank cannot be accurately determined. Whilst optical imagining analysis and SEM methods provide significant information on an individual basis with regards to organic and inorganic constituents in coal, authors such as Jenkins *et al*. (2010) have explored the use of integrated image fusion techniques. O'Brien *et al*. (2011) suggested that the method of combining information from two image systems was tedious and labour intensive and proposed a workflow which involved collecting data from the same coal sample which had been analysed via optical and SEM systems. This workflow was made possible through a new sample preparation method which involved mixing the coal sample with carnauba wax followed by setting the sample face down in epoxy resin. The resulting effect is a surface face which is sufficiently resistant for polishing and optical image analysis. The integrated characterisation method presents some challenges with regards to image processing due to the amount of area required to be analysed. However, once the images from both systems are integrated an improved understanding for the quantitative presence of organic and inorganic constituents is possible.

2.4.2. Chemical analytical techniques

Huggins (2002) divided the various methods of inorganic coal characterisation into:

ii. methods that measure elemental concentrations in the coal
iii. methods that determine mineralogical components
iiii. methods that determine elemental modes

Due to the vast number of chemical characterisation methods which fall under the aforementioned categories (i .to iii.), only those of direct relevance to this study are discussed. It is important to note that the chemical analysis of coal has a broad base of material and several authors have undertaken to study these methods. (Huggins and Huffman, 1996; Huggins, 2002; Ward, 2002; Weber *et al*., 2004; Miller, 2008; Bucknam *et al*., 2009; Stewart, 2009). The chemical techniques used to characterise coal waste and the sulphur speciation methods employed by this study are discussed in the following sub-section.

Proximate analysis

The South African National Standard (SANS 17246:2006) and the International Standards Organization (ISO 17246:2005) for proximate analysis represented a group of standard test methods which include measurement of the following: moisture content, volatile matter which measures (in MJ/tonne) the potential energy generated from combustion, fixed carbon and ash content (Speight, 2005). Based on the standard tests outlined in SANS 17246:2006 and ISO 17246:2005 the properties for the various ranks of coal can be determined.

Leco™ total sulphur

Leco™ sulphur, is an analysis technique which utilises high temperature combustion in order to measure the total sulphur content of a particular sample (AMIRA International, 2002). Sobek *et al* (1978) describes the method as follows: a sample is heated in a Leco Induction Furnace to approximately 1600ºC, a stream of oxygen gas is passed through the sample during heating which promotes the evolution of sulphur dioxide gas which is collected in dilute hydrochloric acid". A series of automated titrations result in a calculated value for the total sulphur in the sample. One drawback involved with this method of chemical characterisation is the interference which may result from high nitrogen concentrations in the sample. Furthermore, halogens (iodine, chlorine, fluorine) present in a sample can also undergo evolution to the gas phase, resulting in lower recorded results for sulphur (Sobek *et al*., 1978). The Leco S method is the most common method of sulphur analysis used in the determination of total sulphur presence and the classification of AMD potential

X-Ray Fluorescence Spectrometry (XRF)

X-Ray Fluorescence (XRF) spectrometry is an elemental analysis technique used to quantify the presence of various major, minor and trace elemental constituents in a material (Lu *et al*., 2001). The technique is based on the measurement of secondary x-rays emitted from a sample which has been excited with high energy x-rays. The secondary fluorescent x-rays occur at characteristic energies for each element and are determined individually by a wavelength-dispersive detector (WDXRD). XRF is routinely used on a wide range of elements such as aluminium (Al), phosphorus (P), titanium (Ti), calcium (Ca) and chromium (Cr) and has even been extended to determine trace elements (U, As, Se and Cs) in coals (Prather *et al*., 1979; Willis, 1988; Johnson *et al*., 1989; Huggins, 2002).

However, there are several disadvantages to the use of XRF as a primary analytical technique. One crucial disadvantage are the detection limits, the comparative sensitivity of XRF is low and when coupled with the absorption of low elements (from Na to Cl) by air, the accuracy of the technique is not as high as for other elemental methods (Huggins, 2002). Given the limitations to trace element determinations with the standard use of XRF, energy-dispersive XRF (EDXRF) is a recent development which has significantly lowered the detection limits for determining trace-elements. EDXRF is performed on coal ash which has been fused and pelletized by the $Li_2B_4O_7$ method. The use of low temperature ashing (LTA) or high temperature ashing (HTA) as a pre-treatment technique to XRF is commonly used. However, both pre-treatment methods have inherent disadvantages the foremost of which is time, ash preparation may take up to several days (in the case of LTA) to attain constant weight, the other problem with using ash for analysis is mineral transformations which contribute to errors in results (Jenkins and Walker, 1978; Huggins, 2002). Therefore, even though there are vast improvements to the instrumentation used during XRF analysis, there are still inherent problems which occur with the actual sample preparation and handling.

Inductively coupled plasma optical emission spectrometry (ICP-OES) and atomic emission spectrometry (ICP-AES)

The optical emission spectrometry technique is an optical absorption technique which measures the atomic emissions from an excited sample to detect the presence of a specific element (Huggins, 2002). Attempts have been made at using OES techniques directly on coal, however, for the most part the method is employed on high temperature ash (HTA). The precision of the technique is typically quoted to be ± 30% due to the interference of some elements with the detection of others (Swaine, 1990; Huggins, 2002). Furthermore, the sensitivity of the technique is also largely dependent on the detection of the emitted radiation by the spectrophotometer. For these reasons, the

technique is not suitable for trace element detection, which is important in the characterisation of potentially hazardous leachate forming coals. OES is a suitable technique to screen large numbers of samples for the presence of major elements which may form part of the group of potentially AMD generating minerals, before applying more accurate techniques. Atomic emission spectrometry applies the same technique as OES but is does provide some advancement due to the superior properties of the ICP excitation source and the multi-sample operation mechanism (Querol *et al*., 1996; Querol *et al*., 2001). Modern ICP preparation techniques utilize the method of direct coal digestion, therefore eliminating the drawbacks associated with low temperature ashing (LTA) and high temperature ashing (HTA) (Huggins, 2002). The primary drawback of ICP is the time required for plasma stabilization (1.5 – 2hours).

The primary emphasis on the aforementioned techniques is that the combined use of two or more of these techniques is far more effective than extensively examining samples through the use of only one method.

2.4.3. Sulphur speciation

There are a number of different forms of sulphur that can contribute to AMD, as well as sulphur forms that do not contribute. As such the method of using total sulphur as an indicator for the determination of AMD potential is inadequate.

There are various studies which discuss methods for sulphur speciation (Gryglewicz *et al*., 1995; Ward, 2002; Stewart *et al*., 2009; Miller *et al.,* 2009). Discussed in this section are two procedures for the speciation of sulphur forms in coal, the International Standards Organization method for the determination of sulphur forms in coal (ISO 157:1996) and the Australian Coal Industry's Research Program method (ACARP Project C16034).

International Organization for Standardization 157:1996 (ISO 157:1996)

The standard ISO method is the most common and internationally accepted method for sulphur speciation and entails the quantitative analysis of sulphate and pyritic sulphur contents of coals.

The procedure utilizes the differential solubilities of sulphates and pyrite in dilute hydrochloric acid (HCl) and nitric acids (HNO_3) such that each can be taken in solution successively and determined directly (ISO 157:1996). The sulphate components are extracted under high temperature conditions (100^oC) by means of dilute hydrochloric acid (HCl) digestion. The pyrite remains in the residue which is then separated by filtration. The filtrate is reserved for precipitation with barium chloride ($BaCl_2$) where the sulphate sulphur content is determined gravimetrically. The residue is reserved

for further extraction with 9% dilute nitric acid (HNO_3) and the iron content is determined by atomic absorption spectrometry (AAS) where is total pyrite content is determined stoichiometrically.
Organic sulphur is insoluble in the reagents used in the procedure therefore, organic sulphur is determined by the difference from the total sulphur content, which is determined from Leco S analysis, and the sulphate and pyritic sulphur contents as determined by ISO method (ISO 157:1996).

This method does not address the separation between non-acid forming sulphate sulphur species, such as gypsum ($CaSO_4 \cdot H_2O$) and epsomite ($MgSO_4 \cdot H_2O$), and the potentially acid forming sulphate sulphur species, such as melanterite ($FeSO_4 \cdot H_2O$). Although the method may be able to determine the sulphate sulphur content of the sample, it is not clear whether these sulphates are acid producing or not. Although elemental sulphur is not expected to be a major sulphur phase in coal wastes, it is important to differentiate between the different sulphur phases in coal wastes and the ISO standard method does not provide a procedure for elemental sulphur (S^0) to be determined. Some authors prescribe the use of HCl leaching for the extraction of jarosite (Li *et al*., 2005). This may result in the overestimation of pyrite as the method assumes all the iron (Fe) leached out during the nitric acid (HNO_3) leach step is associated with pyrite (ISO 157:1996).

ACARP sulphur speciation protocol

The ACARP sulphur speciation method aims to address the shortcomings of the ISO method and provide a comprehensive procedure for isolating the various sulphur forms. The primary shortfall addressed through this method is the differentiation between the acid forming and non-acid forming sulphate phases. The impact of failing to distinguish between the two sulphate phases may result in the overestimation of the AMD potential.

Stewart *et al.* (2009) classified the different sulphur species into six categories, in accordance with their potential for acid formation these include: pyrite, non-acid forming sulphate salts (such as gypsum and epsomite), acid forming soluble sulphate salts (such as melanterite), organic sulphur and jarosite (which are both considered to be low risk in terms of AMD formation) and minor elemental sulphur. Figure 9 shows the procedural method of determining the various sulphur forms of interest.

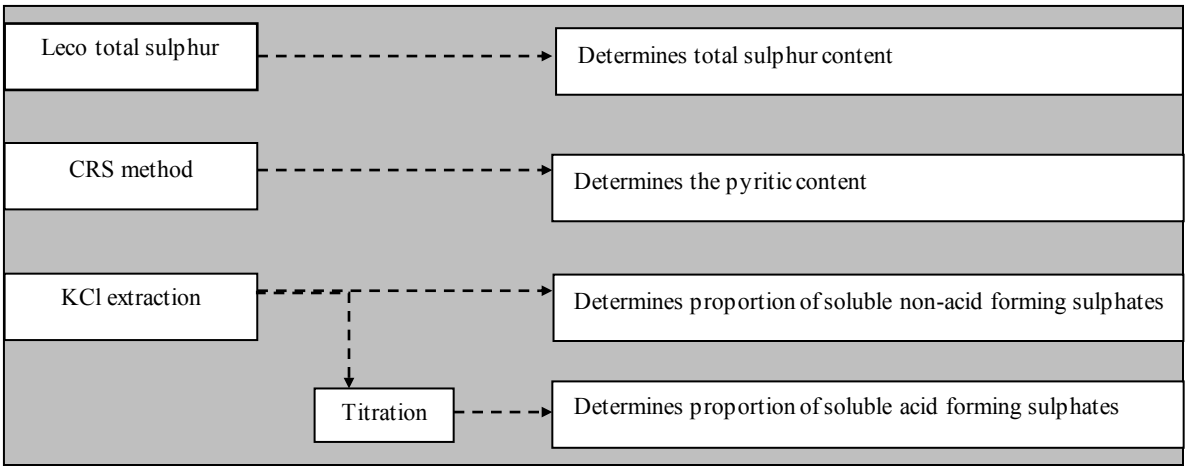

Figure 9: Overview of sulphur speciation procedure developed by Stewart *et al*., (2009)

The Leco sulphur test is first used to determine the total amount of sulphur contained in the sample (Miller *et al.*, 2008; Stewart *et al*., 2009). Pyritic sulphur is determined through the chromium reducible sulphur (CRS) test method. CRS involves the conversion of reduced inorganic sulphur to H_2S gas by hot chromium chloride ($CrCl_2$) solution, trapping the evolved H_2S gas in zinc acetate solution as an aqueous zinc sulphide (ZnS) solution (Miller *et al*., 2009). The ZnS solution is assayed for sulphide content using a spectrophotometery method developed by Cline (1969), designed specifically for the determination of sulphide content in solution. The pyrite content is then determined by means of stoichiometric calculations. The CRS sulphide test has indicated to have reasonable reproducibility, although some variability in results has been observed. Furthermore, elemental sulphur has been shown to be entrained in the measurement of the pyrite (Stewart *et al*., 2009). However, the CRS method includes an option for the removal of elemental sulphur by means of an acetone extraction step (Miller *et al*., 2009).

Based on previous work carried out by Smart *et al*. (2002), it was concluded that pyrite and jarosite are effectively insoluble in water and potassium chloride (KCl) within extraction periods of up to 1hour. The ACARP project expanded on the AMIRA projects' findings and determined that sulphate minerals, excluding jarosite, could be measured by means of the KCl extraction method based on the relative solubilities of the acid sulphate salts and the non-acid sulphate salts. The KCl extraction method involves the extraction of soluble sulphate salts from a sample using 1M KCl for 1 hour at room temperature (Stewart *et al*., 2009). Furthermore, results from the ACARP project indicated that the method is capable of differentiating between soluble acid generating sulphate forms and non-acid generating sulphate forms. This is carried out by way of apportioning part of the extracted solution for titration to determine the acidic content, after which the non-acid sulphate portion is determined by the difference between the total soluble sulphate content and the acid forming sulphate portion (Stewart *et al*., 2009). Organic sulphur was to shown not dissolve in either

the CRS extraction method or the KCl extraction method, therefore, the amount of organic sulphur present in the sample could then be calculated according to Equation (1a)

$$OrganicS = LecoS - \left(PyriteS + S^{0} + AcidS + Non - AcidS\right) \quad \text{Equation (1a)}$$

However, if the presence of jarosite is significant then either the organic sulphur would be over-estimated or the difference could be considered a measure of the low-risk sulphur component in the sample, which would therefore include organic sulphur and jarosite (Stewart *et al.*, 2009). Therefore the low risk sulphur phase would be calculated according to Equation (1b).

$$LowRiskS = LecoS - \left(PyriteS + S^{0} + AcidS + Non - AcidS\right) \quad \text{Equation (1b)}$$

Given that jarosite is insoluble in KCl for extraction periods of 1 hour, Stewart *et al.* (2009) postulated a method for the determination of jarosite. The method follows on from the KCl extraction method after which the residue is harvested for roasting at 550°C to the remove the pyrite content. Thereafter, an HCl extraction step is applied to the solid residue to determine the jarosite content. However, the method has shown to underestimate the jarosite content due to the loss of sulphur as SO_2 gas during the roasting process (Li *et al.*, 2007). The main drawback associated with this method of testing is that it does not address the actual evaluation of organic sulphur in the sample but rather calculates the amount based on difference. Furthermore, the method for determining jarosite is not sufficiently robust to provide reliable results due to the temperature sensitivity during the roasting process.

2.5. Acid potential testing procedure

The development of an acid potential procedure in this study is required in order to ascertain a quantitative assessment of the acid forming potential of the fine coal waste being investigated. Furthermore, the results from the procedure will be used to provide a complete and comprehensive AMD classification of the sample.

The procedure is based on a review of various established and developmental techniques. Ideally, the aim of the acid testing procedure is to:

ii. Understand the potential for acid production in the sample

iii. Evaluate the results of this procedure and transpose them to an understanding of how sulphur species and mineralogy may influence the findings.

2.5.1. Static Tests

Static acid potential tests are generally batch tests which evaluate the balance between acid generating processes and acid neutralising processes which could arise as a result of a sample's mineralogy (Smart *et al.,* 2002). There are several static AMD screening tools which are used to categorise the AMD potential of a sample, these are discussed in this section.

2.5.1.1. Acid Base Accounting (ABA)

This procedure evaluates the balance between the acid generating potential and acid neutralising potential of coal samples (Skousen *et al.,* 2002; Smart *et al*., 2002). The Maximum potential acidity (MPA) and neutralising potential (NP), also known as the acid neutralising capacity (ANC), are determined in order to calculate the net acid producing potential (NAPP) (Skousen *et al*., 2002) which is the difference between these two values.

Maximum Potential Acidity (MPA)

The principle of MPA is that it is calculated from the total quantity of acid forming minerals in the material, and is conventionally based on total sulphur analysis of a sample. This is based on the assumption that all the sulphur contained in the sample is in the form of pyrite and as such the MPA is calculated on this basis according to Reaction (1)

$$4FeS_2 + \frac{7}{2}O_2 + H_2O \Leftrightarrow Fe^{2+} + 2SO_4^{2-} + 2H^+ \qquad \text{Reaction (1)}$$

Based on Reaction (1), the MPA for a sample of coal, containing 1 wt% S as pyrite is 30.6 kg of H_2SO_4 per tonne of material and as such the MPA the formula for MPA is developed according to Equation (2).

$$MPA\ (kg\ H_2SO_4/t) = (Total\ \%\ S) \times 30.6 \qquad \text{Equation (2)}$$

The calculation of MPA according to Smart *et al*. (2002) report tends to overestimate the amount of acid generation which may occur. This is because sulphur can occur in other forms, some of which are slightly less acid generating than pyrite (e.g. jarosite) and others that may be non-acid generating (i.e. sphalerite, galena, chalcocite, gypsum and epsomite).

Acid Neutralising Capacity (ANC)

The acid generated by the oxidation of pyrite may be neutralised due to the presence of various carbonate minerals. According to Smart *et al*. (2002) the ANC is commonly determined by the modified Sobek method, this method involves adding a known amount of standardised hydrochloric acid (HCl) to an accurately weighed amount of sample. A precursor fizz test is conducted to determine the fizz rating and hence the quantity and molarity of the HCl to be added. Once the HCl

is added to the sample, it is allowed to react by heating the mixture before back-titrating it with sodium hydroxide (NaOH). This enables one to determine the amount of unreacted HCl. The amount of acid consumed by the reaction is calculated as the ANC which is expressed as kg H_2SO_4/ton (Smart *et al.*, 2002). The subjectivity of the fizz rating test results in the necessity for extensive repetition of the ANC tests and as such there is usually a high variability in the results (Meek, 1981). Furthermore, Meek (1981) suggested the ANC of rock units containing siderite ($FeCO_3$) were often overestimated when using the modified Sobek method. This is because although $FeCO_3$ is considered a carbonate mineral, continued weathering produces a neutral to slightly acidic solution (Meek, 1981; Shelton *et al.*, 1984). As a result, Meek (1981) suggested the addition of a small quantity of hydrogen peroxide (H_2O_2) to the filtrate of the HCl digested sample in order to oxidize ferrous iron (Fe^{2+}) to ferric iron (Fe^{3+}) which would then be precipitated out at ferric hydroxide ($Fe(OH)_3$) upon titration, yielding a more accurate ANC value . The method of adding H_2O_2 to enhance the oxidation of iron became known as the modified Sobek method with siderite correction (Skousen *et al.,* 1997). Although considered a carbonate mineral siderite does not necessarily provide a buffering capacity as indicated by Reaction (8a). However, under low pH conditions ($Fe(OH)_3$) does not precipitate and siderite becomes acid neutralising according to Reaction (8b) and pyrite oxidation less acid generating.

$$FeCO_3 + \frac{1}{4}O_2 + \frac{5}{2}H_2O \Leftrightarrow Fe(OH)_3 + H_2CO_3 \qquad \text{Reaction (8a)}$$

$$FeCO_3 + \frac{1}{4}O_2 + 3H^+ \Leftrightarrow Fe^{3+} + H_2CO_3 + \frac{1}{2}H_2O \qquad \text{Reaction (8b)}$$

Although the Sobek and Modified Sobek tests both determine the maximum amount of neutralisation available in the sample, neither predict the rate of neutralisation nor can these methods indicate the pH to which the sample can neutralise acidity.

Net Acid Producing Potential (NAPP)

The NAPP is a calculated value of the net capacity for acid production can be determined and also assigns a pH to which acidity can be neutralised. The NAPP is the difference between the MPA and the ANC as shown by Equation (3) (Smart *et al.*, 2002; Weber *et al.*, 2004):

$$NAPP = MPA - ANC \qquad \text{Equation (3)}$$

The NAPP is measured in the same units as ANC and MPA, kg H_2SO_4/ton. If the value for MPA is greater than the value for ANC, the NAPP will be positive which indicates that acid neutralising capacity of the sample will not be able to prevent acid generation. This would further indicate that the sample would have the potential for acid generation. However, if the ANC were to be greater

than the MPA, the NAPP would be a negative value, indicating that the sample may have a sufficient ANC to prevent the occurrence of AMD (AMIRA International, 2002).

ANC/MPA ratio

Another method for assessing the potential for acidity is the ANC/MPA ratio (Skousen *et al.*, 2001). Skousen *et al.* (2001) suggests that this ratio provides the best prediction accuracy for AMD. The ratio indicates the margin of error available within the material before the occurrence of acid generation (Smart *et al.*, 2002). If the ratio is > 1, it indicates an ANC larger than the MPA which is similar to a negative reflecting NAPP. Conversely, if the ratio is < 1, this translates to a positive NAPP value (Smart *et al.*, 2002). Ratios between 1 and 2 can produce either acidic or alkaline waters, whereas ratios greater than 2 are almost always acid neutral (Smart *et al.*, 2002). Table 8 provides an interpretation of the classification guidelines for the ABA tests and the associated ratio.

Table 8: Classification for the interpretation of ABA tests

Test	Result	Units	Classification guideline
Acid Base Account	NAPP > 20	kg H_2SO_4/ton	Acid forming (AF)
	-20 < NAPP < 20		Potentially acid forming (PAF)
	NAPP < -20		Non acid forming (NAF)
ANC/MPA ratio	Ratio < 1	None	Acid forming (AF)
	1 > Ratio > 2		Potentially acid forming (PAF)
	Ratio > 2		Non acid forming (NAF)

2.5.1.2. Net acid generating (NAG) pH tests

Conventional Single Addition NAG tests

The NAG test involves the addition of 250ml of 15% hydrogen peroxide to 2.5g of sample. The reagent is allowed to react with the sample overnight, where acid generating and acid neutralising reactions occur simultaneously. The liquor is then heated to oxidise any remaining sulphides, then vigorously boiled to decompose the remaining peroxide. The result is a liquor from which a direct measurement of the net acid generating potential of the sample can be determined (Smart *et al.*, 2002). The single addition NAG test does not reliably reflect the acid forming potential of sulphidic samples (>1%) since sulphide oxidation may only be partially oxidised during the single addition test (Smart *et al.*, 2002). Investigations carried out by Smart *et al.* (2002), showed that samples with a pyritic content less than 1% (< 1%) were completely oxidised in the single addition NAG test however, those with pyritic sulphur contents greater than 1% were not. This effect is caused by catalytic breakdown of the hydrogen peroxide due to the exothermic nature of the sulphide surface

reactions leaving unreacted surface pyrite in the sample. This may lead to some underestimation of acid forming potentials in samples containing high amounts of pyrite. To overcome this limitation sequential NAG test are carried out. In order to gauge the certainty with which sequential NAG tests may be necessary Smart *et al.* (2002) proposed using a $NAG_{4.5}$/NAPP ratio to determine the relative margin of safety or lack thereof with regards to the likelihood of further acid formation. Should the ratio be found to be less than 0.5 (<0.5) the likelihood for further acid formation is possible. However, this determination cannot be carried out in the absence of considering the pyritic sulphur content.

Furthermore, samples with a high organic matter contents (i.e. > 5-7% total organic carbon) may also interfere with the NAG tests (Smart *et al.*, 2002). Since coal is composed of high amounts of organic material these may react with the hydrogen peroxide to produce organic acids. In samples with low sulphide contents (i.e. < 1%S), organic matter acidity may give an overestimated account of the sulphidic acid potential (Stewart *et al.*, 2003). It is also important to point out that the organic acidity produced during NAG tests does not occur under standard temperature conditions.

Sequential NAG test

The sequential NAG test address' the underestimation error encountered through the single addition NAG tests. The procedure involves a multi-stage series of single addition NAG tests. At the end of each single addition NAG stage, the residue is reserved and NAG tests are repeated until such a time that there is no further catalytic decomposition of the peroxide or alternatively when the measured pH is greater than 4.5 (Smart *et al.*, 2002; Stewart *et al.*, 2006). The number of stages required to complete the decomposition is used as a guide to understand the length of geochemical lag of the sample. In order to complete the sequential test and in turn account for all possible sulphide constituents which may have remained unreacted, the liquor is titrated using sodium hydroxide (NaOH) and left over night to react further. Following this, the process of heating and titrating are repeated until there is no more effervescence and the NAG pH is greater than 4.5. The sequential NAG test is a useful method of ensuring that the sulphur bearing minerals are oxidised and as such that the acid generating potential of the sample is reliably reflected.

Extended boil NAG test

The extended boil NAG test was developed by Stewart *et al.* (2009) on the basis of research which was carried out to quantify and account for the effects of organic matter on the predictability of AMD through the NAG test. Previous investigations, conducted by Stewart (2005) had found that although both pyrite and organic acids react with the hydrogen peroxide (H_2O_2) in the system, pyrite was found to consume the peroxide more quickly. Stewart (2005) found that samples consisting of >

0.7% pyrite would tend to react more readily with the H_2O_2 giving to a rise in temperature, which ultimately results in the decomposition of H_2O_2 before significant generation of organic acid can occur. However, in samples with a pyritic content lower than 0.7% and where the total organic carbon (TOC) was greater than 7%, significant amounts of organic acids are formed resulting in the overestimation of the acid producing potential. Research (Stewart, 2005) has shown that the organic acid compounds produced in the NAG solution composed through vigorous boiling. Solutions with no dissolved organic acids will show no significant change in pH after extended boiling but, samples with organic acids show an increase in pH. It was also determined that uncertainties due to losses in acidity during the extended NAG test may be a result of organic compound interference. Stewart *et al*. (2009) indicated that an extended boil NAGpH greater than 4.5 does not necessarily categorize the sample is non-acid forming (NAF). The research carried out on quantifying and accounting for the effect of organic matter on the NAG test resulted in the development of a modified NAG test involving an extended boil NAG tests and a calculated NAG determination by assaying the NAG solution (Stewart *et al*., 2009). The result of this was a method by which acids derived from pyrite and organic material could be differentiated.

Calculated NAG

For pH levels higher than 4.5, the same filtered solution is assayed for concentrations of cations and anions to determine a calculated NAG value. The calculated NAG value provides a net acidity value (potential) in kg H_2SO_4/tonne by calculating the difference between the acidic components and the neutralising components which are not be associated with the organic acid component. The neutralising components are determined from the concentrations of cations (Ca, Mg, NA, K and Cl) known to be released into the NAG solution and the acidic component is determined from the acid generating sulphur (Stewart *et al.*, (2009). Equation (4) and (5) describe the components used to determine the calculated value for the NAG Acidity (Equation 6).

$$Acid_{Component} = \left\{ {[S]}/{32.06} \right\} \times \left\{ {Vol_{NAG}}/{Wt_{Samp}} \right\} \times 98.07 \qquad \text{Equation (4)}$$

$$Neutrali\sin g_{component} = \left\{ \left(\frac{[Ca]}{40.1} \right) + \left(\frac{[Mg]}{24.3} \right) + 0.5 \times \left(\frac{[Na]}{22.9} \right) + 0.5 \times \left(\frac{[K]}{39.1} \right) - 0.5 \times \left(\frac{[Cl]}{35.45} \right) \times \left(\frac{Vol_{NAG}}{Wt_{sample}} \right) \times 98.07 \right\} \qquad \text{Equation (5)}$$

$$Calculated\,NAG_{Acidity} = (Acid_{Component}) \times (Neutrali\sin g_{Component}) \qquad \text{Equation (6)}$$

To overcome limitations of the various NAG tests, Stewart *et al*. (2009) devised a NAG test protocol specifically for coal samples. The protocol involves a number of decision points based on the outcome of each step. The protocol begins with the conventional single addition NAG test, if the NAGpH of the solution after heating is found to be greater than or equal to 4.5 the sample is

immediately classified as non-acid forming (NAF). However, if the NAGpH is found to be less than 4.5 the solution is divided into three (sample A and B both 100ml and sample C at 50ml). The extended boil test is conducted on sample A, if the solution thereof is found to have a NAGpH greater than 4.5, the calculated NAG step is performed on sample B. Should the pH of sample A be less than 4.5 the sample is immediately classified as potentially acid forming (PAF). A calculated NAG value less than or equal to 0 kg H_2SO_4/tonne renders the sample non-acid forming (NAF), while a value greater than 0 kg H_2SO_4/tonne indicates a PAF sample. Sample C is reserved should a follow up or verification tests be required.

2.5.1.3 Classification of Acid Generating Potential on the basis of Static Tests

The above-mentioned tests are commonly used to classify samples according to their potential to generate acid over the long-term (i.e. over geological time). Depending on the test results, samples can be classified as non-acid forming (NAF), potentially acid forming (PAF) or uncertain (UC). These classifications are further described in the following and the criterion used for classification is presented in Table 9 (Smart *et al.*, 2002).

Non-acid forming (NAF)

A sample classified as NAF may or may not have a significant sulphur content, however, the mineralogy of the sample is such that the availability of acid neutralising constituents is theoretically sufficient enough to overcome any acid produced (Smart *et al.*, 2002).

Potentially acid forming (PAF)

A sample classified as PAF is generally seen to have a sulphur content which exceeds any neutralising capacity that the sample may inherently contain.

Uncertain (UC)

Samples could also fall under the uncertain classification. This classification occurs when there is conflict between the AMD prediction results. This is not an uncommon occurrence in coal samples because the acidity reflected by the tests may be reflective of organic acidity rather than sulphide derived acidity (Smart *et al.*, 2002).

Table 9: Classification for the interpretation of ABA and NAG tests (Smart *et al*., 2002; Stewart *et al*., 2006)

Test	Result	Units	Classification guideline
Acid Base Account	NAPP > 20	kg H_2SO_4/ton	Acid forming (AF)
	-20 < NAPP < 20		Potentially acid forming (PAF)
	NAPP < -20		Non acid forming (NAF)
Conventional & Sequential NAG test	pH_{NAG} >= 4.5 & NAGpH< 0	pH_{NAG} and kg H_2SO_4/ton	Non-acid forming (NAF)
	pH_{NAG} < 4.5 & NAGpH > 0		Potentially acid forming (PAF)
	pH_{NAG} >=4.5 & NAGpH > 0 OR pH_{NAG} < 4.5 & NAGpH < 0		Uncertain (UC)
Extended Boil NAG test	pH_{NAG} < 4.5	pH_{NAG}	Potentially acid forming (PAF)
	pH_{NAG} >= 4.5		Uncertain (UC)
Calculated NAG	$NAG_{calculated}$ =< 0	kg H_2SO_4/ton	Non acid forming (NAF)
	$NAG_{calculated}$ > 0		Potentially acid forming (PAF)

2.5.2. Kinetic tests

Although the established static tests are of value in tracking the acid producing behaviour of coal wastes, the tests do not take into account the relative kinetics of the acid producing reactions and the acid neutralising reactions nor do they provide information on the microbial catalysis that forms part of AMD production. On this basis, the evaluation of various existing and developmental kinetic tests is performed.

Humidity cell tests and column leach tests

Humidity cell tests and column leach tests provide long-term data on the weathering and acid generating characteristics of a sample (Usher, 2008). The tests differ to static tests in that they provide an indication of the combined reaction rates in the system, such as the time related generation of AMD. Humidity cell tests are typically performed across 7 day cycles, of which 3 days are run with dry air, 3 days are run with humid air and the final day is assigned for leaching. The cycle is then re-initiated the following day. The extracted leachate is analysed for pH, conductivity and dissolved species of interest (Usher, 2008). ASTM procedure dictates that cycles should be conducted over a 20 week period in order to provide meaningful data (ASTM D5744-96). Leach column tests provide information on the following: sulphide reactivity, oxidation kinetics, metal solubility and the leaching characteristics of the sample (Smart *et al*., 2002). The tests are performed over a 6 month cycle and involve the loading of a sample into columns or Buchner funnels where a test solution such as deionised water is applied to the surface of the column on a

weekly basis (Smart *et al*., 2002). The leachate collected from these tests is then analysed for acidity/alkalinity (pH), elemental analysis and electrical conductivity (EC). Some adaptations of the test involve inoculating the sample with a bacterium complex in order to assess the microbial effect on leaching.

In general kinetic test are used to compliment or validate geochemical investigations on AMD (Smart *et al*., 2002). However, these tests are known to be both expensive and time consuming and as such several authors recommend that the tests are designed with specific objectives in mind (Blowes *et al.*, 2005; Hornberger and Brady, 1998).

Biokinetic shake flask test

Biokinetic or Microbial shake flask tests are kinetic tests which involve the inoculation of a microbial population to a prepared sample (Hesketh *et al*., 2010). The mixture is then monitored for changes in its pH, over an allotted period of time. In the method proposed by Hesketh *et al*. (2010) a media prepared to a pH of 2 is added to prepared samples. This is followed by inoculating the samples with a range of iron and sulphur oxidising microorganisms such as *Acidithiobacillus ferrooxidans*, *Leptospirillium ferriphilum* and *Acidithiobacillus caldus*. The samples are then placed on an orbital shaking bench and maintained at 37°C for 90 days.

Over this period, the redox potential of each sample is measured, pH readings are recorded and plate counts are conducted to estimate microbial populations. The study completed by Hesketh (2010) was conducted on a copper ore tailings sample and showed that the results of the biokinetic tests can be used to both validate and compliment static prediction tests. Furthermore Hesketh (2010) concluded that microbial shake flask tests can provide information on the relative kinetics of the acid forming and neutralising reactions under conditions of microbial activity. In comparison to the conventional column and humidity cell tests, these tests are simple to set-up and run, and can produce meaningful results in relatively short periods of time (3 months).

2.6. Summary

The environmental effects of coal mining and processing are already evident in the reports of the deteriorating water qualities at the Loskop dam and Olifants river catchment areas (Section 1.2). Literature has shown that a significant amount of run-of-mine (ROM) coal reports as waste annually, this figure was approximated to 63 Million tonnes in 2007, of which 11.3 Million tonnes were accounted for as ultra-fine material. Furthermore, South African coal is described as fairly unpredictable particularly with regards to the large compositional variability seen across the seams (Section 2.1.1). With a growing concern that fine coal wastes pose a more significant influence on

the environment than coarser waste material, the lack of quantifiable data which speaks to this concern goes further to show the absence for the understanding of coal related AMD in South Africa. Furthermore, the significant quantities of unpredictable waste material will continue to pose a serious environmental and health risk if the true nature of their AMD producing potential is not quantified.

Literature has shown that the lack of quantifiable data is owed partly to the absence of a standardised approach to the assessment of the AMD potential in coal. Coal consists of a multiplicity of components, both organic and inorganic. The challenge therein is correctly quantifying the acid accumulation due to sulphides and acid formation from organic matter. Standard sulphur speciation tests also fail to distinguish between acid forming sulphate species and non acid forming sulphate species. The determination of pyrite through the standard ISO 157 sulphur speciation method is also associated with much uncertainty. Although tests have been developed by authors (Stewart *et al*., 2009) in attempts to address shortcoming and challenges associated with the standard AMD characterisation tests, these tests are associated with a number of uncertainties themselves. Current AMD prediction tools are limited to first order predictions or static tests and kinetic tests which do not account for all the aspects involved with the AMD generation in coal materials. Furthermore, standard AMD characterisation tests have been developed for sulphide wastes from the processing of hard-rock ores and these tests do not address the particular challenges associated with coal such as the issue of the various forms of sulphur and the presence of organic carbon. As such, the inclusion of a number of prediction tools into a framework which would address these shortcomings would ensure an accurate account for long-term AMD prediction.

The review has covered a number of analytical and AMD characterisation tools including conventional, established tests (such as XRD, ABA, NAG and the ISO157:1996 sulphur speciation protocol) and novel tests, some of which have been developed specifically for assessing coal (such as the extended boil NAG tests and the ACARP sulphur speciation test). The integration of these tools into an acid mine drainage (AMD) protocol would provide a comprehensive evaluation framework for determining the true nature of the AMD potential of coal in South Africa. The advantage of developing a framework would be that the assessment of the AMD potential in coal and coal wastes would have a standardised approach. Of significant importance to this framework is determining which methods are most suitable for the accurate and reliable characterisation of the sulphur chemistry and acid generating potential of the coal material. The information reflected in this review has been considered to develop a research approach and method, by which the resultant data will be used in order to address the key research objectives outlined in the introduction.

CHAPTER 3

METHODS AND MATERIALS

This chapter includes an overview and a brief description of the sample selected. A description of the experiments, methods and materials used for the case study are also presented here. Further details of the methods used can be found in the Appendix. The experimental approach for the case study uses five different experimental routes to characterise a coal waste sample. Figure 10 indicates the experimental methods employed in this study, namely: physical characterisation, mineralogical characterisation, chemical characterisation, sulphur speciation and acid mine drainage potential characterisation. The results gathered from these techniques are presented in chapter 4 as the case study results and will be used to answer the key questions proposed in section 1.4.

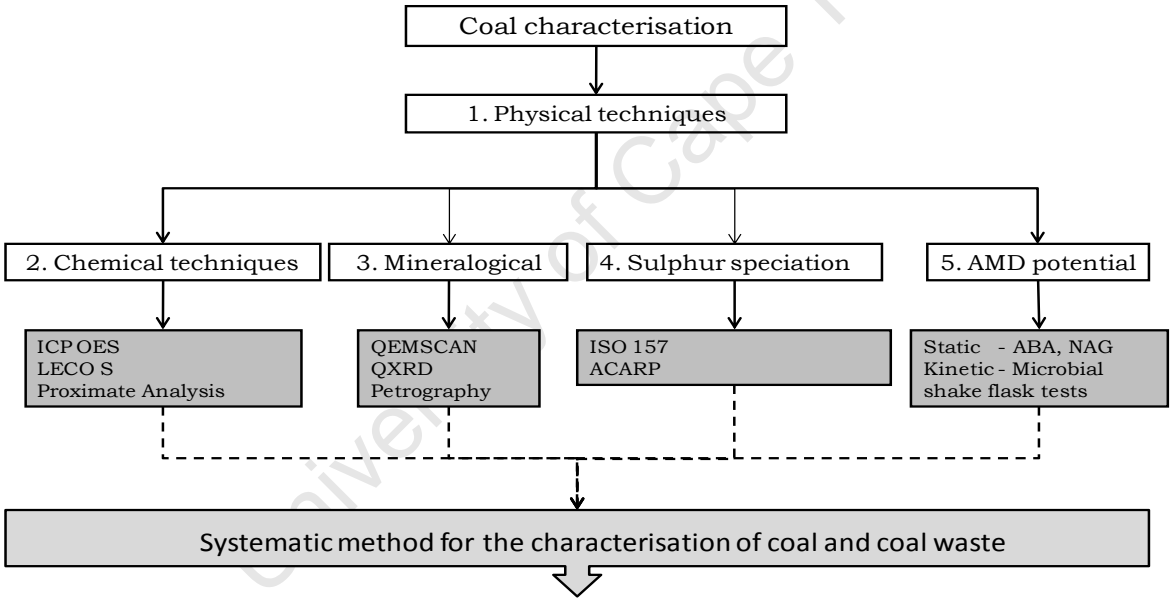

Figure 10: Schematic representation of experimental approach and methods employed

CHAPTER 3 METHODS AND MATERIALS

3.1. Sampling

The sample selected for this case study originated from the Middleburg coalfields region in South Africa. The plant from which the sample originates produces both export quality coal and lower grade thermal coal. The plant consists of two circuits A and B. Circuit A is fed ROM coal and has two main output streams, namely export quality product and waste. The waste from circuit A reports as feed to circuit B which also has two main output streams, namely Eskom grade thermal coal and waste. The sample used by this case study was obtained from the thickener underflow waste (tailings) stream of circuit B as illustrated by Figure 11.

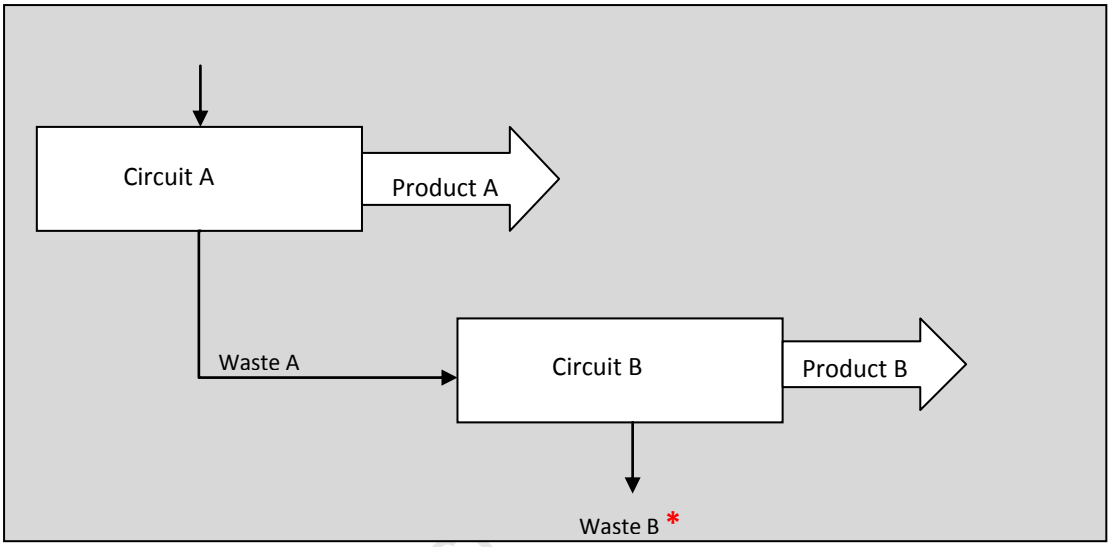

Figure 11: Circuit flowsheet of Middleburg plant from which ultra fine coal waste was sampled. Asterisk represents the sampling location.

3.2. Sample preparation and physical characterisation

A 50 kg coal thickener underflow sample was collected from the point of generation at the colliery and delivered in a sealed container to the University of Cape Town, Department of Chemical Engineering. The sample was air dried, quartered and coned on a tarpaulin in order to achieve manageable 5 kg representative samples. Each 5 kg sample was then split using a riffle splitter to obtain 1 kg representative aliquots. The 1 kg samples were placed in re-sealable plastic bags and stored in 10 litre (L) plastic drums. The samples were used for the characterisation case study investigation as well as a coal desulphurisation investigation conducted by Kazadi Mbamba (2011).

CHAPTER 3 METHODS AND MATERIALS

In order to physically characterise the coal sample, the sample was screened to determine the top size, particle size distribution (PSD) and 80 percent passing size (d_{80}) as indicated by Table 10

.

Table 10: Particle size distribution of screened sample with a top size of 1mm and a d50 of 267µm

Size fraction (µm)	Cumulative % passing (PSD)
-75	7.3 ± 0.21
+75 - 106	17.5 ± 0.28
+106 - 180	22.8 ± 0.41
+180 - 212	35.7 ± 0.31
+212 - 355	41.2 ± 0.39
+355 - 500	61.8 ± 0.62
+500 - 850	77.0 ± 0.83
+ 850	99.8 ± 0.04

The sized samples and the bulk feed sample were subsequently prepared and stored for further characterisation test work indicated by Table 11.

Table 11: Indication of the test work performed on the sized samples

Size fractions (µm)	Characterisation test work
Bulk	Chemical characterisation: (Leco S, ICP-OES, Proximate Analysis) Mineralogical characterisation: (Petrography, QXRD)
-75 +75- 106 +106 - 180 +180 - 212 +212 - 355	Chemical characterisation: (Leco S, ICP-OES, Proximate Analysis) Mineralogical characterisation: (QXRD, QEMSCAN) Sulphur speciation: (ISO 157:1996, ACARP) AMD predication : (ABA, Single addition NAG, sequential NAG, microbial shake flask)

3.3. Chemical characterisation techniques

3.3.1. Total sulphur analysis by Leco™

The total sulphur concentration of the sample was determined using a LECO S632 analyzer by the ALS Laboratory Group. This method utilises high temperature combustion and infrared spectrophotometery in order to measure the total sulphur content of a particular sample. The total sulphur results are presented in chapter 4.

3.3.2. Elemental analysis by ICP-OES

The concentration of the major and minor elements was determined using ICP-OES at ALS Laboratory Group in Witbank. In accordance with the method used by the laboratory, these samples were ashed by means of high temperature combustion in air at a temperature 800 ºC for 2 hours. The ash was then subjected to low temperature acid digestion with a hydrofluoric acid/hydrochloric acid (HF/HCl) mixture in a polypropylene bottle. Boric acid (H_3BO_3) was added to the mixture to complex excess fluoride. The resulting solution was then analyzed by ICP-OES. A detailed methodology for ICP-OES is provided in Appendix A.1.1.

3.3.3. Proximate Analysis

Proximate analyses of the coal were conducted to determine (1) moisture, (2) volatile matter, (3), fixed carbon and (4) ash content. The proximate analysis was performed on all the sized samples as well as the bulk sample. This was performed by the ALS Laboratory Group in Witbank in accordance with the international standard organisation method (ISO 17246:2005).

3.3.4. Sulphur speciation

The methods used for the determination of sulphur forms in coal are discussed in this section and further detailed experimentation methods are presented in Appendix A.1.2. and A.1.3.

Determination of forms of sulphur - ISO 157:1996

The ISO 157 procedure specifies methods for determining pyritic and sulphate sulphur contents in coal. The organic sulphur content is determined by subtracting the sum of these percentages from the total sulphur amount, as determined by the Leco S method described in Section 2.4.2.

The first procedure in the method involved the separation of sulphate and pyritic sulphur by means of boiling 2 – 8 g of coal sample with dilute HCl for 30 min. The insoluble residue was then separated from the filtrate. The sulphate sulphur dissolved in the filtrate and was determined gravimetrically by precipitation with barium chloride ($BaCl_2$). The mass percentage of the sulphate sulphur was calculated according to Equation (7).

$$SS_{Total}(\%) = \frac{m_2 - m_3}{m_1} \times 13.74 \qquad \text{Equation (7)}$$

Where:

m_1 is the mass in grams (g) of the test portion taken for HCl acid extraction.

m_2 is the mass in grams (g) of the barium sulphate found in the determination.

m_3 is the mass in grams (g) of the barium sulphate found in the blank test.

The pyritic sulphur component, which remains within the insoluble residue, can be determined by further extraction with 9% dilute nitric acid (HNO_3). This step dissolves the pyritic iron into solution thereby enabling one to determine the iron content by atomic absorption spectrometry (AAS). The pyritic sulphur content is determined from the pyritic iron concentration, assuming a stoichiometry where 1 mole of pyrite (87.84 $g.mol^{-1}$) per mole of Fe (55.84 $g.mol^{-1}$) is used.

Determination of forms of sulphur –ACARP

The ACARP sulphur speciation protocol specifies a method for determining each of the following: pyritic sulphur, elemental sulphur, and sulphate sulphur (acid forming sulphate sulphur and non acid forming sulphate sulphur) and jarosite (Stewart *et al*., 2009). For the purposes of this study, the elemental sulphur method and jarosite S method were not included on the basis that elemental sulphur poses a minor acid generation risk and the existing jarosite S method is not sufficiently robust to provide reliable data.

Determining pyritic sulphur – Chromium Reducible Sulphur method (CRS)

The CRS has been extensively reported on by Miller *et al.* (2008) and Ahern *et al.* (2004). The method involves the conversion of reduced inorganic sulphur to H_2S by hot acidic $CrCl_2$ solution, trapping the evolved H_2S gas in zinc acetate as zinc sulphide (ZnS). The experiments were conducted in an acid fume hood with a set up similar to the one illustrated in Figure 12. The system was sealed to contain the evolved H_2S gas.

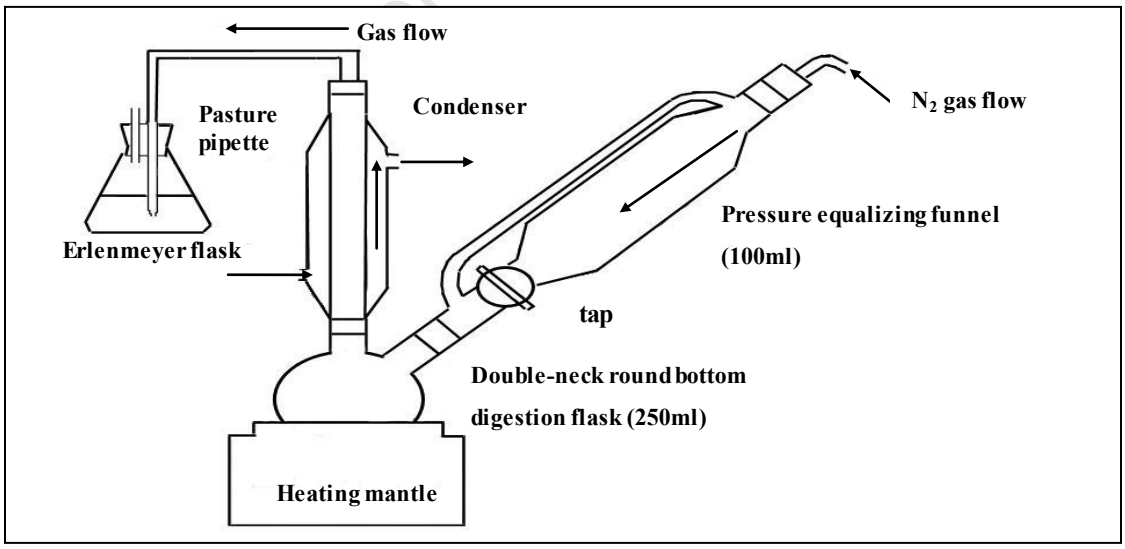

Figure 12: Schematic representation of the apparatus used in the chromium reducible sulphur test for the determination of pyritic sulphur. (Source: Ahern *et al*., 2004).

Technical grade chromium powder (2 g), ethanol (10 ml) and the coal waste sample (0.545 g) were placed in the double-neck round bottom digestion flask and purged with nitrogen (N_2) gas for 2 min. 6M HCl (60 ml) was introduced into the vessel where the mixture was then heated to a gentle boil for 20min. The ZnS solution was assayed for sulphide content using a Helios α UV-Vis spectrophotometer and the pyrite content of the original sample was calculated using a stoichiometry where 1 mole of pyrite (MW = 87.84) per 2 moles of S (MW = 32.08) is used.

Determining soluble sulphate sulphur – Potassium Chloride method (KCl)

The soluble sulphate sulphur content was determined by a KCl extraction procedure. 80ml of inert KCl solution and 2 g of coal waste sample was placed in a plastic bottle and shaken vigorously for a period of 1 hour. The mixture was then filtered using 0.45 µm filter paper and the liquor was separated into two equal parts. One part of the liquor was titrated with NaOH (0.05M) to a pH of 7 and the remaining liquor was assayed for dissolved sulphur using ICP-OES.

Equation 4 and 5 show the calculations by which the acid forming sulphate sulphur and the total KCl extractable sulphur species were quantified. Equation (8) relates to the titrated liquor and Equation (9) relates to the total amount of sulphate sulphur contained in the coal sample.

$$SS_{Acid}(\%) = \frac{Vol_{NaOH} \times Mol_{NaOH} \times Vol_{Extract} \times \left(32.06/2\right)}{Wt_{sample} \times Vol_{titrated} \times 10} \quad \text{Equation (8)}$$

$$SS_{Total}(\%) = \frac{[S] \times Vol_{Extract}}{Wt_{sample} \times 10000} \quad \text{Equation (9)}$$

Where:

SS is the soluble sulphur as a percentage (%)

[*S*] is the concentration of sulphur in grams per litre (mg/L)

Vol_{NaOH} is the volume of NaOH titrated in litres (mL),

Mol_{NaOH} is the concentration of NaOH in molarity (M),

$Vol_{Extract}$ is the volume (mL) of total leach liquor obtained after extraction,

$Vol_{titrated}$ is the volume (mL) and

Wt_{sample} is the original mass in grams (g) of the sample.

The percentage of non acid forming sulphur was then calculated as a difference between the total percentage extractable sulphates and the acid forming sulphates.

Determining Low risk sulphur – By difference

The low risk sulphur component of the total sulphur was determined by difference. This is calculation is expressed by Equation (1b).

$$LowRiskS = LecoS - \left(PyriteS + S^0 + AcidS + Non - AcidS\right) \quad \text{Equation (1b)}$$

Analysis of dissolved sulphide (S^{2-}) in solution

The amount of dissolved sulphide in solution was determined by means of a sulphide assay. The assay is a modified method of the methylene blue method developed by Fischer (1898). Cline (1969) proposed the use of a single reagent containing N, N-dimethyl-ρ-phenylenediamine sulphate. The reagents and dilution concentrations presented in Table 12 were used to determine the concentrations of the dissolved hydrogen sulphides (H_2S, HS^-, S^{2-}) in the assay samples.

Table 12: Reagent concentrations and dilution factors used in the sulphide sulphur assay in the various concentration ranges as suggested by Cline (1969)

Sulphide concentration (µmole/litre)	Diamine concentration (g/500ml)	Ferric concentration (g/500ml)	Dilution factor (ml:ml)	Path length (cm)
1 – 3	0.5	0.75	1:1	10
3 – 40	2.0	3.0	1:1	1
40 – 250	8.0	12.0	2:25	1
250 - 1000	20.0	30.0	1:50	1

The Helios α UV-Vis spectrophotometer was used to measure the relative absorbance wavelength of each sample, this was read at a wavelength of 670 nm. A detailed description of this method is presented in Appendix A.1.3.

3.4. Mineralogical characterisation

Various mineralogical techniques were used to characterise the composition of the bulk coal waste sample and separated size fractions. The methods used are described in this section and further description of the methodologies can be found in Appendix A.2.

3.4.1. Petrography

The petrographic analysis was conducted by Petrographics SA. The analysis was done on the bulk sample and was prepared according to the South African National Standards (SANS) 7404-2:1985 method. Approximately 10 ml of epoxy resin and hardener were mixed thoroughly. To

this resin mixture, approximately 26 g of representative bulk coal sample was added and thoroughly stirred. The block moulds in which the resin sample would cure were cleaned and coated with a mould release agent before being heated to ± 90 ºC in a drying oven. Once heated the moulds were filled with the resin mixture and allowed to set at 90 ºC. Particle grit was removed by washing the sample blocks with water or alternatively immersing them in an ultra-sonic cleaning bath. Silicon carbide paper was used as the grinding medium to remove any deep scratches visible on the surface of the objective sample block. The sample blocks were finally polished with a prepared slurry medium of alumina and water. The polishing took place on a water saturated lap cloth for 2 min and finally on a slurry saturated lap cloth for 2 min.

The prepared sample is examined using a reflected light microscope and the maceral groups are identified under an immersion medium with a suitable refractive index. The maceral groups are identified by their relative reflectance, colour, size and morphology. The proportions of the maceral groups are determined by a point count procedure. A total of at least 500 point counts is required according to the standard method for determining maceral group composition (SANS 7404-3:1994)

3.4.2. Quantitative X-ray diffraction (QXRD)

QXRD analyses were performed in duplicate, the sample preparation involving splitting the sample into duplicate representative samples of 3.5 g each. Each 3.5g sample was then micronized for 10 min to achieve a particle size range of -10 μm. 90% ethanol solution was used for cleaning any remaining sample from the mill. The samples were then dried under drying lamps. Powder QXRD spectra were obtained by using a Bruker D8 Advance powder diffractometer with Vantec detector and fixed divergence and receiving slits with Co-Ka radiation. The phases were identified using Bruker Topas 4.1 software and the relative phase (weight %) were estimated using the Rietveld method. The QXRD analysis provides a preliminary mineralogical assessment of the samples and the results also provide a comparison against which the QEMSCAN data can be compared.

3.4.3. QEMSCAN

The QEMSCAN analysis was conducted at the Eskom Research and Innovation Centre (ERIC), Rosherville, Johannesburg. The analysis was done on each sample size fraction. Furthermore, as indicated in Section 3.4.4, the residue from the draw and fill microbial shake flask tests was retained for QEMSCAN analysis. Each sample was split to produce a representative 0.2 g sample and each size fraction was composited, such that two blocks per size fraction would be

analyzed. Mould blocks (30mm in size) were prepared by heating the blocks in an oven to 80 ºC for 30 min. The inside of each block was brushed with an oil coating to prevent the wax from sticking to the mould walls. Carnauba wax flakes were melted in a microwave for ± 5 min. The melted wax was poured into the prepared moulds to the 3/4 level mark. The 0.2 g samples were then added to the hot wax in the moulds and stirred in a figure of eight pattern in order to avoid segregation. The samples were cooled at 60 ºC for 40 min as shown in Figure 13. Prepared sample blocks were checked for defects or spoils, if these were found, the samples were re-heated to 100 ºC and mixed in a figure of eight pattern once more and then cooled at 60 ºC.

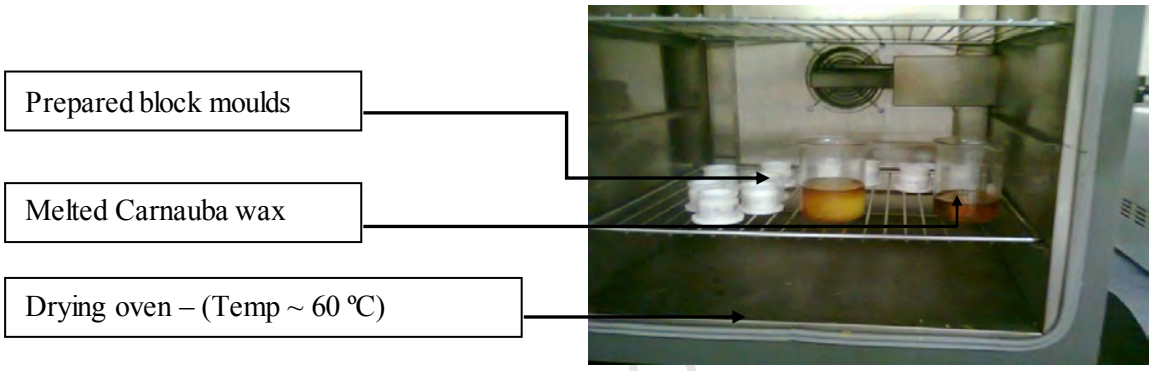

Figure 13: Prepared sample blocks in a 60 ºC drying oven for QEMSCAN analysis conducted at ERIC Rosherville, Johannesburg

Grit and deep scratches were removed by a surface grinding process together with a final polishing step. A detailed description of the preparation process including the surface polishing process is presented in Appendix A.2.2. The final preparation stage prior to analysis was the coating of carbon (graphite) onto the polished surface of each sample. Eskom utilized a Zeiss EVO 50 SEM for their QEMSCAN image analysis, the measurements of which were validated against the ICP-OES data provided to ESKOM. The raw data attained through QEMSCAN was processed using IExplorer software. This user-specified software was used to categorises the following minerals according to their proportional content: Kaolinite [$Al_4Si_4O_{10}(OH)_2 \cdot H_2O$], Quartz ($SiO_2$), Pyrite ($FeS_2$), Sulphate minerals ($SO_4^{2-}$), Siderite ($FeCO_3$), Calcite ($CaCO_3$), Dolomite [$CaMg(CO_3)_2$] and coal. The software was used to analyse the modal presence of the minerals, the degree of association of pyrite with these minerals and the extent of pyrite liberation within the coal samples tested.

CHAPTER 3 METHODS AND MATERIALS

3.5. AMD potential prediction tests

The acid generating potential of the coal waste samples was conducted according the AMD prediction tests outlined in Section 2.5. An overview of these procedures is outlined in this section.

3.5.1. Static tests – Acid base accounting (ABA)

Maximum Potential Acidity (MPA)

The MPA is calculated stoichiometrically from the total sulphur as measured by Leco tests according to Equation (10) (Smart *et al.*, 2002).

$$MPA(kgH_2SO_4 / tonne) = (TotalS) \times 30.6 \quad \text{Equation (10)}$$

A modification of the MPA value was also determined by calculating the maxium acid potential based on the combined average sulphide (S^{2-}) content determined from QXRD, CRS, and ISO 157:1996 methods according to Equation (11).

$$MPA_{S^{2-}}(kgH_2SO_4 / tonne) = (AverageS^{2-}) \times 30.6 \quad \text{Equation (11)}$$

Acid neutralising capacity (ANC) – Skousen method with siderite correction

The modified Sobek method (Skousen *et al.*, 1997) was adopted for this study. This method involves the addition of hydrogen peroxide H_2O_2 which oxidizes the ferrous iron in the dissolved siderite, yielding lower alkalinity predictions. The method was run on duplicate samples for each of the coal waste size classes. A precursor fizz rating test was done on each sample by adding a several drops of 25% HCl to a 1g sample of coal waste, as indicated in Appendix A.3.1. Based on the rating determined for each sample, the quantity and molarity of the HCl to be used in the ANC test could be obtained. Table 13 shows the appropriate volumes and acid-base additions for the ANC determination.

Table 13: Fizz rating and acid-base additions based on the Environmental Geochemistry International Pty Ltd methodology for ANC determination

Reaction	Fizz Rating	HCl molarity (M)	HCl volume (ml)	NaOH molarity (M)
None	0	0.5	4	0.1
Slight	1	0.5	8	0.1
Moderate	2	0.5	20	0.5
Strong	3	0.5	40	0.5
Very Strong	4	1.0	40	0.5
Carbonate	5	1.0	60	0.5

Once the appropriate amount of HCl was added to the sample, the solution pH was measured to ensure that it was between 0.8 and 1.5. If the pH was found to be outside of this range, the fizz rating was readjusted according to Table 13 and the ANC tests repeated. The solutions were boiled for 5min and allowed to cool. The solutions were filtered and pH measurements were taken. 5ml of 30% H_2O_2 was added to the solution and this was allowed to boil for a further 5min. Once cooled, the samples were back titrated to a pH of 7 and the NaOH volume was recorded. The procedure was repeated for 72 hours with an addition of 5ml H_2O_2 after each 24 hour cycle. A blank test sample was created for each fizz rating attained, these test sample were subjected to the sample procedures as the rest of the flasks, however, no coal sample was present in these flasks.

The value for ANC was calculated as shown by Equation 12 and is a measurement of the amount of acid consumed by the neutralising agents in the sample.

$$ANC = \frac{\left[Vol_{HCl} - Vol_{NaOH} \times C\right] \times M_a \times 49}{W} \qquad \text{Equation (12)}$$

Equation 13 shows the computation of *C*.

$$C = \frac{Vol_{HCl} inBlank}{Vol_{NaOH} inBlank} \qquad \text{Equation (13)}$$

Where:

M_a is the concentration of HCl as molarity (M).

W is the mass of the sample in grams (g).

Vol_{HCl} is the volume of HCl (in litres L) added as instructed by the fizz rating.

Vol_{NaOH} is the volume (L) of NaOH titrated.

A stoichiometric conversion factor of 49 is used to give the units kg H_2SO_4/tonne of material.

Net acid producing potential (NAPP)

The NAPP (expressed in kg H_2SO_4/tonne of material) for a sample is a calculated value which measures the balance between the effect of the acid producing potential and the acid neutralising potential. Equation (3 – Section 2.5.1.1) shows how the NAPP is calculated.

$$NAPP = MPA - ANC \qquad \text{Equation (3) - Section 2.5.1.1}$$

3.5.2. Static tests – Single addition Net Acid Generating (NAG) test

The single addition NAG tests were performed by reacting 15% H_2O_2 with 1.25g of coal sample in a 250 ml Erlenmeyer flask as indicated in Appendix A.3.2. The peroxide was allowed to react

with the sample overnight and the flask was covered with a watch glass and placed in a fume hood. The following day, the pH of the sample mixture was recorded and the flask was gently heated on a heating mantle for at least 2hours or until effervescence had stopped. Once cooled the pH of the mixture was recorded and the sample filtered. The filtrate was back titrated with 0.1 M NaOH to pH 4.5 and then pH 7. The volume of the base required at each instance was also recorded. The NAG at pH 4.5 and pH 7 respectively were calculated as indicated in Equation (14).

$$NAG = \frac{49 \times Vol_{NaOH} \times M_b}{W} \qquad \text{Equation (14)}$$

Where:

Vol_{NaOH} is the volume of NaOH in litres (L).

49 is the stoichiometric conversation factor.

M_b is the concentration of the base (NaOH) in molarity (M).

W is the mass of the sample is grams (g).

3.5.3. Static tests – Sequential Net Acid Generating (NAG) test

Sequential NAG tests were conducted as it is not uncommon for some unreacted sulphide minerals to remain in the mineral during a single addition NAG test. This occurs when the H_2O_2 breaks down before oxidising with all the sulphide minerals present. The method was the same as presented for the single addition NAG tests, however, the filtered residue was retained and the procedure was repeated on the residue. This is continued until the after-boil pH was found to be greater than 4.5 and no further reaction with H_2O_2 could be seen.

3.5.4. Kinetic tests – Microbial AMD prediction tests

The shake flask tests for the case study were conducted using two different scenarios, the first was a draw and fill system which involved the removal of 90% of the supernatant upon each sampling instance. The second scenario was a batch system where no supernatant was removed throughout the testing period. The tests were conducted by weighing out 7.5 g of sample into 250 ml Erlenmeyer flasks, 150 ml of autotrophic basalt salt solution (ABS) at a pH of 2 (acidic) and at a pH of 6 (circum neutral) was introduced into respective flasks. A measured amount (7.5ml) of a mixed culture of bacterium was introduced into each flask. The draw and fill shake flask tests were conducted in triplicate and the batch tests were conducted in duplicate. The prepared flasks were then covered with aluminium foil and placed on an orbital shaking platform at 150 rpm as shown in Figure 14. The flasks were maintained at 37 ºC for a minimum of 70 days.

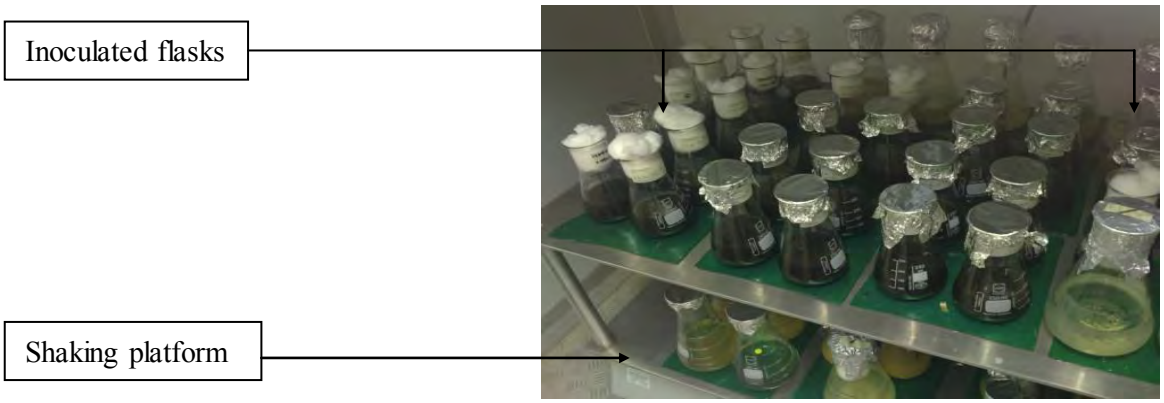

Figure 14: Microbial shake flask tests conducted in the 37 degree room at the Centre for Bioprocessing Engineering Research (CeBER) Unit at the Department of Chemical Engineering.

Redox potential, pH, ferrous iron and total iron in solution were all recorded at each sampling instance. After completion of the tests, the sample residue was retained for QEMSCAN analysis. Table 14 and Table 15 shows a matrix of all the draw and fill and batch experiments conducted respectively for each coal waste sample.

Table 14: Matrix indicating the draw and fill shake flask tests performed and the conditions applied to thereto

Sample	pH condition = 2	pH condition = 6
	Microbial conditions: Biotic	
	X= Performed	O = Not performed
-75µm	X	X
+75µm - 106µm	X	X
+106µm -180µm	X	X
+180µm - 212µm	X	X
+212µm - 355µm	X	X
Sample	**pH condition = 2**	**pH condition = 6**
	Microbial conditions: Abiotic	
	X= Performed	**O = Not performed**
-75µm	X	X
+75µm - 106µm	O	O
+106µm -180µm	O	O
+180µm - 212µm	O	O
+212µm - 355µm	X	X

Note: (1) X, denotes that the experiment was performed for the size fraction under the conditions indicated

(2) O, denotes that the experiment was not performed for the size fraction under the conditions indicated

Table 15: Matrix indicating the batch shake flask tests performed and the conditions applied thereto

Sample	pH condition = 2	pH condition = 6
	Microbial conditions: Biotic	
	X= Performed	O = Not performed
-75µm	X	X
+75µm - 106µm	O	O
+106µm -180µm	X	X
+180µm - 212µm	O	O
+212µm - 355µm	X	X
Sample	**pH condition = 2**	**pH condition = 6**
	Microbial conditions: Abiotic	
	X= Performed	**O = Not performed**
-75µm	X	X
+75µm - 106µm	O	O
+106µm -180µm	X	X
+180µm - 212µm	O	O
+212µm - 355µm	X	X

Analysis of dissolved iron (Fe) in solution

Ferrous iron (Fe^{2+}) and total iron (Fe) which had to be recorded for each sampling instance of the microbial shake flasks tests were determined using the 1-10 phenanthroline method (Komadel and Stucki, 1988). The analysis was conducted using the Helios α UV-Vis spectrophotometer at a wavelength of 510 nm and the solution concentration of each sample was calculated using a standard curve.

CHAPTER 4

CASE STUDY RESULTS

This chapter describes the results for the physical characteristics of the bulk coal samples and presents and discusses the results of each of the chemical, mineralogical and acid generating characterisation tests described in Chapter 3. A cross-comparison and detailed interpretation of the characterisation results is provided in Chapter 5.

4.1. Physical characterisation

The results of the particle size analysis are presented in Figure 15.

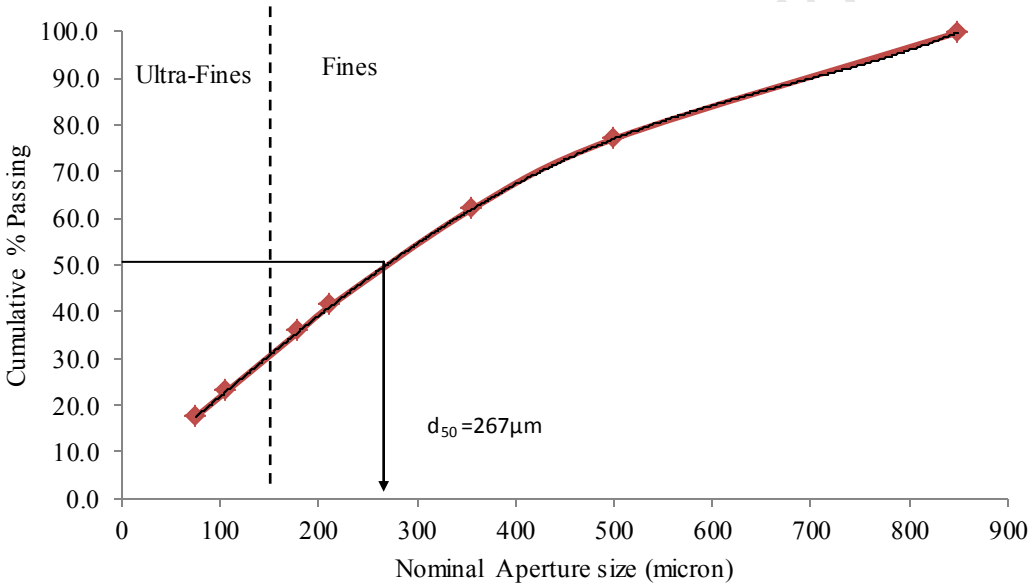

Figure 15: Particle size distribution (PSD) curve with d50 and size classification of particle

The coal tailings sample was classified and the top size was found to be < 1mm in size with a d50 of 267µm. It was determined that approximately 18 % of the bulk sample is in the ultra-fine range and 82% is classified as fine material according to the classification guidelines outlined by de Korte (2002).

4.2. Chemical characterisation

The chemical characterisation techniques discussed in Chapter 3 were applied to the bulk sample and the sized coal tailings samples. The results of the characterisation tests are provided in this section.

4.2.1. LECO™ total sulphur

Total sulphur characterisation was carried out by LECO™ analysis and the results thereof are presented in Table 16.

Table 16: Measured weight percentage of sulphur in coal tailings

Sample (μm)	Leco™ Total Sulphur (% weight coal)
Bulk	1.10 ± 0.03
- 75	2.08 ± 0.04
+ 75 – 106	1.62 ± 0.04
+ 106 – 180	1.07 ± 0.03
+ 180 – 212	1.01 ± 0.03
+ 212 – 355	1.03 ± 0.03

Note: standard uncertainties are in accordance with ALS Laboratory Group and Dept of Chemical Engineering UCT

The smallest size fraction analysed (-75μm) had the highest amount of total sulphur present and the sulphur content decreased with increasing particle size. The total sulphur for the bulk tailings sample was 1.10 % by weight, this corresponds with the sulphur range of inertinite rich thermal coal and vitrinite rich coking coal waste streams (Falcon and Ham, 1988; Koper, 2004; de Korte, 2007). DME (2001) reported that ultra-fine tailings typically report a total sulphur content of < 2 %, the results presented in Table 16 correlate with the DME findings.

4.2.2. Proximate analysis results

The proximate analysis conducted on the tailings samples included moisture, ash, volatile matter and fixed carbon assays and the results thereof are presented in Table 17.

Table 17: Proximate analysis results for the coal tailings sample, reported on an air-dried basis.

Analysis	Content (mass %)					
	Bulk	-75	+75 -106	+106 -180	+180 -212	+212 -355
Inherent Moisture	2.30 ± 0.00	3.30 ± 0.00	3.00 ± 0.00	2.70 ± 0.00	2.90 ± 0.00	2.61 ± 0.00
Ash	33.5 ± 0.67	44.1 ± 0.88	40.7 ± 0.81	33.3 ± 0.67	34.0 ± 0.68	33.3 ± 0.67
Volatiles	19.2 ± 0.04	17.6 ± 0.04	17.6 ± 0.04	18.9 ± 0.04	17.8 ± 0.04	18.6 ± 0.04
Fixed Carbon	45.0 ± 1.05	35.0 ± 1.51	38.7 ± 1.66	45.1 ± 1.05	45.3 ± 1.06	45.5 ± 1.06

Note: the standard uncertainty as reported in accordance with ALS Laboratory Group.

The fixed carbon matter, which essentially is the solid combustible material in coal after the determination of moisture and volatile matter, is greatest in the three largest size fractions. The higher deportment of ash to the finer fraction (-75μm and -75 + 106μm) is consistent with the

results reported by de Korte (2007). The formation of ash occurs as a result of chemical changes to the mineral matter of coal (mineral matter refers to the inorganic constituents such as silicate minerals, carbonate minerals, pyrite etc) by thermal conversion. Since ash is related to the inorganic composition of coal, the mineral matter content can be calculated using the Parr formula (Equation 15).

$$mm\% = 1.08A\% + 0.55S\%_{Total} \qquad \text{Equation (15)}$$

Where:

mm % is the mineral matter content by weight % (*%w/w*)

A% is the percentage ash of the sample

$S\%_{Total}$ is the percentage total sulphur of the sample (Leco S)

Figure 16 shows the presence of the various combustion products in the sized and bulk samples including the calculated mineral matter.

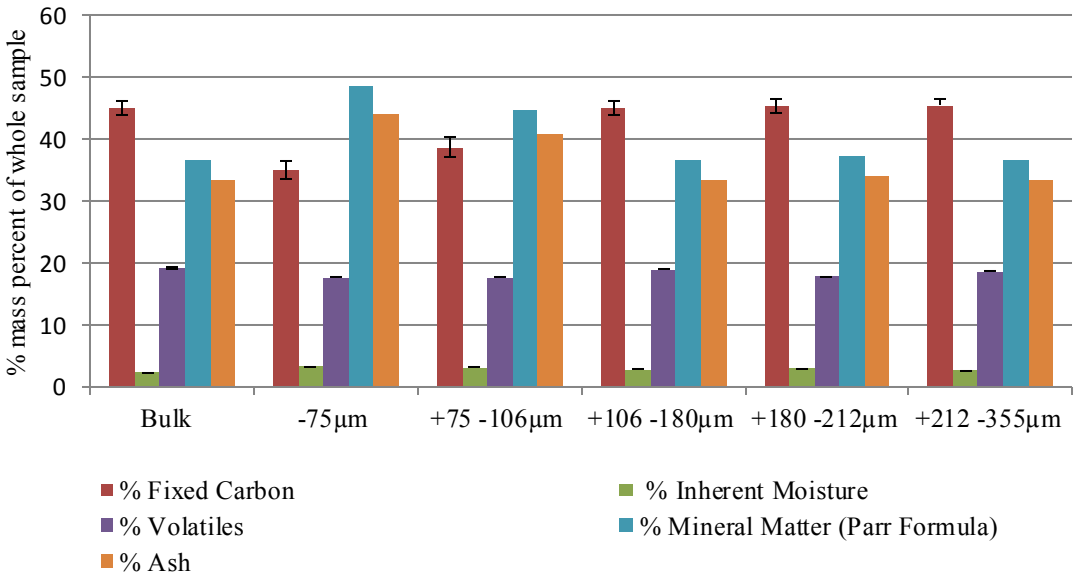

Figure 16: Graphic representation of proximate analysis results including the calculated mineral matter

The -75 µm size fraction contained the highest percentage mineral matter. The amount of volatile material was found to be largely consistent across the various size fractions (±18 %).

Table 18 shows a tabulated comparison between typical South African waste qualities reported in literature (DME, 2001) and the qualities determined by Leco S and proximate analysis for the bulk tailings sample

Table 18: Comparison of bulk tailings characteristics with those reported in the literature

Analysis	Reported values (DME, 2001)	Tailings sample(1)
Ash (%)	10 - 50	33.5
Sulphur (%)	< 2	1.10
Volatiles (%)	17 - 27	19.2
Fixed carbon (%)	41 - 56	45.0

Note: (1) Tailings sample, proximate analysis reported on an air-dry basis.

The results for the bulk tailings sample presented in Table 18 correlates with the quality of South African ultra-fine slurry, reported by the literature (DME, 2001).

4.2.3. ICP-OES elemental analysis results

ICP-OES was used to determine the total elemental analysis for commonly occurring inorganic elements. The elemental results of the ash samples are presented in Table 19.

Table 19: Total elemental analysis for the coal tailings size fractions (reported on a whole coal basis, air-dried basis).

		Content (mass %)					
Element		Bulk	-75µm	+75-106µm	+106-180µm	+180-212µm	+212-355µm
[Si]	± 0.78	8.52	10.88	9.97	9.33	9.42	9.41
[Al]	± 0.31	3.94	4.94	4.31	3.74	4.05	3.77
[Fe]	± 0.18	1.46	3.57	2.35	1.40	1.48	1.24
[Ca]	± 0.09	1.07	1.69	1.37	1.19	1.04	1.11
[K]	± 0.02	0.24	0.41	0.31	0.22	0.23	0.19
[Mg]	± 0.04	0.08	0.24	0.17	0.11	0.13	0.11
[P]	± 0.02	0.10	0.08	0.08	0.08	0.08	0.08

Note: The standard uncertainty associated with the each element is reported in accordance with ALS Laboratory Group.

The -106 µm size fractions have consistently higher inorganic element concentrations than the +106 µm size fractions. Furthermore, the elemental concentrations for the three largest size fractions (covering the size range +106-355 µm) are very similar whereas in the smaller size fractions (-106+ 75µm and -75 µm) there is significant variation in the concentrations of Si, Fe and Al as shown by the change in gradients for the curves in Figure 17.

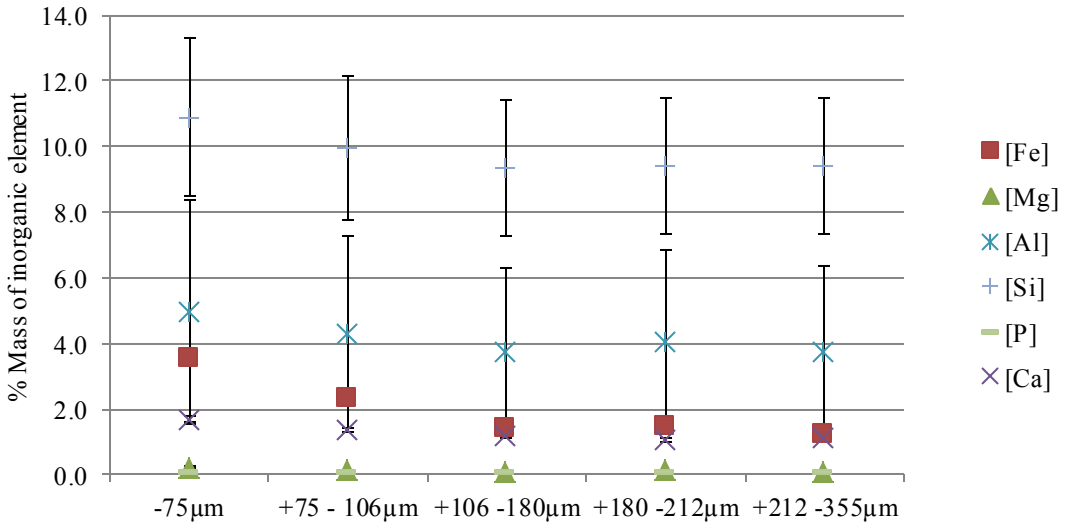

Figure 17: Variation in elemental concentrations across the size fractions coal waste samples

4.3. Mineralogical characterisation

The tailings size fractions and biokinetic leach residues (derived in accordance with the draw and fill method described in Section 3.5.4) were subjected to mineralogical characterisation.

4.3.1. Petrography results

The bulk sample was assessed petrographically according to three major fundamental and independent parameters: organic composition, rank and grade. The organic composition of the sample was inertinite rich and the total inertinite content was determined to be ±77 % on a volume, mineral-matter free basis. The sample contained less than 20 % vitrinite and only 47 % of the total macerals classified were found to be reactive. Approximately 11% of the organic phase was found to be severely disintegrated indicating some extent of weathering. However, 63 % of the bulk sample was classified as fresh coal which indicates that the extent of oxidation and weathering was not extensive.

According to the ISO 11760 – 2005 standard and the random reflectance measurements conducted on the sample, the sample was characterised as a Bituminous Medium Rank C coal. The measured standard deviation of the reflectance distribution showed a standard deviation of < 0.1, this is typical of a single seam non-blend coal sample. A detailed petrography assessment is presented in Appendix A.5.4.

4.3.2. QXRD analysis results

Given that one of the primary objectives of the case study was to examine how the mineralogy and particle size distribution of the tailings sample influences the potential for AMD formation in coal tailings, a QXRD investigation of the tailings size fractions was undertaken, the results of which are presented in Table 20.

Table 20: Mineralogical analysis by quantitative x-ray diffraction results for the coal tailings size fractions.

% of mineral phase						
Class (µm)	Quartz SiO_2	Kaolinite $Al_4Si_4O_{10}(OH)_2 \cdot H_2O$	Epsomite $MgSO_4 \cdot H_2O$	Gypsum $CaSO_4 \cdot H_2O$	Jarosite $KFe_3(OH)_6(SO_4)_2$	Pyrite FeS_2
- 75	34	52	2	8	< 1.0	3
+ 75 - 106	34	55	3	5	2	2
+ 106 - 180	38	54	< 1.0	3	2	3
+ 180 - 212	34	58	< 1.0	5	1	2
+ 212 - 355	35	58	< 1.0	3	2	2
% of whole coal						
- 75	17	29	< 1.0	1	< 1.0	< 1.0
+ 75 - 106	16	27	< 1.0	2	<1.0	<1.0
+ 106 - 180	13	22	< 1.0	2	<1.0	<1.0
+ 180 - 212	13	22	< 1.0	1	< 1.0	< 1.0
+ 212 - 355	13	22	< 1.0	1	<1.0	<1.0

Note: Results are reported on an air-dried basis
The Goodness of Fit (GOF) for the various size ranges are as follows: -75 µm = ±1.70, +75-106 µm = ±1.76, +106 -180 = ±1.86, +180-212 µm = ±1.81, +212- 55 = ±1.88

According to the results, the concentration of pyrite is higher in the three smaller size fractions (-75µm, +75 - 106µm and +106 - 180µm). Other sulphur bearing minerals included: epsomite ($MgSO_4.7H_2O$), gypsum ($CaSO_4$) and jarosite [$KFe_3(SO_4)_2(OH)_6$]. According to literature these sulphates are formed as secondary products in the weathering of pyrite. The majority of the secondary sulphates were concentrated in the finer fractions of the tailings sample (-75µm and +75 – 106µm). The higher sulphates content in the finer fraction corresponds with the higher concentration of pyrite. However, jarosite was found to have a slightly higher presence in the largest size fraction. It is also important to note that no acid neutralising minerals, such as calcite or dolomite, could be detected by QXRD. As discussed in Section 2.4.1 mineralogical analysis by QXRD is restricted by the detection limits of the technique (± 2 % of the mineral phase). It is for this reason that a comprehensive mineralogical account of both major and minor

mineral phases was conducted through a QEMSCAN analysis. These results of are reported in Section 4.3.3.

4.3.3. QEMSCAN analysis results

QEMSCAN analyses were conducted on the coal tailings sample, the residue from the acidic (pH 2) microbial shake flask tests and the circum-neutral (pH 6) microbial shake flask tests. The following section presents the modal results for the untreated coal samples.

Modal Report for untreated samples

The detailed modal results for the QEMSCAN assessments are presented in Appendix A.5.1 The condensed mineral report for the untreated samples has been tabulated in Table 21 and the proportions of minerals and coal in each size fraction are presented in Figure 18. The mineral constituents presented in Table 21 and Figure 18 are user defined and were chosen based on their relevance to the characterisation of the AMD potential in the samples, in accordance with the literature.

Table 21: Condensed QEMSCAN modal report on the untreated (size fractions) reported on a whole sample basis air-dried basis.

Mineral	Content (mass % of whole coal)				
	-75µm	+75-106µm	+106-180µm	+180-212µm	+212-355µm
Kaolinite $[Al_4Si_4O_{10}(OH)_2 \cdot H_2O]$	21.6	19.8	22.5	24.9	22.6
Quartz (SiO_2)	23.9	20.2	27.4	24.2	17.9
Pyrite (FeS_2)	4.4	6.8	7.9	6.9	2.6
Sulphate minerals (SO_4^{2-})(1)	1.6	2.1	0.7	0.5	0.1
Siderite ($FeCO_3$)	2.4	4.9	1.5	1.7	1.4
Calcite ($CaCO_3$)	7.0	6.3	6.7	5.5	2.2
Dolomite $[CaMg(CO_3)_2]$	1.2	1.1	0.7	0.8	0.5
Coal	37.9	38.4	32.4	35.5	52.6
Other	0.1	0.3	0.1	-	-
Mineral Matter (MM)(2)	62.1	61.6	67.6	64.5	47.4
Ash forming minerals(3)	44.5	44.0	48.7	46.7	28.7

Notes: (1) proportions of sulphates were calculated based on the normalised sulphate contributions from alunite $[KAl_3(SO_4)_2(OH)_6]$ and gypsum ($CaSO_4 \cdot H_2O$).

(2) mineral matter calculated according to PARR formula

(3) mass percentage of ash forming minerals was calculated on this basis of the amount of material remaining after combustion (Speight, 2005).

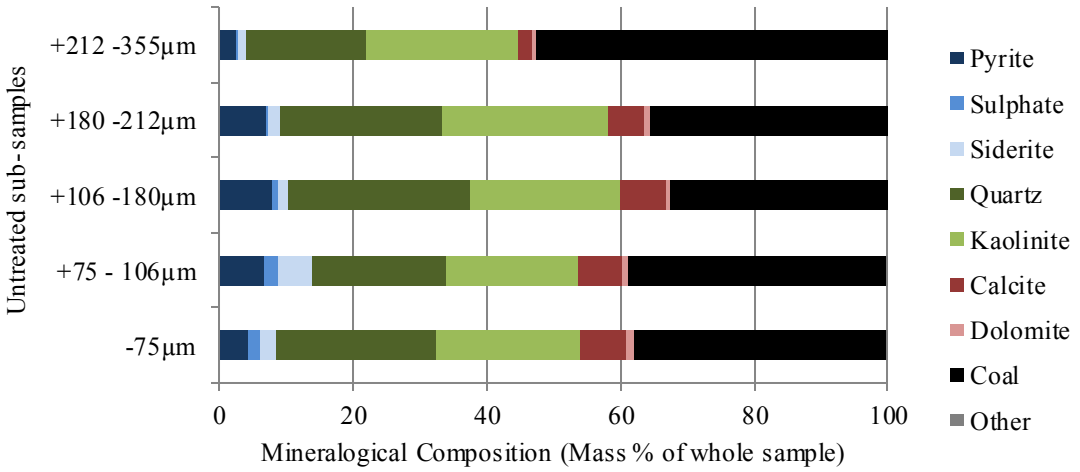

Figure 18: Condensed proportions of organic and inorganic constituents determined by the QEMSCAN modal report

The relatively inert minerals, quartz and kaolinte, contributed the highest proportion of mineral constituents of all the size fractions. Size fractions: +180 - 212µm and +160 - 180µm contained the highest concentrations of these two minerals in total. The QEMSCAN assessment identified calcite and dolomite, which were not detected by means of the QXRD analysis. The -75µm size fraction was found to contain the highest proportions of these carbonate minerals. Siderite was also exclusively identified using QEMSCAN and was shown to be concentrated in the mineral phase of the +75 - 106µm size fraction. The mineral group described as 'other' in Table 21 and Figure 18 refers to a combined suite of trace or minor minerals constituents. The QEMSCAN analysis found that the mineral phase of size fraction +106 – 180µm contained the highest proportion of pyrite (7.92%) and the lowest proportion was found to be contained in +212 - 355µm fraction (2.62%). The significant difference (86%) in pyrite content between QEMSCAN analysis for the +106 – 180µm size fraction and QXRD analysis points to possible segregation during sample preparation (Goodall and Scales, 2007).

Pyrite Liberation and Mineral Association

QEMSCAN enables a user to not only pre-define the minerals of interest to be reported on but also assess the extent of mineral liberation and mineral associations. As discussed in Section 2.4.1 mineral liberation is directly related to the amount of exposed reactive free surface area for oxidation. The extent of pyrite liberation is expressed as the exposed "free" surface area and has been defined according to the following categories: locked phase, which refers to 0-30% pyrite liberation, middlings phase, which refers to 30 – 80% pyrite liberation and liberated

phase, which refers to 80 – 100% liberation. The extent of liberation of the untreated size fractions is presented in Table 22.

Table 22: Mineral liberation report for pyrite in the untreated coal tailings sample

Sub sample	% Locked phase	% Middlings phase	% Liberated phase
-75µm	17.4	73.5	9.1
+75-106µm	17.6	74.3	8.1
+106-180µm	5.9	57.0	37.1
+180-212µm	7.3	64.6	28.1
+212-355µm	12.4	78.1	9.6

Note: The extent of surface area exposed (mineral liberation) was defined as follows: locked 0% to <=30%, middlings <=40% to <=80%, liberated >80%

According to Table 22, pyrite primarily occurs as in the middlings phase across the entire size range. The +106-180µm and +180-212 µm size fractions contained the greatest percentage of liberated pyrite (37.1% and 28.1% respectively) and the lowest percentage of locked pyrite (5.9% and 7.3% respectively).

Mineral-mineral associations were mapped out to provide an indication of the association of pyrite with other minerals. The primary focus thereof was to establish the extent to which inert (non-reactive) minerals and acid neutralising minerals are associated with pyrite in coal. The results of the mineralogy association report, generated on the basis of the extent of exposed mineral grain surface perimeter, have been summarised in Table 23.

Table 23: Mineral association report for pyrite in the coal tailings sample

	Extent of pyrite association (% of total)				
Sample	-75µm	+75 - 106µm	+106 - 180µm	+180 - 212µm	+212 - 355µm
Background[(1)]	26.4	33.98	26.0	24.0	7.8
Kaolinite $[Al_4Si_4O_{10}(OH)_2 \cdot H_2O]$	25.5	15.89	21.8	21.9	17.9
Quartz (SiO_2)	1.6	2.39	2.2	1.9	2.1
Sulphate minerals (SO_4^{2-})[(1)]	1.2	0.85	2.6	2.4	3.8
Siderite ($FeCO_3$)	1.7	5.86	1.0	1.8	1.4
Calcite ($CaCO_3$)	4.2	2.93	7.5	8.0	12.5
Dolomite $[CaMg(CO_3)_2]$	0.2	0.10	0.2	0.2	0.1
Coal	35.5	33.81	35.9	36.5	48.6
Other[(2)]	3.7	4.20	2.9	3.4	5.9

Notes: (1) "Background" refers to the % association of pyrite with the mounting carnauba wax (Section 3.4.2) used during sample preparation
(2) "other" refers to a combined suite of minerals constituents identified as either trace or minor

The perimeters of the pyrite grains contained in the coal tailings samples show greater association with coal than any other constituent. Translated this means that pyrite is strongly associated with the organic phase of coal structure. The perimeter association of pyrite with the background in each size fractions remained above 20% barring the largest sample (+255 - 355µm) which only registered a 7.8% association with the background. This means that of the total perimeter of pyrite available, at least 20% is exposed as 'free' surface on which oxidation reactions can potentially take place. Pyrite is more strongly associated with the relatively inert mineral of kaolinite than the acid neutralising minerals of dolomite and calcite.

4.4. Sulphur speciation results

Sulphur speciation was conducted by two chemical characterisation methods namely the ISO 157 and the ACARP method. The results of both characterisation techniques are reported and compared within this section.

4.4.1. Sulphur forms – ISO 157

The ISO 157 method was used to determine the pyrite and sulphate sulphur components of the samples. The organic sulphur component was calculated by way of the difference between the total sulphur (measured through Leco S analysis) and the components determined through the ISO 157 method. Table 24 shows the distribution of the various sulphur forms in the sized tailings samples.

Table 24: ISO 157 sulphur speciation results for the size fractions

	Concentration of sulphur forms (mass %)		
Sample	Pyritic S	Sulphate S	Organic S (By difference)
- 75µm	1.05 ± 0.05	0.52 ± 0.01	0.51 ± 0.06
+ 75- 106µm	0.86 ± 0.04	0.29 ± 0.01	0.33 ± 0.05
+ 106- 180µm	0.72 ± 0.04	0.11 ± 0.00	0.24 ± 0.04
+180- 212µm	0.67 ± 0.03	0.09 ± 0.00	0.25 ± 0.04
+212- 355µm	0.64 ± 0.03	0.05 ± 0.00	0.34 ± 0.03

Note: The standard uncertainty is reported in accordance with ALS Laboratory Group.

As discussed in Section 4.2.1, the sulphur content of the size fractions is highest in the smallest size fractions and is seen to decrease toward the larger fractions. Pyritic sulphur and sulphate sulphur exhibit a similar trend as total sulphur, with 1.05 ± 0.05% pyritic sulphur in the -75 µm sample and only 0.64 ±0.03 % in the +212 -355µm sample. The samples were found to contain more organic sulphur than sulphate sulphur, barring the -75 µm size fraction which contained

equal amounts of organic and sulphate sulphur (organic S 0.51 ±0.06 %, sulphate S 0.52 ±0.01 %). Table 25 presents the distribution of the sulphur forms as a percentage of total sulphur in each size fraction.

Table 25: Distribution of sulphur forms in accordance with ISO157 speciation results

Sample (micron)	Relative distribution of sulphur forms (% of total)		
	Pyrite	Sulphate	Organic S
- 75µm	50.48 ± 2.7	25.00 ± 0.26	24.52 ± 0.89
+ 75 - 106µm	58.11 ± 1.8	19.59 ± 0.00	22.30 ± 0.25
+ 106 - 180µm	67.29 ± 2.4	10.28 ± 0.02	22.43 ± 0.38
+180 - 212µm	66.34 ± 2.2	8.91 ± 0.02	24.75 ± 0.43
+212 - 355µm	62.14 ± 2.0	4.85 ± 0.005	33.01 ± 0.79

According to Table 25, pyritic sulphur accounts for over 50% of the total amount of sulphur contained in each sample. Organic sulphur represents up to 33% of the total sulphur and sulphate sulphur contributed to the remainder (4.85 ±.0.00%, 25.00 ±0.25%). The ISO 157 method determined that sulphate sulphur provided the least contribution of sulphur to the total sulphur content in each size fraction. The proportion of sulphate sulphur (contained within the mineral phase) is seen to decrease toward the larger size fractions

4.4.2. Sulphur forms – ACARP

The ACARP method was used to determine the following sulphur forms: pyritic, organic, acid forming sulphate sulphur and non-acid forming sulphate sulphur. Pyritic and sulphate sulphurs were determined by CRS extraction and KCl extraction respectively. Each test was conducted in duplicate for all size fractions tested. Low risk sulphur which mainly consists of organic sulphur but may contain traces of elemental sulphur and some jarosite was calculated as the difference between the empirically determined species and the total sulphur (LECO™). The various chemical methods described in Section 3.5.2 were used to produce the results presented in Table 26 and Figure 19.

Table 26: Sulphur forms characterised according to ACARP sulphur speciation method for the untreated size fractions

Size fraction	Concentration of sulphur forms (mass %)							
	Pyritic sulphur		Acid sulphates[2]		Non-acid sulphates[3]		Low risk sulphur (Diff)[4]	
- 75µm	0.96	± 0.29[1]	0.00	±0.00	0.71	± 0.11	0.41	± 0.40
+ 75-106µm	0.79	± 0.31	0.00	±0.00	0.45	± 0.11	0.38	± 0.42
+ 106-180µm	0.80	± 0.34	0.00	±0.00	0.25	± 0.10	0.02	± 0.44
+180-212µm	0.10	± 0.02	0.00	±0.00	0.18	± 0.06	0.73	± 0.08
+212-355µm	0.11	± 0.00	0.00	±0.00	0.12	± 0.17	0.80	± 0.17

Note: (1) Error is indicated by the standard deviation, where n = 2.
(2) Potential acid sulphate minerals - Melanterite ($FeSO_4 \cdot 7H_2O$), roemerite [$FeSO_4 \cdot Fe_2(SO4)^3 \cdot 12H_2O$], alunite [$KAl_3(SO_4)_2(OH)_6$]
(3) Potential non-acid sulphates - Gypsum ($CaSO_4 \cdot H_2O$)
(4) Potential low risk sulphur – organic sulphur and elemental sulphur (S^0) and jarosite

According to the ACARP method, pyritic sulphur and the non-acid sulphate species are concentrated in the smaller size fractions (-75µm, +75 - 106µm, +106 - 180µm). The inverse trend was observed for the low risk sulphur component (composed of organic sulphur and jarosite). Koper (2004) reported that the concentration of low risk sulphur forms generally changes with respect to significant changes in ash content. Based on the proximate analysis results for ash content (Table 17), the results for the ACARP low risk sulphur tests are not immediately understood. According to the ACARP method none of the size fractions contained any measurable acid forming sulphate species. Figure 19 outlines the proportional contribution of the various sulphur forms to the total sulphur content as a percentage (%).

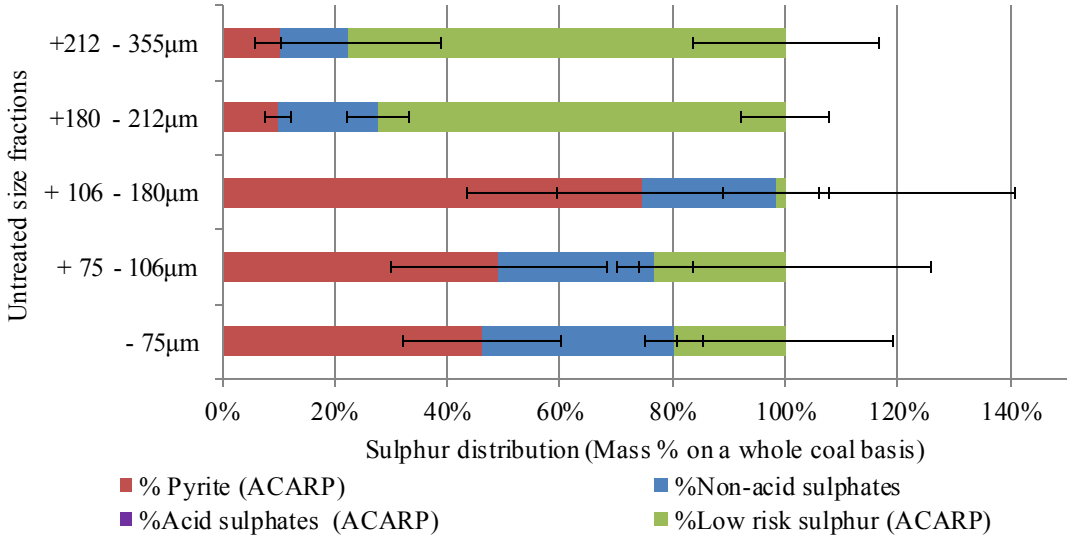

Figure 19: Sulphur distribution in the untreated size fractions in accordance with the ACARP method

The standard deviations indicated in Table 26 and shown in Figure 19 are relatively high, accounting for an uncertainty in excess of ± 30% in the measured amounts of pyritic sulphur and sulphate sulphur for some of size fractions (-75µm, +75 - 106, +106 - 180µm). The effect of this seems to render the calculated value for the low risk sulphur content as highly uncertain given that the percentage error is far higher than the calculated amount. The poor reproducibly may be due to the heterogeneity of the sample which is aggravated by the small amounts of sample used (< 1g). The concentrations of pyrite of both sulphur speciation methods display a decreasing trend toward the coarser fractions this is in contrast to the QEMSCAN results which displays a more bell shaped trend. In addition, the QEMSCAN results for pyrite show a bias in concentration across all the size fractions when compared to the pyrite concentrations in sulphur speciation results. This difference is trend and concentration may be as a result of insufficient sample preparation for the QEMSCAN samples.

Furthermore, the very low pyritic sulphur results in the larger particle size ranges indicates that the method may not be suited to deal with samples which are not pulverised. Literature, (Sullivan *et al*, 2002; Ahern *et al*, 2004) indicates that samples for acid sulphate soil analysis be finely ground to ensure homogeneity as well as optimum recovery of pyrite from the chromium reducible sulphur method. McElnea *et al*. (2002) have also stressed the necessity to adjust sample size in accordance with the expected pyritic sulphur content, to ensure reproducibility and accuracy of results.

4.5. AMD prediction tests

Static and kinetic tests were used to formulate a prediction of the AMD potential for the samples. The static tests selected for the investigations included: acid base accounting (ABA), net acid generation (NAG) tests and sequential NAG tests. Microbial shake flask tests provided kinetic data for the response of the samples to a bioleaching environment. This section presents the results for the assessment of the AMD potential for the tailings samples based on the tests discussed and the mineralogy presented in Sections 4.2 – 4.4.

4.5.1. Acid base accounting (ABA)

Maximum acid producing potential (MPA)

ABA tests were conducted across all the sized coal tailings samples. A MPA value was determined for the total sulphur values of each sample. MPAs were also calculated for the pyritic sulphur content measured by the various mineralogical and chemical characterisation techniques. Detailed data is provided in Appendix A.4.3 and selected results are presented in

Table 27. The MPA for each size fraction was calculated according to Equation (2) in Section 2.5. In the case of the calculation of MPA from mineralogical data, the pyritic S content of pyrite was calculated as 53.45 % by mass.

Table 27: MPA results in kg H_2SO_4/tonne, attributed to pyritic sulphur and total sulphur.

Size fractions (µm)	Total S (LECO)	Pyritic S^{2-} (QXRD)	Pyritic S^{2-} (QEMSCAN)	Pyritic S^{2-} (ISO)	Pyritic S^{2-} (CRS)
-75	63.65 ± 1.27*	24.47 ± 0.98†	71.90 ± -	32.13 ± 0.86*	29.35 ± 8.86*
+75-106	49.57 ± 0.99	22.51 ± 0.23	111.11 ± -	14.06 ± 0.70	24.31 ± 9.51
+106-180	32.74 ± 0.01	18.34 ± 0.37	129.09 ± -	22.03 ± 0.59	24.44 ± 10.25
+180-212	30.91 ± 0.01	18.71 ± 0.19	112.75 ± -	20.50 ± 0.55	3.05 ± 0.71
+ 212-355	31.52 ± 0.01	18.33 ± 0.37	42.49 ± -	19.58 ± 0.52	3.27 ± 0.00

Note: * denotes the standard error, where n = 2.
† denotes the "Goodness of Fit" GOF
‡ MPA values were calculated excluding size fractions + 180 - 212µm and + 212 - 355µm.

The results indicate that MPA calculated from the total sulphur content is significantly higher than the MPA calculated on the basis of pyritic sulphur. According to Smart *et al*. (2002), the standard MPA calculation tends to overestimate the potential for acid generation as it assumes that all the sulphur is present as acid forming species. As indicated by the sulphur speciation results, significant quantities of the sulphur in coal are present in forms which have a low (jarosite) to negligible (organic S) acid generating capacity.

Examination of the data shows that the smallest size fraction (-75µm) in each of the techniques represented the highest potential for acid formation (QXRD = 24.47 kg H_2SO_4/tonne ±0.98, ISO = 32.13 kg H_2SO_4/tonne ±0.86 kg H_2SO_4/tonne, CRS = 29.35 kg H_2SO_4/tonne ±8.86 kg H_2SO_4/tonne). The reasons for the high propensity of acid generation in the finer fractions of the tailings sample are not clear. Devasahayam (2007) points out this may be attributed to the correlation between the particle breakdown and the rate of oxidation of sulphide within the finer size range. However, the extent of mineral liberation and the availability of liberated pyrite may also play a role in this trend. MPA values for the two largest size fraction (+ 180 - 212µm and +212 - 355µm) indicate clear outliers, with the MPA values calculated on the basis of the CRS sulphide sulphur method being significantly lower than the other values. As discussed in the previous sub-section, the CRS method gave relatively low sulphide sulphur values for the coarser particle size fractions, which were not pulverised prior to analysis.

Acid Neutralising Potential (ANC)

Tests to determine the acid neutralizing capacity (ANC) of each of the untreated size fractions were conducted in duplicate. Table 28 shows the results for the Skousen method with siderite correction according to the procedure outlined in Section 3.5.1.

Table 28: ANC results for the untreated size fractions

Size fractions	ANC (kg H_2SO_4 / tonne)
- 75µm	31.90 ± 0.25
+ 75 - 106µm	27.69 ± 0.58
+ 106 - 180µm	29.81 ± 0.04
+180 - 212µm	31.47 ± 2.58
+212 - 355µm	28.21 ± 2.95

Note: Error is indicated by the standard deviation, where n = 2.

The acid neutralising capacity across all the size fractions was determined to be generally uniform. However, the standard error for the two larger size fractions (+212 - 355µm, +180 - 212µm) was higher than the smaller size fractions. As discussed previously sample size and particle size distribution may affect the relative availability of acid generating and acid neutralising components in a sample (Stewart *et al*., 2009). Furthermore, the homogeneity of samples in the larger size range may also impact on the accuracy of results.

Classification

The net acid producing potential (NAPP) was determined from the MPA and ANC results in accordance with Equation (3) Section 2.5.1.

$NAPP = MPA - ANC$ (kg H_2SO_4/tonne) Equation (3) - Section 2.5.1

Table 29 shows results for the standard NAPP values determined according to Equation (3) using the ANC results from Table 29 and the MPA results in Table 27. Table 29 also shows the non-standard NAPP referred to as the average combined sulphide NAPP where the MPA has been calculated according to the average combined presence of pyritic sulphur as determined through the ISO 157, ACARP and QXRD methods.

Table 29: Acid base accounting results for the standard NAPP calculation and the combined average calculation based on the average pyritic sulphur content across the CRS, ISO and QXRD characterisation techniques.

Sample (μm)	Standard NAPP (kg H_2SO_4/tonne)(1)	Classification	Average combined S^{2-} NAPP (kg H_2SO_4/tonne)(2)	Classification
- 75	31.75 ± 1.03(3)	Acid forming	-3.25 ± 3.32	Potentially acid forming
+ 75 - 106	21.88 ± 0.41	Acid forming	-3.32 ± 2.90	Potentially acid forming
+ 106 - 180	2.93 ± 0.03	Potentially acid forming	-8.21 ± 3.70	Potentially acid forming
+ 180 - 212	-0.57 ± 2.57	Potential acid forming	-17.39 - 2.09	Potentially acid forming
+ 212 - 355	3.31 ± 2.93	Potentially acid forming	-14.48 - 2.66	Potentially acid forming

Note: (1) Standard NAPP calculations conducted using LECO (S) total sulphur value to calculate MPA
(2) Average combined NAPP calculations conducted using the average combined value of pyritic sulphur determined from the CRS method, ISO 157 standard and QXRD to calculate the MPA
(3) Error is indicated by the standard deviation, where n = 2.

The classification guide described in Table 8, Section 2.5.1.1 was used to qualify the acid generating potential based on the NAPP outcomes in Table 29. All the size fractions possess some degree of acid formation. The standard NAPP values for the two smaller size fractions (-75μm and +75 - 106μm) were found to be acid forming and the three larger size fractions were classified as potentially acid forming. Even though the NAPP values calculated on the basis of sulphide sulphur were lower than those calculated on the basis of total sulphur (standard NAPP), the average combined sulphide samples were still classified as potentially acid forming (PAF) in accordance with ABA test method.

4.5.2. Net acid generating (NAG) tests

NAG tests were conducted to improve the prediction of AMD by examining the accelerated chemical oxidation of pyrite and other possible sulphide minerals. Single addition NAG test were conducted to provide a preliminary AMD classification and sequential NAG tests were carried out to enhance the prediction results by ensuring all sulphide minerals were oxidised during the tests. Detailed results are presented in Appendix A.4.3 and a summary is provided in this Section.

Single addition NAG pH tests

The results of the single addition NAG tests are presented in Table 30. The results provide a preliminary AMD classification for the coal tailings samples. The AMD classification guidelines indicated in Table 9, Section 2.5.1.3 were used for the classification of the acid potential.

Table 30: Single addition NAG pH tests for the coal tailings samples

Sample (µm)	After-boil NAG pH	$NAG_{pH4.5}$ (kg H_2SO_4/t)	NAG_{pH7} (kg H_2SO_4/t)	Class
-75	2.50 ±0.02(1)	29.01 ±0.39	43.32 ±13.72	Potentially acid forming
+75-106(2)	2.89 ±0.00	20.97 ±0.00	26.66 ±0.00	Potentially acid forming
+106-180	2.84 ±0.00	21.36 ±0.98	30.58 ±0.78	Potentially acid forming
+180-212	3.00 ±0.12	18.42 ±3.92	39.69 ±9.70	Potentially acid forming
+212-355	2.97 ±0.05	18.23 ±1.37	32.54 ±8.23	Potentially acid forming

Note: (1) Error is indicated by the standard deviation, where n = 2.
(2) Single addition NAG test was not performed in duplicate.

According to the classification criteria for NAG testing (Section 2.5.1.2) the tailings samples were classified as potentially acid forming (PAF). Each size fraction indicated a positive value for the equivalent mass of sulphuric generated at both pH 4.5 and 7. The NAG values obtained by titrating to a pH value of 7 (NAG_{pH7}) were significantly higher than those obtained by titrating to pH 4.5 ($NAG_{pH4.5}$). In the case of base metal sulphide ores, these differences have been attributed to the hydrolysis and precipitation of divalent metal ions (e.g. Cu, Zn, Ni) in the pH range 4.5-7 (Stewart *et al*., 2009). Negligible amounts of divalent metal ions are, however, expected to be present in the case of coal. Although no attempt was made to positively identify those species in the NAG solutions consuming alkali in the pH range 4-7, it is possible that this effect may be reflective of organic acid generation through the reaction of peroxide (H_2O_2) with the organic phase in the samples (See discussions in Section 2.5.1.2, Chapter 2).

Sequential NAG pH tests

Sequential NAG testing were conducted for the untreated tailings samples. The experimental steps for the single addition NAG tests were repeated until an after-boil NAG pH greater than 4.5 was noted. Table 31 presents the results of the three stage sequential tests conducted for the untreated size fractions.

Table 31: Sequential NAG results for the untreated size fractions

		Size fractions (µm)				
		-75	+75-106 (2)	+106-180	+180-212	+212-355
Stage 1	NAGpH	2.50 ± 0.02(1)	2.89 ± -	2.83 ± 0.01	3.00 ± 0.12	2.97 ± 0.04
	$NAGpH_{4.5}$(3)	29.0 ± 0.39	21.0 ± -	21.4 ± 0.98	18.3 ± 3.82	18.2 ± 1.37
	$NAGpH_{7.0}$(4)	43.3 ± 13.7	26.7 ± -	30.6 ± 1.76	39.7 ± 9.70	32.5 ± 8.23
Stage 2	NAGpH	2.68 ± 0.01	3.18 ± -	2.74 ± 0.01	2.74 ± 0.01	2.73 ± 0.00
	$NAGpH_{4.5}$(3)	51.9 ± 2.47	69.1 ± -	58.1 ± 1.88	61.4 ± 4.49	62.0 ± 3.63
	$NAGpH_{7.0}$(4)	89.3 ± 4.70	109.2 ± -	97.8 ± 2.28	104.4 ± 10.2	102.2 ± 4.16
Stage 3	NAGpH	5.51 ± 0.21	4.80 ± -	5.04 ± 0.07	4.68 ± 0.08	4.76 ± 0.00
	$NAGpH_{4.5}$(n.d)					
	$NAGpH_{7.0}$(n.d)					

Note: (1) Error is indicated by the standard deviation, where n = 2.
(2) The +75 – 106µm was not performed in duplicate, where the standard deviation could not be determined
(3) $NAGpH_{4.5}$ reflective of the cumulative mass of H_2SO_4 generated per unit tonne (H_2SO_4/tonne) at pH 4.5
(4) $NAGpH_7$ reflective of the cumulative mass of H_2SO_4 generated per unit tonne (H_2SO_4/tonne) at pH 7

According to the results shown in Table 31, the majority of acid generation occurred in stage 2, with the NAG_{pH7} values increasing to a greater extent than those of $NAG_{pH4.5}$ .These results indicate that the formation of acid during the single stage NAG tests was " incomplete". The increases in the NAG values during the second stage are, however, unlikely to be attributed to an increase in the extent of pyrite oxidation, as the sulphide sulphur content is <1% in all size fractions (Smart *et al.*, 2002). Rather, these increases can probably be attributed to the reaction of hydrogen peroxide with carbonaceous matter. As discussed in Chapter 2 (Section 2.5.1.2), the formation of organic acids due to the partial oxidation of carbonaceous materials by hydrogen peroxide can lead to high NAG values during both single and sequential NAG tests that are unrelated to acid formation from sulphides (Stewart *et al.*, 2009).

4.6. Kinetic AMD prediction results

The objective of conducting biokinetic AMD prediction tests was to enhance the prediction of AMD by examining the relative geochemical dissolution rates of the acid producing and acid neutralising minerals in the tailings samples, under conditions of microbial activity. Two testing scenarios were conducted, a batch testing procedure and a draw and fill (semi-continuous) procedure. The results of these kinetic tests are described and reported within this section and all detailed results are presented in Appendix A.6. The microbial shake flask tests were conducted according to the detailed methodologies provided in Appendix A.4.1.

4.6.1. Draw and fill microbial shake flask tests

Draw and fill microbial shake flask tests were carried out under two conditions to simulate two different scenarios. A circum-neutral fed environment was simulated by using an autotrophic basalt solution (media) at pH 6 and an acid fed environment was simulated using ABS at pH 2. The draw and fill method works on the principle of a simulated semi-continuous process where 90% of the supernatant is removed on a regular basis.

Acid fed environment

In this scenario, the samples were inoculated with a biokinetic culture (pH 1.87) and an autotrophic basal salt (ABS) solution at pH 2.0 was added as media. In order to isolate and examine the geochemical reactivity of the samples, abiotic flasks were prepared for two of the size fractions -75µm and +212 - 355µm. Abiotic flasks were prepared similar to the biotic (inoculated) flask however, the biokinetic culture was not introduced into these flasks. Furthermore, the abiotic experiments were conducted for 74 days and pH measurements were taken during the course of this period. The biotic experiments were conducted for 87 days during which pH, redox potential and ferrous and total iron measurements were taken

Results are shown for the variation in pH (Figure 20) for both abiotic and biotic conditions. The results for redox potential (Figure 21) and ferric iron generation (Figure 22) over a time period of 87 days have also been presented. The figures have been divided into 3 regions I to III, denoting the draw and fill regime undertaken in each region.

I. Draw and fill every 2-3 days

II. Draw and fill every 7-8 days

III. Draw and fill every 14 days

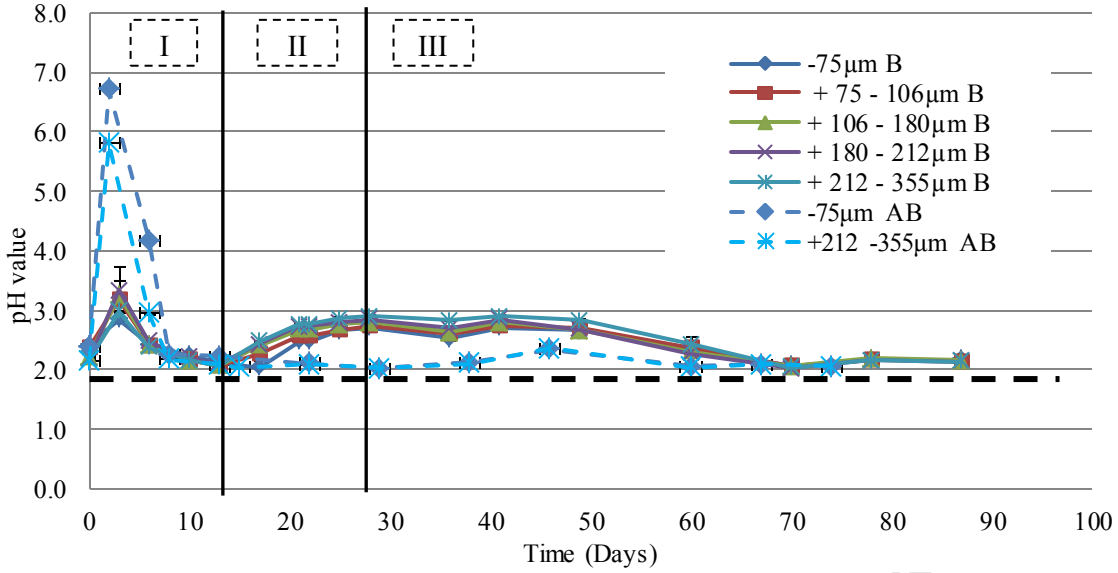

Figure 20: pH as a function of time for size fractions, where "B" is an indication that the tests were conducted under biotic conditions and "AB" indicates abiotic conditions. The dotted line indicates the pH of the fresh ABS solution at each draw and fill instance.

Initially an increase in pH is seen across all the flasks which can be attributed to the leaching of readily soluble acid neutralising carbonate minerals. Under abiotic conditions the pH levels increase in excess of pH 5, whereas the biotic samples experience an increase to approximately pH 3. Drawing out the supernatant liquor containing the solubilised acid neutralising minerals resulted in the steady decrease of the pH in the biotic and abiotic samples after day 3. However, the samples remained net acid neutralising until day 10. The abiotic samples were observed to stabilise in Region II and continued to present very little change in pH activity in Region III. This is indicative of the acid neutralising reactions and acid generating reactions occurring at the same rate and to the same extent. For the biotic samples the pH was observed to increase steadily above pH 2.5 in Region II and III. This indicates that the continued addition of acid enhances the neutralising capacity to a point where it is proceeding to a greater extent than acid formation due to pyrite oxidation. Possible acid neutralising reactions which may be occurring under these conditions include: the re-dissolution of ferric hydroxide (formed in region I), the dissolution of siderite (according to Reaction 8b), and/or the dissolution of kaolinite, according to reaction (9).

$$FeCO_3 + \frac{1}{4}O_2 + 3H^+ \Leftrightarrow Fe^{3+} + H_2CO_3 + \frac{1}{2}H_2O \qquad \text{Reaction (8b)}$$

$$Al_4Si_4O_{10}(OH)_6H_2O + 10H^+ \Leftrightarrow 4H_4SiO_4 + 4Al^{3+} + H_2O \qquad \text{Reaction (9)}$$

After 70 days of leaching the pH levels in the inoculated samples progressively stabilised owing to the kinetic rates of acid neutralisation and production occurring simultaneously and/or occurring to the same extent.

Figure 21 and Figure 22 show the variation in redox potential and ferric iron concentration over the time course of 87 days. The figures are sub-divided into regions I, II and III, indicating the draw and fill regime.

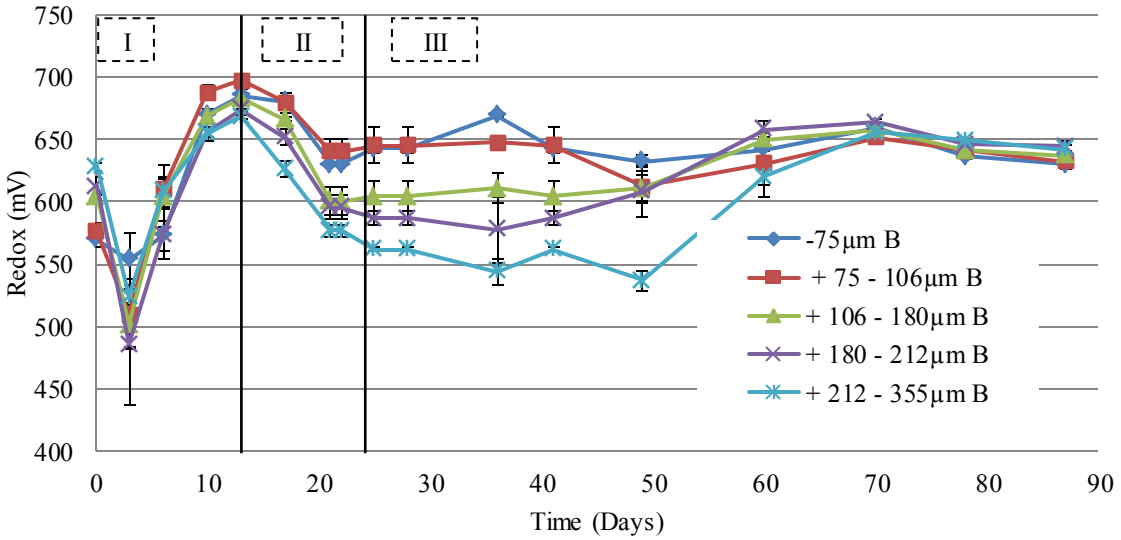

Figure 21: Redox potential measured against an Ag/AgCl electrode as a function of time where "B" is an indication that the tests were conducted under biotic conditions. Errors are shown as standard deviation where n=3.

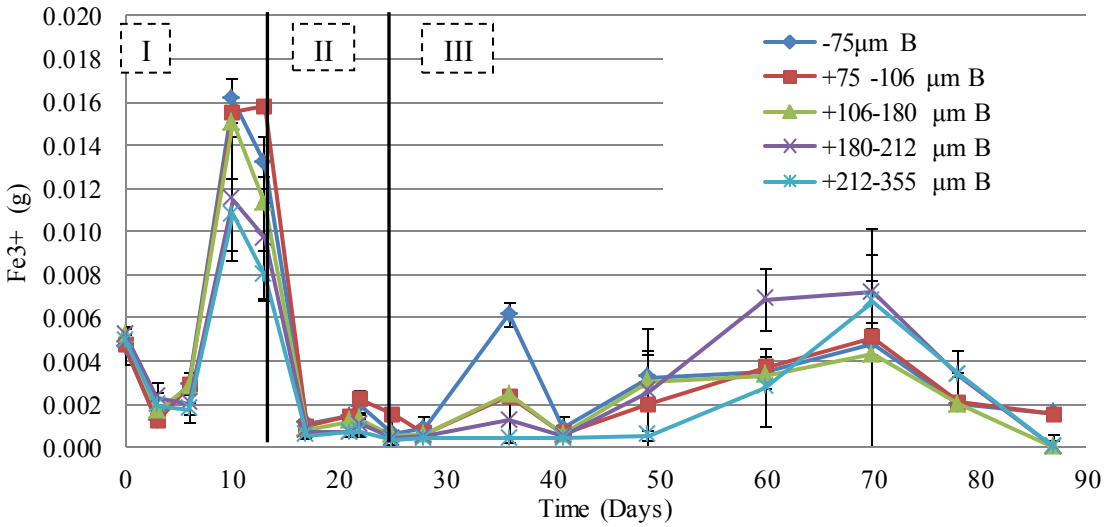

Figure 22: Ferric iron generation in the pH 2 systems as a function of time, where "B" is an indication that the tests were conducted under biotic conditions. Error denote the standard deviation where n = 3.

Initially the redox potentials and ferric iron (Fe^{3+}) generation indicate a rapid decrease across all the size fractions owing to the leaching of readily soluble acid neutralising minerals under the

acidic conditions. This observation is consistent with the rapid increase in the pH values in Figure 20 for the first 3 days of testing.

After approximately 13 days of testing the redox potential increased above 650mV in all the size fractions. This was consistent with the increase in the ferric ions (Fe3+) generated at 13 days (Figure 22). Redox potentials in the region of ±650mV (observed at 13 days) are generally considered an indication of microbial activity therefore it can be assumed that the onset of microbial activity occurred during this time period. The Fe^{3+} concentrations followed the same trends as those of pH indicating that the Fe^{3+} concentrations were controlled by the precipitation of ferric oxyhydroxides or jarosite ($KFe_3(OH)_6(SO_4)_2$). Trends in terms of redox potential and ferric concentrations are consistent with the time-related changes in pH, with the redox potentials and ferric concentrations increasing as the pH decreases.

Circum-neutral fed environment

A second scenario of draw and fill tests aimed to assess the reactivity of the tailings samples in a non-pH controlled circum-neutral fed environment. As with the acid fed environment, the samples were inoculated with the same biokinetic culture (pH 1.87) and an ABS solution at pH 6.0 was added as media. Results are shown for the variation in pH (Figure 23) and redox potential (Figure 24) over a time period of 87 days. The figures have been divided into 3 regions I to III in accordance with the draw and fill regime discussed for the acid fed environment.

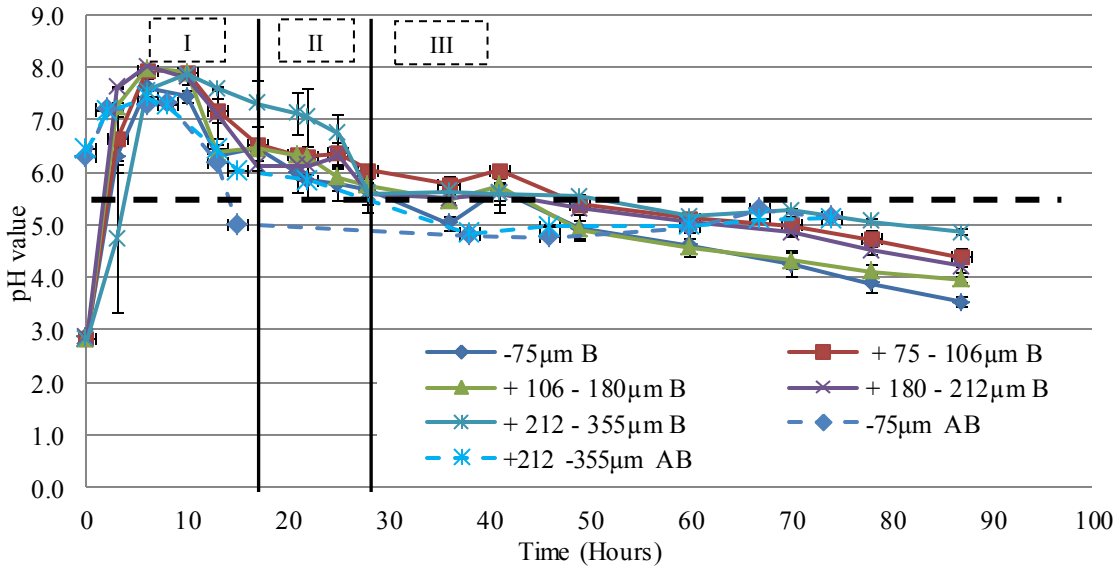

Figure 23: pH as a function of time for size fractions, where "B" is an indication that the tests were conducted under biotic conditions and "AB" an indication of abiotic conditions. The dotted line indicates the pH of the fresh ABS solution at each draw and fill in indicates the pH of the fresh ABS solution at each draw and fill instance. Errors are shown as a standard deviation where n=3.

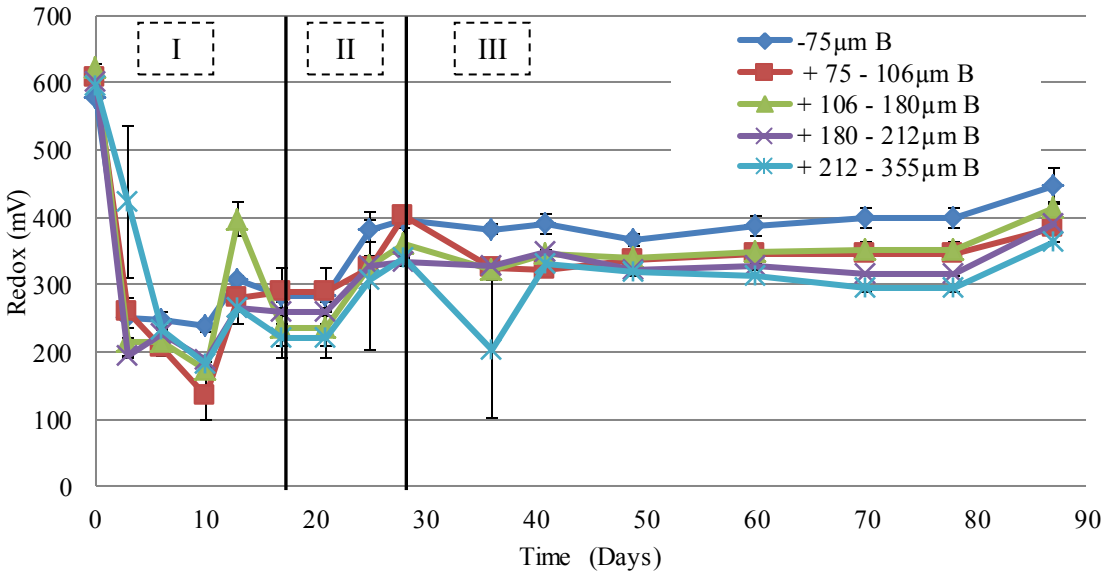

Figure 24: Redox potential measured against an Ag/AgCl electrode as a function of time in a circum-neutral environment where "B" is an indication that the tests were conducted under biotic conditions . Errors are shown as standard deviation where n=3.

The high redox potentials (> 550mV) and low pH values (< 3.0) measured on day 0 are primarily attributed to the initial inoculation of the flasks with the biokinetic culture with redox potentials of 710mV and a pH of 1.87. From day 0 to day 10 (Region I) the pH is observed to increase rapidly to pH 8. This is indicative of readily soluble acid neutralising minerals leaching into solution as a result of the slightly acidic conditions (pH 3) at the start of the tests (day 0). The redox potential for the same time frame (0 – 10 days) shows rapidly decreasing values which correlate with the pH trends observed. After 10 days of testing, an increase in the redox potentials (Figure 24) and a decrease in the pH level (Figure 23) was seen across all the samples. The samples appeared to be initially net acid neutralising. However, the neutralising capacity relative to the acid forming capacity appeared to decrease rapidly after the first 10 days, with all the samples becoming net acid generating after 40 days. Trends indicate that longer time periods would have resulted in a further decline in pH and increase in redox potential. The net acid generating behaviour under circum-neutral pH conditions is unexpected, as such conditions are generally not considered to be optimal for pyrite oxidising strains of bacteria

Figure 25 shows the ferric iron concentration over the time course of 87 days for the circum-neutral tests.

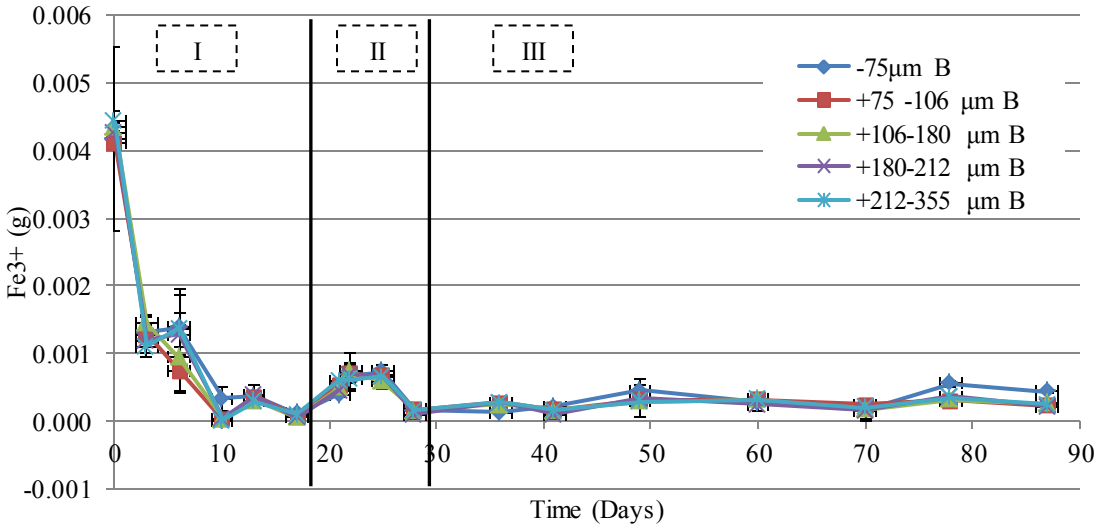

Figure 25: Ferric iron generation in the pH 6 systems as a function of time, where "B" is an indication that the tests were conducted under biotic conditions. Error denote the standard deviation where n = 3.

The initial Fe^{3+} concentration of 0.004g can be attributed to the presence of micro-organisms from the 7.5mL of inoculums used at the start of the bioleaching process. The rapid decrease in Fe^{3+} is further indicative of the rapid formation of ferric oxyhydroxides at the pH values of the test solutions indicated in Figure 23.

Modal Report for residues for the draw and fill biokinetic tests

The bioleach residues from the acid fed and circum-neutral fed bioleach tests were reserved for QEMSCAN analysis, the condensed mineral report of these have been tabulated in Table 32 and Table 33 respectively.

Table 32: Condensed QEMSCAN modal report on the pH 2 (bioleach) sub-samples reported on a whole sample basis.

	Content (mass % of whole coal)				
Mineral	-75µm	+75 - 106µm	+106 -180µm	+180 -212µm	+212 -355µm
Kaolinite [$Al_4Si_4O_{10}(OH)_2 \cdot H_2O$]	23.8	22.9	27.7	32.0	23.8
Quartz (SiO_2)	16.6	17.4	14.2	20.1	16.6
Pyrite (FeS_2)	0.0	0.3	2.4	0.1	0.0
Sulphate minerals (SO_4^{2-})(1)	0.1	0.0	0.1	0.1	0.1
Siderite ($FeCO_3$)	0.5	1.0	1.7	0.6	0.5
Calcite ($CaCO_3$)	0.0	0.0	0.0	0.0	0.0
Dolomite [$CaMg(CO_3)_2$]	0.0	0.0	0.0	0.0	0.0
Coal	59.0	58.2	54.1	47.1	59.0
Other	0.0	0.2	0.0	0.0	0.0
Mineral Matter (MM)(2)	41.08	41.81	46.00	52.94	41.08
Ash forming minerals(3)	23.48	24.21	27.10	35.14	22.48

Notes: (1) proportions of sulphates were calculated based on the normalised sulphate contributions from alunite [$KAl_3(SO_4)_2(OH)_6$] and gypsum ($CaSO_4 \cdot H_2O$).
(2) mineral matter calculated according to PARR formula
(3) mass percentage of ash forming minerals was calculated on this basis of the amount of material remaining after combustion (Speight, 2005).

The relatively inert minerals of quartz and kaolinite contributed to the highest proportion of mineral constituents across all the sub-samples. Approximately 100% dissolution of pyrite appeared to have taken place across all the sub-samples barring one sample (+106 -180µm). This size fraction was also found to have had the highest initial proportion of pyrite in the untreated samples (7.9%). The effective dissolution of pyrite in the +106 - 180µm sample was calculated to be approximately 70%. The presence of siderite was also found to have decreased from an average of 2.38% ± 0.65 to 0.86% ± 0.23. This is likely attributed to the continued addition of acidic media giving rise to the dissolution of siderite resulting in the slight increase in pH observed in region II and III of Figure 20. The absence of measurable calcite ($CaCO_3$) and dolomite $CaMg(CO_3)_2$ is reflective of the rapid dissolution of these readily neutralising minerals in the initial stages of the investigation which appear as peaks in pH curve in region I of Figure 20.

Table 33: Condensed QEMSCAN modal report on the pH 6 (bioleach) sub-samples reported on a whole sample basis.

	Content (mass % of whole coal)				
Mineral %	-75µm	+75 - 106µm	+106 -180µm	+180 -212µm	+212 -355µm
Kaolinite [$Al_4Si_4O_{10}(OH)_2 \cdot H_2O$]	29.2	26.1	27.8	24.7	28.8
Quartz (SiO_2)	25.7	26.1	18.6	20.0	26.1
Pyrite (FeS_2)	0.1	2.1	2.5	1.4	3.8
Sulphate minerals (SO_4^{2-})(1)	0.0	0.0	0.0	0.0	0.1
Siderite ($FeCO_3$)	0.5	1.6	1.0	1.3	1.9
Calcite ($CaCO_3$)	0.0	0.0	0.0	0.0	0.0
Dolomite [$CaMg(CO_3)_2$]	0.0	0.0	0.0	0.0	0.0
Coal	44.3	44.2	50.1	52.6	39.2
Other	0.1	0.1	0.0	0.0	0.1
Mineral Matter (MM)(2)	55.68	55.85	49.98	47.45	60.90
Ash forming minerals(3)	38.08	38.25	31.08	29.65	42.30

Notes: (1) proportions of sulphates were calculated based on the normalised sulphate contributions from alunite [$KAl_3(SO_4)_2(OH)_6$] and gypsum ($CaSO_4 \cdot H_2O$).
(2) mineral matter calculated according to PARR formula
(3) mass percentage of ash forming minerals was calculated on this basis of the amount of material remaining after combustion (Speight, 2005).

Pyrite was detected in all 5 size fractions, with the highest measured presence of 3.8% in the +212µm–355µm sample. The acidic nature of the culture meant that the overall initial pH of the inoculated media was approximately pH 3. The absence of measurable carbonate minerals can be attributed to the rapid dissolution of these minerals in the initial stages which resulted in a rapid increase in the pH from pH 3 to pH 7.

4.6.2. Batch microbial shake flask tests

Batch microbial shake flask tests can be considered to simulate the effect of an extremely low flow of pore water through a dump, where the dump remains stagnant for long periods of time. The tests were conducted under two conditions to simulate a circum-neutral environment where the media used was at a pH of 6 and an acidic environment where the media used was at pH 2. The batch procedure undertook to assess the reactivity of the tailings samples under biological influence in a non-pH controlled environment. Unlike the draw and fill tests, supernatant media was not removed and replaced upon each sampling instance. As discussed in Section 3.5.4, the batch tests were conducted for the following size fractions: -75µm, +106 - 180µm and +212 - 355µm.

Acid fed environment

150mL of autotrophic basalt salt solution was adjusted to pH 2, thereafter 7.5g of sample was added into the prepared media after which the prepared flasks were inoculated with the 7.5mL of biokinetic culture (pH 1.9). The batch microbial shake flask tests were conducted for 74days. In order to determine the geochemical behaviour of the samples in the absence of microbial activity, an abiotic system was prepared for each flask in the batch tests according to the method described in Appendix A.4.1. The experiments were conducted for 74 days during which, pH and redox potential were taken

Figure 26 presents the results for the variation in pH as a function of time under biotic "B" and abiotic "AB" conditions. Results for the redox potentials measured during the tests are also included within this section (Figure 27).

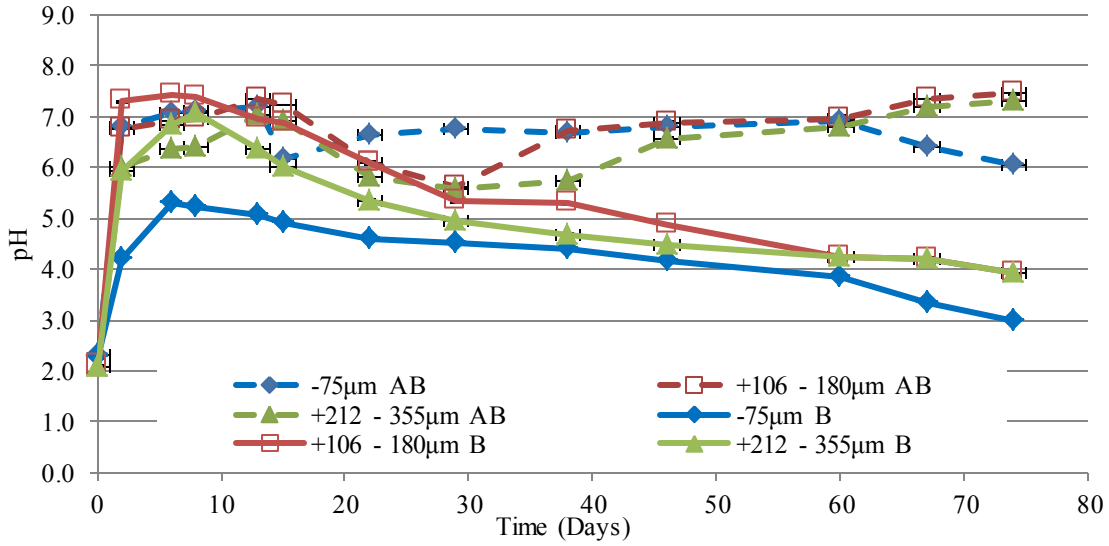

Figure 26: pH as a function of time for the biotic "B" and abiotic "AB" conditions of the batch acid microbial shake flask tests. Errors are shown as standard deviation where n=2.

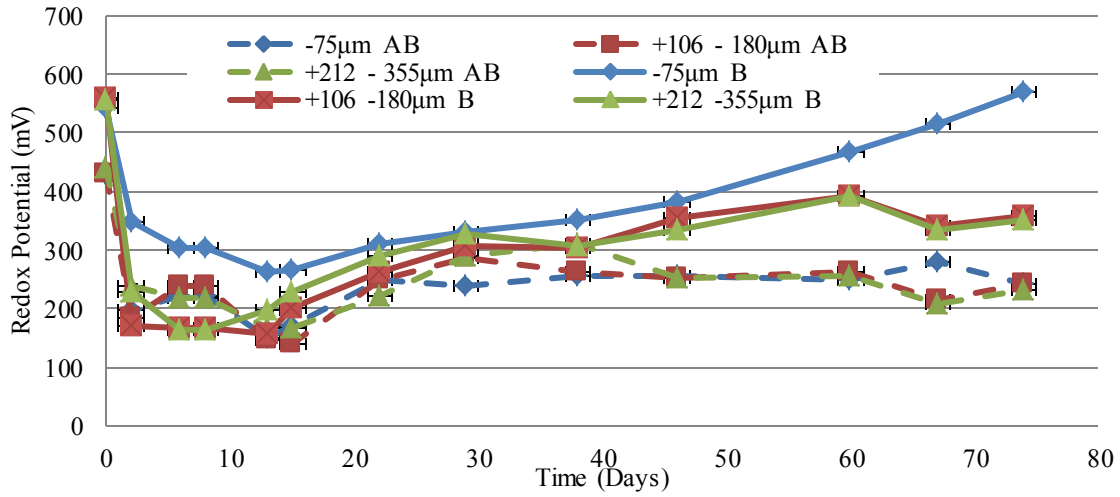

Figure 27: Redox potential measured against an Ag/AgCl electrode as a function of time in a batch acidic (pH 2) environment. Errors are shown as the standard deviation where n=2. 'B'indicating biotic (inoculated system), 'AB' indicating abiotic system

As in the case of the draw and fill tests, the batch leach tests showed an initial increase in pH across all the samples indicative of the leaching of readily soluble acid neutralising carbonate minerals into solution. After approximately 15 days of leaching the pH levels of the biotic tests steadily decreased, this is indicative of acid generating reactions having begun to dominate the environment. The biotic samples indicate an overall net acid generating potential which is reflected in the steady decrease in pH across the biotic samples. In comparison, the abiotic tests indicate an overall acid neutralising potential indicated by the rapid increase in pH from day 0 (pH = 2) and minimal change in circum-neutral pH (±6.0) achieved after 15 days. This comparison is indicative of the role of bacterial strains in the acid generating behaviour of all the coal size fractions from a period of 20 days onwards.

Circum-neutral environment

A second scenario of batch tests was also set up, these aimed to assess the reactivity of the tailings samples in a circum-neutral batch environment. The samples were inoculated with the same biokinetic culture (pH 1.9) and an ABS solution which was prepared to a pH of 6.0. The batch microbial shake flask tests were conducted for 74 days. Similar to the batch acid fed tests, an abiotic system was prepared for each flask in the batch system according to the method described in Appendix A.4.1. The experiments were conducted for 74 days during which, pH and redox potential were taken

Figure 28 presents the results for the variation in pH, results for the redox potentials measured during the tests are presented in Figure 29.

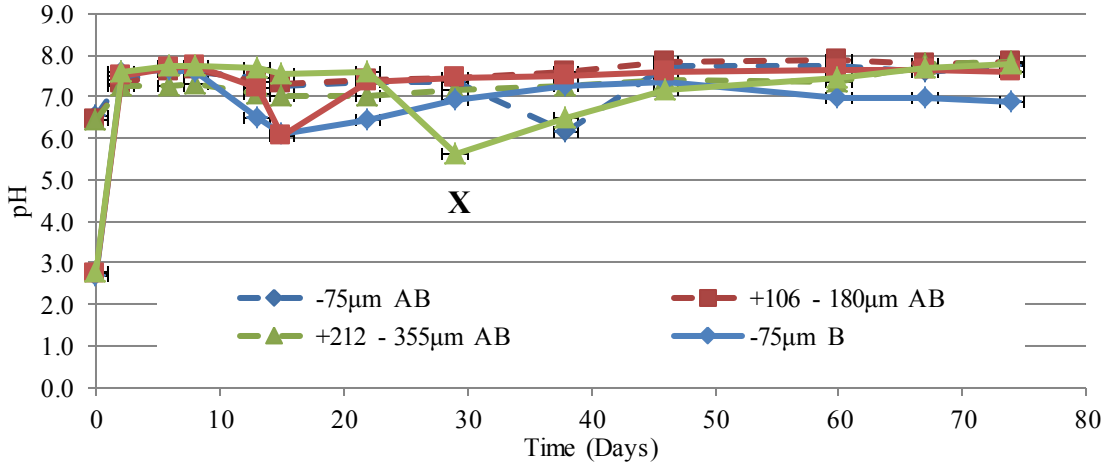

Figure 28: pH as a function of time for the biotic "B" and abiotic "AB" conditions of the batch acid microbial shake flask tests. Errors are shown as the standard deviation where n=2.

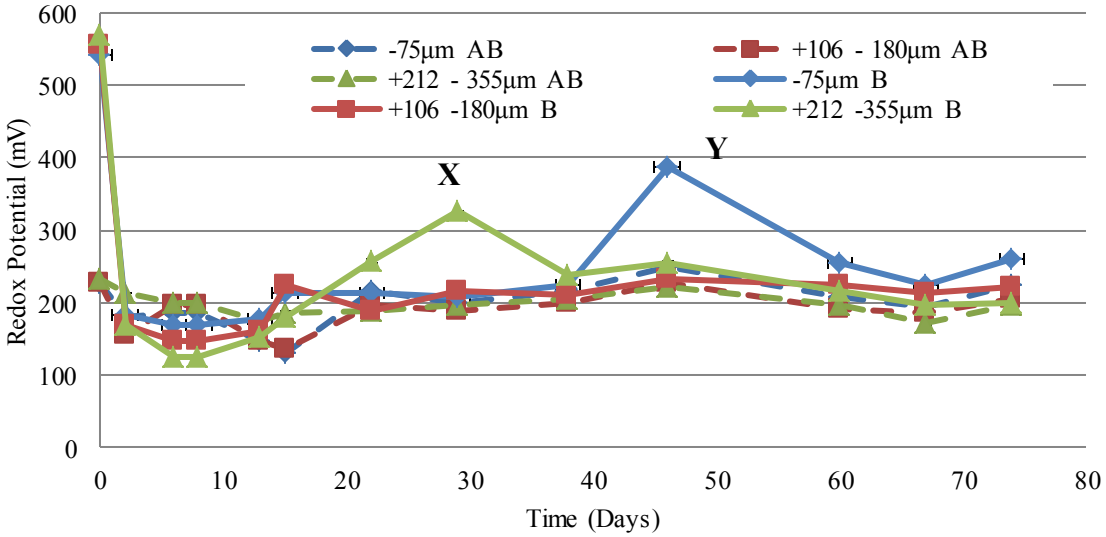

Figure 29: Redox potential measured against an Ag/AgCl electrode as a function of time in a batch circum-neutral (pH 6) environment. Errors are shown as the standard deviation where n=2. 'B'indicating biotic (inoculated system), 'AB' indicating abiotic system

The inoculated tests (biotic) initially present with high redox potentials (> 550mV) and low pH values (< 3.0), this can attributed to the initial inoculation of the flasks with the biokinetic culture (redox potentials of 668mV and a pH of 1.9). Under biotic conditions the redox was observed to decrease between 0-5 days and the pH increased for the same time frame. As in previous tests, this can be attributed to the dissolution of readily soluble acid neutralising minerals leaching into solution under the low pH conditions presented at the start of the experiments. The stable pH and redox potential values after 5 days are indicative of negligible microbial activity or oxidative dissolution of pyrite under these leach conditions. Slight variation in the pH was observed for the largest size fraction (+212 - 355µm) in the biotic experiment at 30 days (labelled point "X") reflecting outliers to the experimental data.

CHAPTER 5

DISCUSSION

The results of the various characterization tests were presented and discussed on an individual basis in Chapter 4. This chapter provides a more detailed analysis and synthesis of these results with a view to answering the key research questions namely:

i. In which minerals and macerals are the various forms of sulphur and acid neutralising constituents distributed through the coal tailings,
ii. How does the mineralogy, texture and particle size distribution of the coal tailings influence their acid generating potential?
iii. What analytical techniques and test methods are suitable for the accurate and reliable characterisation of the sulphur chemistry and acid generating potential of coal tailings?
iv. How can the methods and techniques in (iii) be combined in the form of a systematic and meaningful framework for the characterisation of coal and coal waste streams?

More specifically this chapter sets out to evaluate and compare the different characterisation tests thereby addressing questions (iii) and (iv) and to analyse the related effects of mineralogy and particle size distribution on the acid generating potential of fine coal waste, thereby addressing questions (i) and (ii).

5.1. Evaluation and comparison of the characterisation methods

This section evaluates and compares the various analytical techniques and characterisation methods used to quantify chemical forms of sulphur (Section 5.1.1), mineral composition (Section 5.1.2) and acid generating potential (Section 5.1.3).

5.1.1. Sulphur speciation techniques

Three major sulphur forms were identified in the samples namely: pyritic sulphur (S^{2-}), sulphate sulphur (SO_4^{2-}) and low risk sulphur (comprising of organic sulphur and jarosite). Sulphur characterisation was undertaken using two methods of speciation, ISO 157 standard method and the ACARP method.

The sulphate sulphur determined by means of the ACARP method was found to be consistently higher than that as determined by the ISO method, this is evident in Figure 30, showing the parity between the ACARP and ISO methods for the sulphate sulphur results.

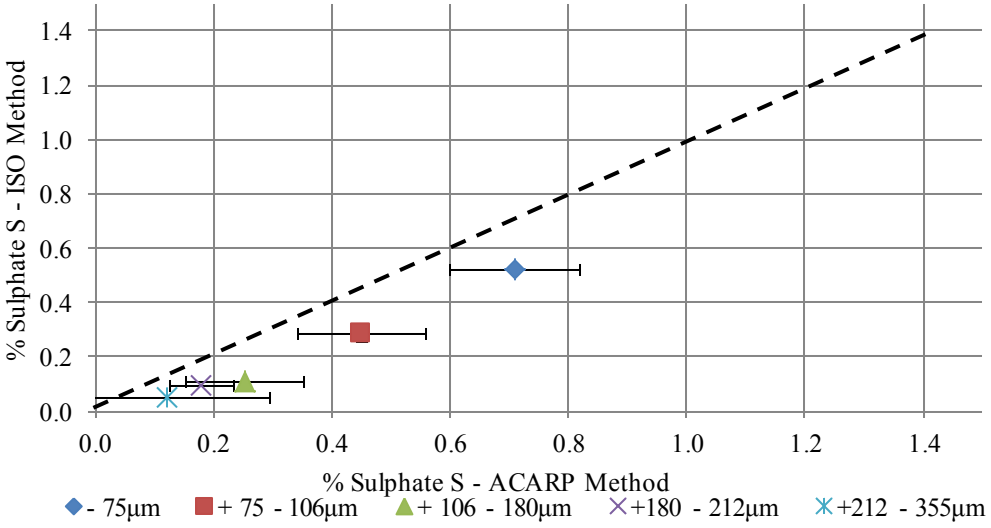

Figure 30: Parity comparison of sulphate sulphur as measured by the ISO 175 and ACARP sulphur speciation methods

The reason for this is difference is not clear as the conditions of the HCl leach procedure adopted by the ISO method are more aggressive than the KCl extraction method adopted by ACARP. However, Czerewko *et al*. (2003) pointed out that, methods which adopt a gravimetric determination of sulphate sulphur through the precipitation of barium sulphate (such as the ISO method) can be subject to weighting errors if tests samples do not contain appreciable quantities of sulphate (SO_4^{2-}). Hence the reliability of the ISO 157 method is likely to be strongly dependant on the mineralogy of the sample.

The two methods for the determination of pyritic sulphur give relatively consistent results for the smaller size fractions, as evident in the parity chart in Figure 31.

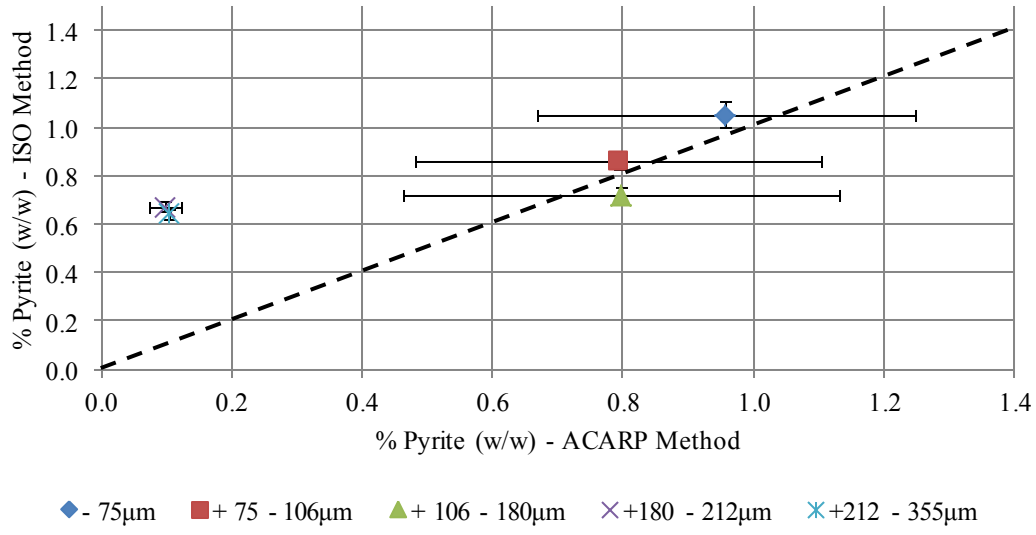

Figure 31: Parity comparison of pyrite as measured by the ISO 175 and ACARP sulphur speciation methods

In general the CRS method is considered to be a reliable and accurate method for determining sulphide sulphur. The ISO method, on the other hand, makes a number of assumptions. The ISO method uses a hydrochloric acid (HCl) leach step to remove sulphate sulphur before assessing for pyrite in the residue. The concern therein is that literature also prescribes HCl leaching for the extraction of jarosite and the final analysis of the nitric acid (HNO3) liquor assumes that all the iron (Fe) assayed is originally associated with the pyrite phase (Li *et al*., 2005). The validity of these assumptions and hence the reliability of the ISO sulphur speciation method is likely to be strongly dependant on the mineralogical composition. Czerewko *et al*. (2003), raises the same point and goes further to say that nitric acid digestion may not necessarily dissolve all the pyrite present leading to underestimation. However, similarity in the results for the smaller size fractions indicates that these assumptions may be valid for typical South African coal wastes.

The standard deviations for the ACARP method and the CRS sulphide sulphur are relatively high and this is an aspect of this method which will need to be addressed through future work. It is also important to point out that only one representative sample was submitted for the ISO method, thus the standard deviations were only reported on one sample. Additionally a fundamental difference in sample preparation may account for the differing results. The ISO 157 method calls for 2-8 grams of sample with a particle size distribution reflecting 100% passing -75μm (ISO 157:1996). The CRS method requires 0.545 grams of sample with a 100% passing size of -75μm (Stewart *et al*., 2009). Several authors have highlighted the difficulty in characterising coal due to its heterogeneous nature, others have emphasized the necessity to adjust sample size and grind finely when conducting the CRS test procedure (McElnea *et al*., 2002; Sullivan *et al*., 2002).

5.1.2. Techniques for quantifying mineral composition

The chemistry of the coal tailings samples was assessed using ICP-OES, proximate analysis and sulphur speciation. According to Harvey and Ruch (1984) sulphate minerals and pyrite can occur as finely disseminated grains, layers, nodules or cleats within the structure of coal. The distribution of sulphur to the smaller size fractions is indicative of finely disseminated grains of sulphur bearing minerals (i.e. FeS_2) in the coal tailing sample. These results were complemented by the ICP-OES analysis which determined that the elements of iron [Fe], aluminium [Al] and calcium [Ca] were found to be concentrated in the two smaller size fractions. These elements are typically associated with the sulphur bearing minerals of pyrite (FeS_2) alunite ($KAl_3(SO4)_2(OH)_6$) and gypsum ($CaSO_4 \cdot H_2O$) and kaolinite ($Al_4Si_4O_{10}(OH)_2 \cdot H_2O$) which is the primary source of [Al] in coal. According to Speight (2005) the elements identified are also closely associated with ash forming minerals in coal. The

petrographic study found the tailings sample to have a high ash content and low volatile matter content, which was found to be in line with the South African coal waste characteristics reported by the DME, (2001). According to Roberts (1988) a low vitrinite content (< 20%) found in a coal sample favours a low presence of organic and pyritic sulphur.

Mineralogical techniques to quantify the mineral composition of the coal tailings samples included, QXRD and QEMSCAN. Both methods also identified pyrite (FeS_2) as the primary acid producing minerals. The disparity in the pyrite results for the two methods was examined by means of the parity chart in Figure 32.

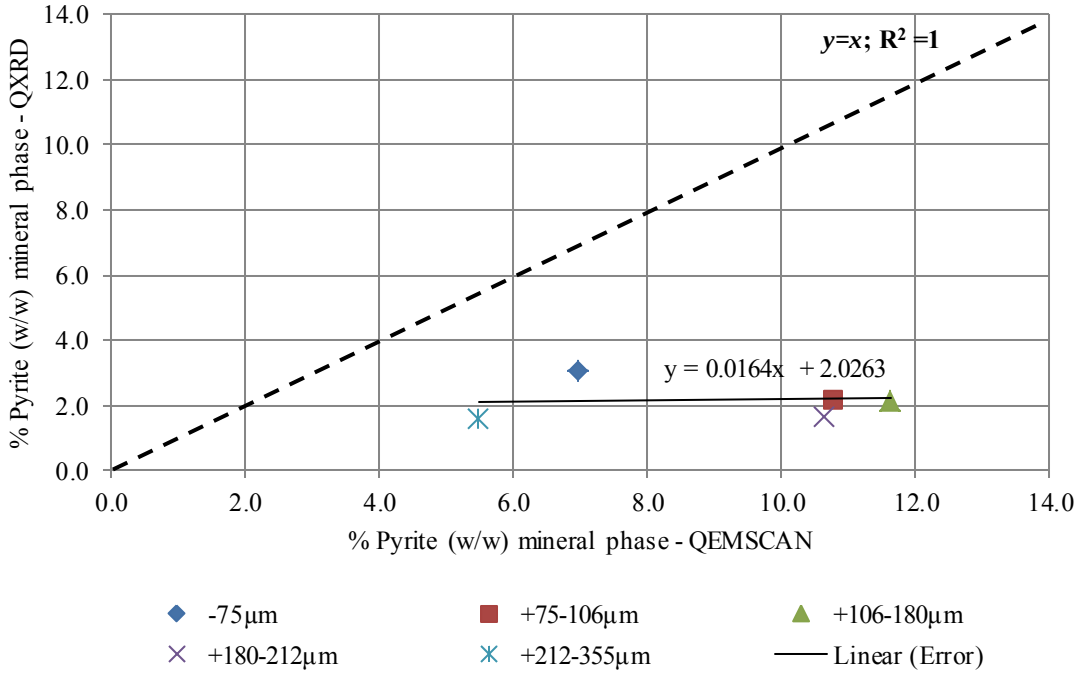

Figure 32: Parity comparison of pyrite as measured by QXRD and QEMSCAN

A linear regression determined a relatively modest gradient of 0.0164 for the compared results indicating higher concentrations of pyrite determined through QEMSCAN than QXRD. The high concentrations of pyrite reported by the QEMSCAN analysis could be an indication of possible segregation in the samples. Goodall and Scales (2007) reported on segregation, which is an artefact of inadequate sample preparation usually resulting in a biased distribution in favour of heavier minerals. Segregation typically occurs when certain minerals such as pyrite and siderite have significantly higher densities (S.G. 5.02 and S.G. 3.96) than the surrounding material (i.e. coal S.G. 1.55) in the sample. This error is also propagated in the reporting of the other mineral results in QEMSCAN since the total concentration of mineral matter remains constant.

Sulphates such as alunite, jarosite, gypsum and epsomite were identified through QXRD and QEMSCAN, the results of which have been compared in Figure 33, by means of linear regression.

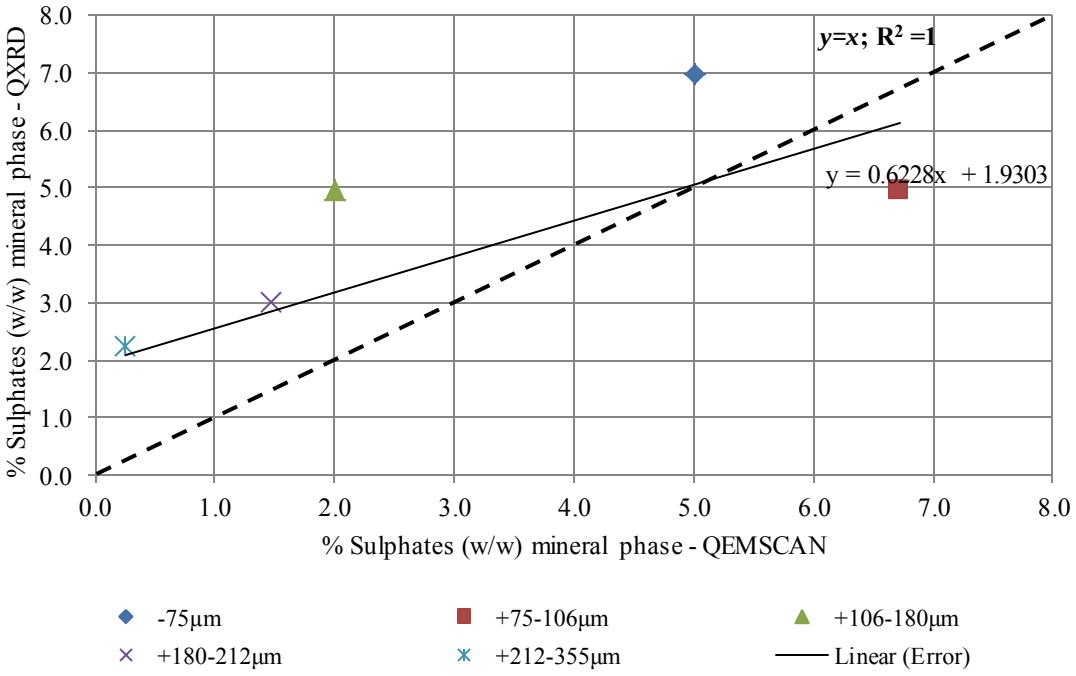

Figure 33: Parity comparison of sulphates as measured by QXRD and QEMSCAN

QXRD measured higher concentrations of sulphate minerals across most size fractions. The reason for this result is unknown as QEMSCAN is widely regarded as a more reliable quantitative tool due to its high degree of sensitivity. Both these methods confirmed that the relatively inert minerals of silica and kaolinite contributed the highest proportion of the minerals phase. A Parity comparison of silicate minerals as measured by QXRD and QEMSCAN is shown in Figure 34.

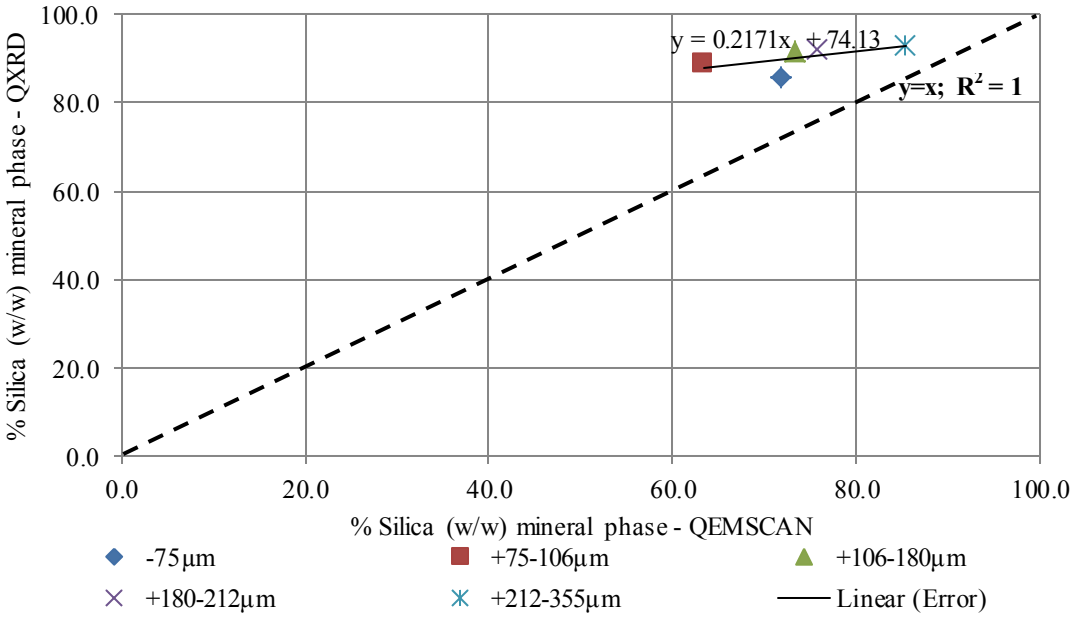

Figure 34: Parity comparison of silicates as measured by QXRD and QEMSCAN

The results for QXRD were found to be consistenly higher than QEMSCAN. Van Alphen (2007) points out that a 1994 collaborative study using CCSEM (computer controlled scanning electron microscopy) conducted by Galbreath *et al.*, (1996) found that the reproducibility of kaolinite measured in coal to be the poorest amongst other minerals such as calcite and pyrite. Van Alphen (2007) accounts for this due to the finely disseminated nature of kaolinite included in coal. Future test work to compare the reproducibility between QEMSCAN and QXRD results may be necessary. The QXRD assessment did not detect the presence of carbonate minerals in the samples. However, QEMSCAN analysis found calcite, dolomite and siderite across all the size fractions (Table 21 - Section 4.3.3.). The sensitivity of QXRD to the detection of minerals with concentrations of approximately 2.0% and less may potentially be low. This best describes the lack of quantitative QXRD data for these minerals.

5.1.3. Empirical AMD characterisation tests

Static and kinetic (dynamic) AMD characterisation tests were conducted to formulate a prediction for the AMD potential of coal tailings in the fine to ultra-fine size range. The results of the AMD prediction tests are discussed herein.

Static AMD prediction tests

Acid base accounting (ABA) and net acid generating tests (NAG) were performed to determine acid potential. Combined classification plots of NAGpH against NAPP for total sulphur and sulphide sulphur are presented in Figure 35 and Figure 36 respectively.

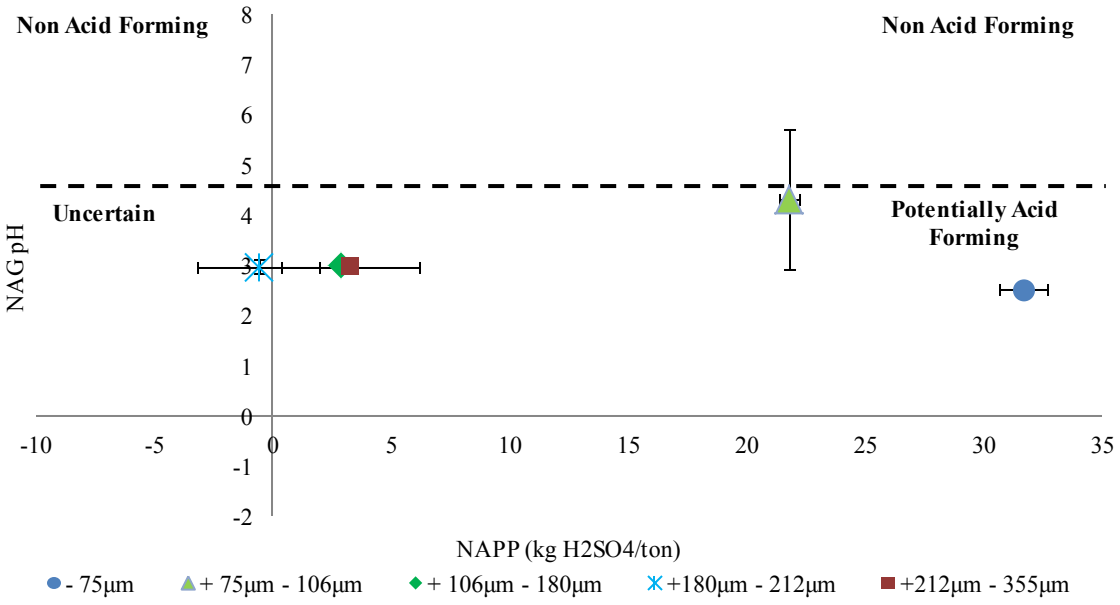

Figure 35: Combined classification plot of NAGpH against NAPP for total sulphur

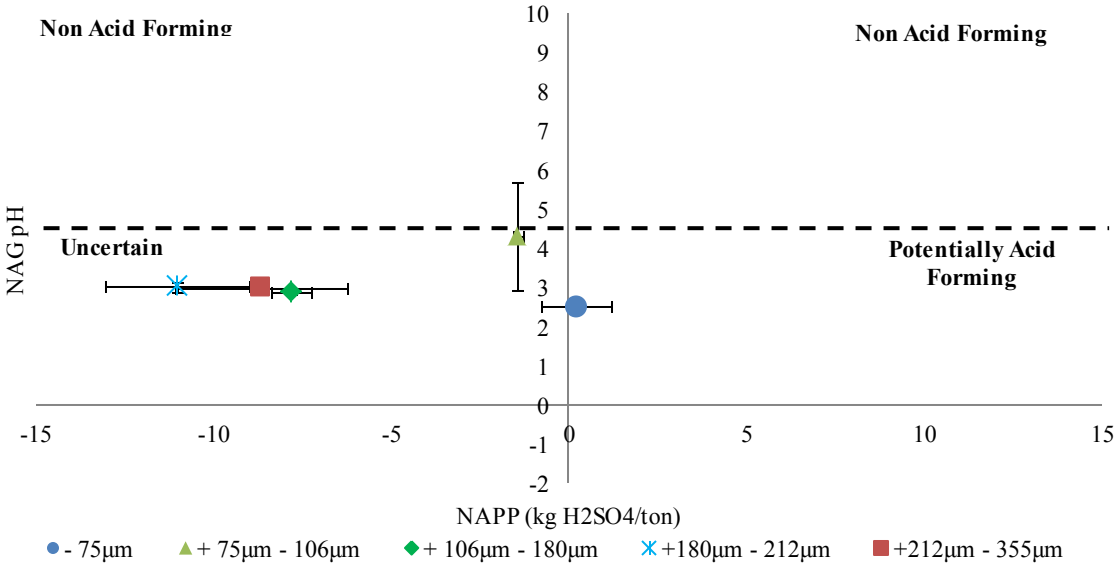

Figure 36: Combined classification plot of NAGpH against NAPP for sulphide sulphur measured by ISO method

Almost all the samples indicated a classification of potentially acid forming when the total suphur content was applied to calculate the NAPP. However, after an adjustment of the NAPP to take into account only the sulphide sulphur contribution it was found that almost all the samples fell into the uncertain category as seen in Figure 36. This highlights how using total sulphur to determine NAPP overestimates acid potential. Additionally the uncertain categorization even after adjustment of the NAPP may be due to the overestimation through the NAG tests. According to Smart *et al.* (2002) and Stewart *et al.* (2009) the interaction of the total

organic carbon (TOC) and the hydrogen peroxide (H_2O_2) during the boiling stage of experimentation tends to overestimate the potential for acid generation in the NAG tests.

Static AMD prediction tests provide reasonable quantitative information on the oxidation of pyrite. However, the standard acid potential tests were developed for the determination of acid potentials in sulphidic rock and not coal. Therefore, by nature, tests such as the NAG pH tests tend to overestimate the potential for acid generation. Furthermore, static tests do not provide a quantitative representation on the relative kinetic processes associated with AMD in a mine waste system, where several processes have to be taken into consideration including acid neutralisation, bacterial influence and environmental conditions (Hesketh, 2010).

Kinetic microbial shake flask AMD prediction tests

Microbial (Biokinetic) shake flask tests were conducted simulating two scenarios namely: batch and draw and fill. The results of these tests have been presented in Section 4.6 and the effects of microbial activity on the AMD generating potential of coal tailings under these conditions have been explored in this section.

All the kinetic experiments indicated a rapid increase in pH at the onset of the leach tests. This is consistent with the dissolution of readily soluble acid neutralising minerals such as calcite. Hesketh (2010) highlighted that in an open system (which is typical of a waste disposal scenario) majority of the acid consuming capacity would be lost in the early stages of the life of the deposit. QEMSCAN analysis conducted on the biokinetic residues aimed to examine the mineralogy of the residues and identify participatory acid neutralising minerals in the microbial leach experiments. The absence of calcite and dolomite across all the size fractions in the bioleach residues indicates their likely participation in the rapid increase in pH observed during the initial stages of the biokinetic tests. The predominantly neutralising environment created by the dissolution of these minerals during the initial stages delayed the onset of acid generation. This action would have also diminished the neutralising capacity measured through the static AMD tests, indicating the likelihood that the final pH values in the biotic experiments may have been even lower than those measured at termination. This is also demonstrated in Figure 37 where the incomplete oxidation of pyrite is evident by the remaining concentration of pyrite in each size fraction.

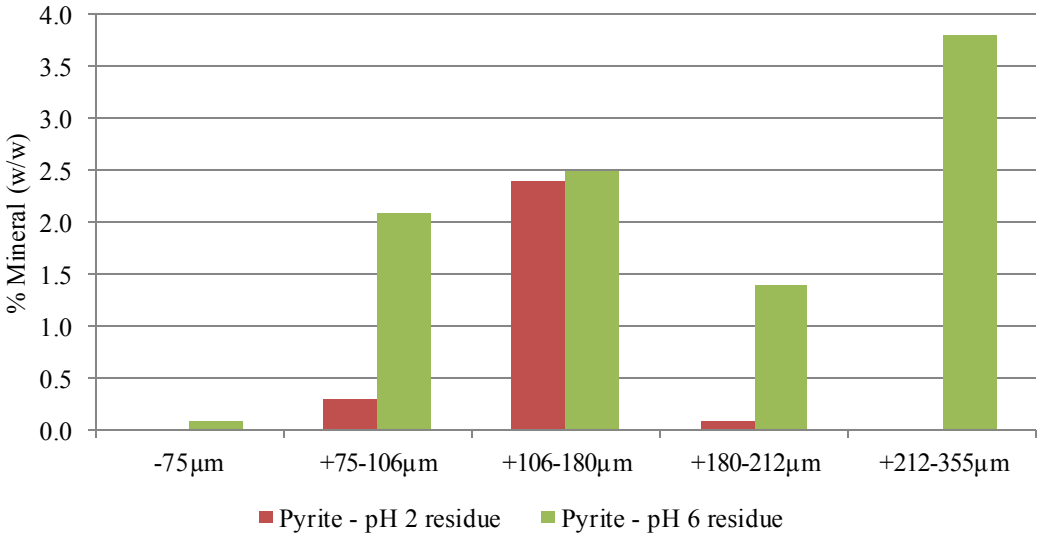

Figure 37: Pyrite concentration in the feed and draw and fill residues of the microbial shake flask tests.

The effect of the microbial activity on AMD potential

The effect of microbial influence is best represented in the batch test experiments. The pH of the inoculated acid fed samples consistently decreased after 3 days of experimentation and were still declining at a significant rate when the tests were terminated, this trend is illustrated in Figure 26 – Section 4.6.2. The abiotic batch tests represented by three size fraction (-75µm, +106 – 180µm, +212 – 315µm) remained relatively neutral. This highlights the propagating effect that microbial activity is likely to have on the long term acid generating potential of coal wastes.

5.2. Related effects of mineralogy and particle size distribution on AMD potential

The effect of mineralogy and particle size differentiations on the AMD potential of coal waste under different test conditions is examined in the following section.

5.2.1. Particle size distribution and the effect on AMD potential

The NAPP results have consistently shown that particle size distribution plays a major role in AMD potential. Figure 38 shows an increasingly negative NAPP trend toward the larger particle sizes, indicating a lower acid producing potential in the larger particle sizes. This is due to the higher pyritic sulphur content in the smaller size fractions, resulting in a higher MPA trend toward the smaller size fractions.

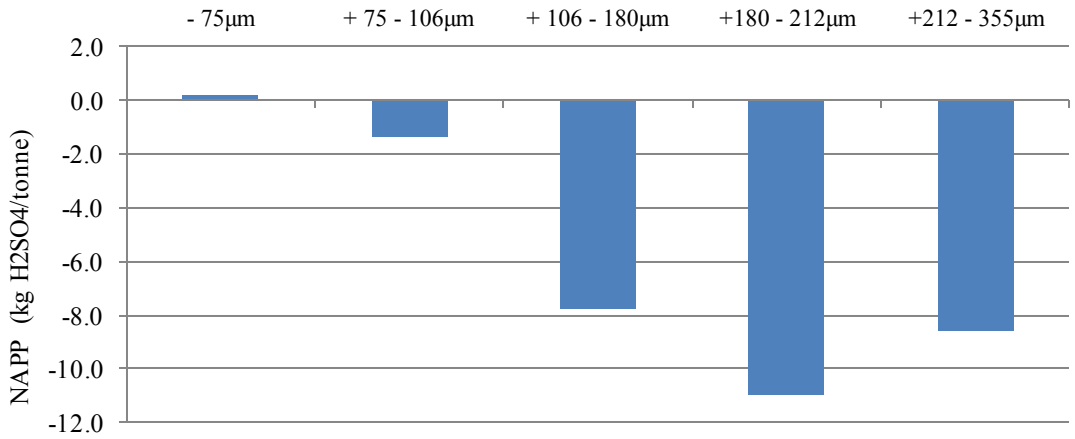

Figure 38: NAPP based on ISO measured sulphide sulphur as a function of particle size

The NAG tests performed indicated a corresponding trend to the ABA results. Lower NAG pH values were recorded for the smaller size fractions and an increasing NAG pH trend toward the larger size fractions is evident in Figure 39.

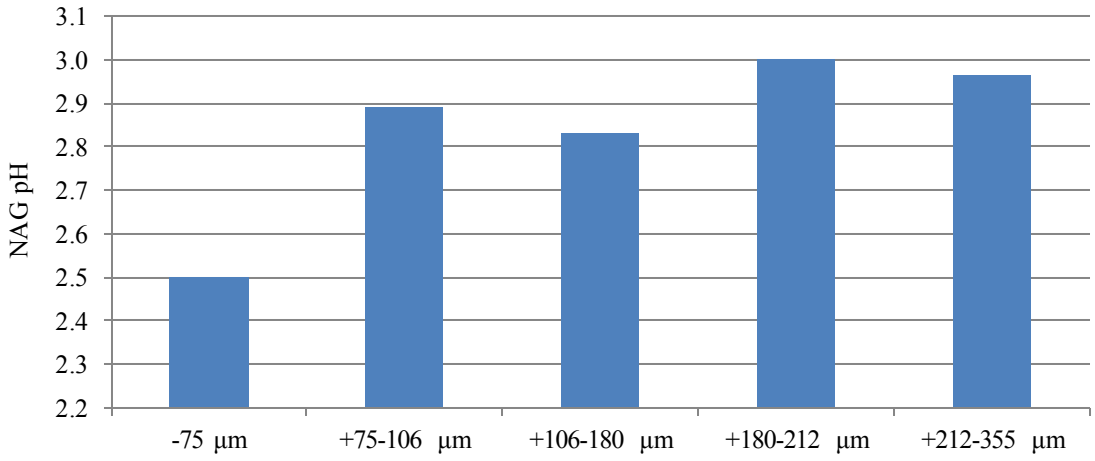

Figure 39: NAG pH as a function of particle size

The biokinetic results presented in Figure 40 clearly reflect a correlation between AMD potential and particle size.

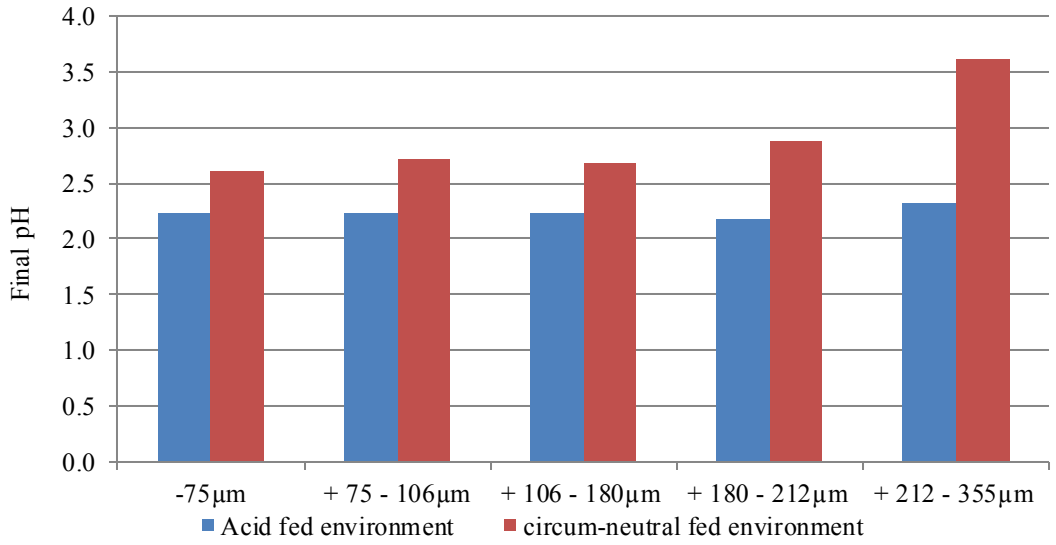

Figure 40: Measured final pH of the draw and fill biokinetic tests at point of termination

The pH at termination of the tests provides an indication of the net effect of the relative acid producing and acid neutralising reactions which occurred over the duration of the tests. Higher pH values relative to lower values point to a less acidic net effect. The biokinetic results point to a measurably higher AMD potential in the smaller size fractions than the larger size fractions, this is likely due to the higher pyritic sulphur content in the finer fractions. The mineralogical analysis conducted on the biokinetic residues, however, also appear to indicate that the complete oxidation of pyrite was preferential in the finest sized samples, which may be indicative of surface area or grain size dependent effects. However, there appears to be no correlation between particle size and the extent of reaction in the neutralising minerals.

5.2.2. Comparison of the biokinetic tests results and the static AMD tests

In order to validate the biokinetic results a comparison between the static AMD results and the biokinetic results was conducts, with particular emphasis on the pH conditions resulting from the oxidation of pyritic sulphur. The results of three selected size fractions have been presented in Table 34.

Table 34: Comparison of biokinetic tests and static AMD tests

Sample (µm)	Pyrite* (%)	NAG pH	Batch final day pH	ANC (kg H_2SO_4)	Classification
-75	1.05	2.50	2.99	31.90 ± 0.25	Acid forming
+106-180	0.72	2.83	3.91	29.81± 0.04	Uncertain
+212-315	0.64	2.97	3.93	28.21± 2.95	Uncertain

The final measured pH of the batch tests was plotted against the single addition NAG pH by means of a parity chart in Figure 41. The resultant variation in the pH values may be indicative of the incomplete oxidation of pyrite in the larger size fractions in the biokinetic tests. Although Hesketh (2010) also points out that the decomposition of the reacting peroxide during the NAG tests may also lead to the incomplete oxidation of pyrite. Notwithstanding the above, there exists a relationship between the sulphide concentrations, size fractions and pH values in the data, represented by an R^2 value of 0.9313. This close relationship highlights the efficacy of the biokinetic tests in validating the static test findings of a relationship between particle size distribution and AMD potential.

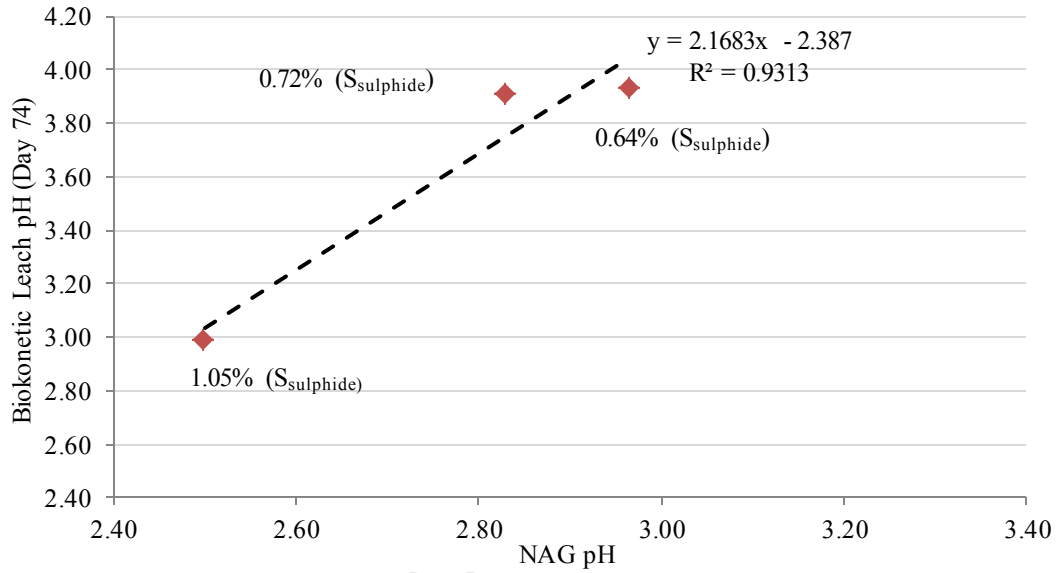

Figure 41: Comparison of the batch biokinetic final measured pH against the NAG pH

CHAPTER 6

CONCLUSIONS AND RECOMMENDATIONS

The research conducted for this project aimed at developing a quantitative understanding of the various sulphur species and other inorganic minerals within a coal tailings stream. The information gathered could then be used for the development of a framework for the characterisation of AMD in coal and coal waste streams. In order to achieve this, laboratory based experiments were structured in a case study format using a fine coal waste sample. The case study was carried out in order to address the following key questions:

i. In which minerals and macerals are the various forms of sulphur and acid neutralising constituents distributed in coal tailings?

ii. How does mineralogy, texture and particle size distribution (PSD) influence the acid generating capacity of coal tailings?

iii. What analytical techniques and test methods are suitable for the accurate and reliable characterisation of the sulphur chemistry and acid generating potential of coal tailings?

iv. How can these methods and techniques be combined in the form of a systematic and meaningful framework for the characterisation of coal and coal waste streams?

The case study approach utilized five different experimental routes to characterise the coal waste sample, namely: physical characterisation, mineralogical characterisation, chemical characterisation, sulphur speciation and AMD potential characterisation. The primary outcomes of the study, in line with the aforementioned key questions are summarised in Section 6.1 and recommendations are presented in Section 6.2.

6.1. Case study outcomes

The case study sample was found to contain 1.10% sulphur, most of which was found to be in pyritic form. The particle size distribution of the sample indicated that 75% of the sample was classified as fine to ultra-fine material. Preliminary mineralogical analysis found the sample to be slightly weathered. This indicated that the process of AMD had already been initiated in the fresh tailings sample. The key findings of the experimental test work and the significance thereof are highlighted in the following sections.

6.1.1. Mineralogical characteristics - Particle size distribution and texture

Based on the findings in literature (Section 2.3) the mineralogical characterisation techniques presented in Section 3.4 were applied to the coal tailings sample. The case study identified three categories of mineral constituents, namely: acid forming minerals, acid neutralising minerals and inert minerals. Dolomite and calcite were identified as the primary acid neutralising constituents. Quartz and kaolinite were identified as the inert clay and oxide components in the sample. Pyrite (FeS_2) was identified as the primary acid producing sulphur form and jarosite ($KFe_3(OH)_6(SO_4)_2$) was identified as the lower risk sulphur form. The presence of jarosite ($KFe_3(OH)_6(SO_4)_2$) confirmed the preliminary petrographic analysis which suggested that the sample was in a weathered state. Pyrite accounted for approximately 0.54% of the bulk tailings sample, as measured by QXRD. This translated to a maximum acid potential of 16.52kg H_2SO_4/ton of sample. Pyrite was also found to be fairly liberated in the samples, with a grain perimeter exposure rate of no less than 20%. The QEMSCAN results have also demonstrated how easily data integrity can be compromised. It is for this reason that the extent of reporting on results relating to pyrite morphology and grain size has been limited in the text.

6.1.2. Related effects of mineralogy, texture and particle size distribution on AMD

The net effect of the acid producing minerals and acid neutralising minerals identified in the mineralogical assessment was explored through AMD prediction tests. Static testing methods included acid base accounting (ABA) and net acid generation (NAG) tests. ABA tests showed that the smallest size fraction containing 2.08% $S_{(total)}$ had the highest potential for acid formation, with a NAPP of 63.65 kg H_2SO_4/ton compared to a NAPP value of 3.313 kg H_2SO_4 for the largest fraction.. In the case of wastes containing a high content of low-risk sulphur such as coal, the ABA test tends to overestimate the acid potential. This was demonstrated when the total pyritic content was substituted for total sulphur in the ABA method. The smallest size fraction showed an NAPP of 0.23 kg H_2SO_4/ton and the largest fraction an NAPP of -8.62 kg H_2SO_4/ton. For this reason the combined use of static AMD prediction tests with the biokinetic AMD prediction tests was deemed necessary. The use of biokinetic tests not only provided qualified insight into the relative rates of acid generating and acid consuming reactions but also validated and complemented the static tests. The biokinetic tests validated the relationship between particle size and AMD potential found in the static tests. This highlighted textural importance of pyrite and how a finely disseminated texture is likely to lead to the deportment of pyrite to the smaller size fraction of a particle size distribution. The shake flask tests also demonstrated that although a measured acid neutralising capacity may provide short term

alleviation, fluid flow and the movement of effluent in a natural system will likely lead to the loss or depletion of this capacity.

6.1.3. Sulphur speciation and AMD characterisation techniques

The sulphur speciation methods identified pyritic sulphur, sulphate sulphurs and deduced the presence of organic sulphur within the tailings samples. Though the data indicated discrepancies between the ISO 157 and the ACARP protocol results, similar trends were observed across both methods. Both methods found pyritic sulphur to be highly concentrated in the smaller fractions of the tailings sample. Pyritic sulphur accounted for over 50% of the total amount of sulphur contained in each sample. The ACARP tests showed that the sulphate sulphur accounted for in the samples was attributed to non-acid forming sulphur components. However, several inconsistencies related to inadequate sample preparation compromised the results of the CRS method.

6.1.4. A systematic AMD protocol

Hesketh (2010) proposed a systematic assessment for the viability of alternative methods for the mitigation of AMD from sulphide tailings. A similar approach was taken in this study by creating a framework consisting of methods and techniques for the characterisation of AMD in coal tailings. The methods used in this case study examined four primary areas, namely, chemical characterisation techniques, mineralogical characterisation techniques, sulphur characterisation and laboratory AMD prediction. The aim of focusing on these areas was to identify key analytical techniques and test methods which could be included in the AMD framework outlined in Figure 42.

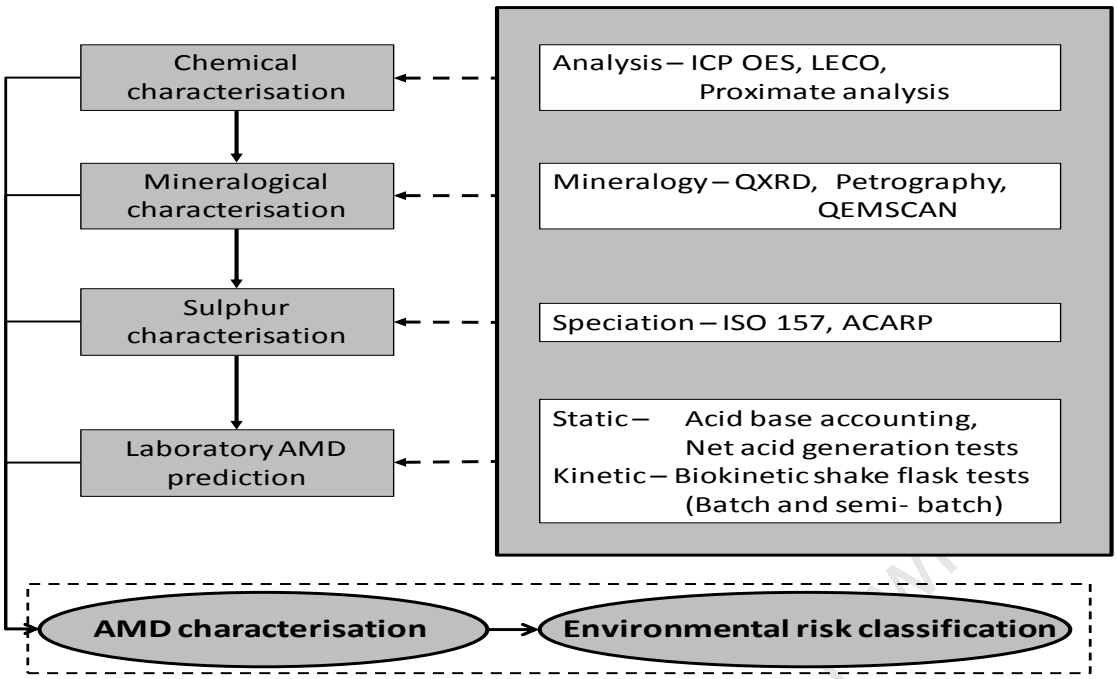

Figure 42: Schematic outline of the analytical tools to be used in the proposed AMD characterisation framework

The case study has shown that characterisation methods cannot be carried out in isolation of one another. The primary techniques outlines in Figure 42 are discussed in further detail below.

Chemical and mineralogical characterisation techniques

Quantitative x-ray diffraction (QXRD) has generally provided a reliable and inexpensive method of quantifying mineralogical constituents in coal. However, QXRD lacks reliability at low concentrations (less than ± 2%) and is therefore only suitable for quantifying primary minerals. The inclusion of methods such as inductively coupled plasma optical emission spectrometry (ICP-OES) and quantitative evaluation of minerals by scanning electron microscopy (QEMSCAN) not only provides detailed elemental analysis but also information on mineral associations and the extent of mineral liberation.

Sulphur characterisation

Conventionally, sulphur characterisation has been performed through the ISO 157 method. The case study has shown that the ACARP systematic method of determining sulphur forms allows one to distinguish between acid forming sulphates and non-acid forming sulphates. Size distribution analysis of sulphur has shown the relationship between certain sulphur forms and particle size. Sulphur speciation techniques to include quantitative determinations of pyrite, elemental sulphur, acid sulphates, non-acid sulphates, jarosite and organic sulphur have been the subject of several authors studies (Miller *et al.*, 2008; Stewart *et al.*, 2009). The case study

highlighted the dependence of sample size on sulphur mineralogy in the ACARP method through poorly reproduced data. Further assessment of the two sulphur speciation protocols is required in order to produce more reliable data.

Acid mine drainage prediction

This case study has shown that static AMD prediction tests can provide quantitative classifying information on a sample, however, this is not without a significant level of uncertainty. The biokinetic shake flask tests provide integral information on the long-term behaviour of coal tailings. Furthermore, the modification of the tests to demonstrate the behaviour under circum-neutral conditions provides a contrasting reference to the acid fed worst case" scenario. The adaptability of the biokinetic tests to semi-batch conditions provides useful information on the relative rates of acid generating and acid consuming reactions, not only under microbial oxidation conditions but also in a pseudo open system. The case study has also shown the interdependence across characterisation techniques. This was demonstrated through the AMD prediction tests which identified a higher AMD producing trend toward the smaller size fractions. The interpretation of the AMD prediction tests was complemented by the sulphur speciation analysis which identified higher levels of pyritic (acid generating) sulphur in the small size fraction.

6.2. Recommendations for further work

This protocol outlined in Section 6.1.4 combines a number of analytical techniques and tests in a systematic manner. The development of this protocol was, however, only based on a single coal tailings sample. The variable characteristics of the various coal bodies across the different beneficiation circuits in South Africa, as well as the number of coal waste streams produced within each circuit, requires that further application and refinement of this protocol is needed to build up a coal waste database with a specific emphasis on AMD generating potential.

This study has also indicated that further development of many of these techniques is required in order to improve their consistency and reliability. Specific recommendations arising from this study include:

1. Further evaluation and comparison of the two sulphur speciation protocols, with specific emphasis on sample preparation techniques and reproducibility.
2. Refinement and standardisation of the biokinetic AMD prediction protocol including batch and semi-batch methods across a range of samples should be examined. In

particular, this study indicates that longer leach periods (>90 days) may be required for coal wastes in comparison to base metal sulphide waste streams.

3. In order to overcome the uncertainties associated with the standard single addition NAG tests, sequential NAG tests are often employed. However, due to the high organic carbon content of coal, further investigation to determine the relative contributions of total organic carbon (TOC) versus sulphides to the acidity of the sequential NAG is necessary. This will aid in establishing an understanding of the degree to which organic acidity interferes.
4. Improved sample preparation techniques for QEMSCAN should be explored to address heavy mineral segregation common with coal samples reducing reliability of results.

REFERENCES

7. Reference

Ahern, C.R., McElnea A.E. and Sullivan LA. 2004. "Acid sulfate soils laboratory methods guidelines". Published by the Department of Natural Resources, Mines and Energy, Indooroopilly, Queensland, Australia, ISBN 1 920920 66 8.

Akabzaa, T.M., Armah, T.E.K. and Baneong-Yakubo, B.K. 2007. "Prediction of acid mine drainage generation potential in selected mines in the Ashanti Metallogenic Belt using static geochemical methods", *Journal of Environmental Geology*, vol.52, pp. 957-964.

Akcil, A. and Koldas, S. 2006. "Acid Mine Drainage (AMD): causes, treatment and case studies". *Journal of Cleaner Production*, vol. 14, no. 12-13, pp. 1139-1145.

Alewell, C., Matzner, E. and Lükewille, A. 1992. "Reversibility of soil acidification by reduction of acid input – an experiment with undisturbed soil columns". In: *Responses of Forest Ecosystems to Environmental Changes*. A. Teller, P. Mathy and J.N.R. Jeffers (eds.). *Journal of Applied Science,* pp. 789-790

Álvarez-Ayuso, E., Querol, X. and Tomás, A. 2006. "Environmental impact of coal combustion-desulphurisation plant: Abatement capacity of desulphurisation process and environmental characterisation of combustion by-products". *Journal of Chemosphere*, vol. 65, no: 11, pp. 2009-2017.

Banwart, S.A., Evans K.A. and Croxford, S. 2002. "Predicting mineral weathering rates at field scale for mine water risk assessment". In: *Mine Water Hydrogeology and Geochemistry*. P.L. Younger and N.S. Robins. The Geological Society of London, Bath, U.K,

Bell, F.G., Bullock, S.E.T., Hälbich, T.F.J. and Lindsay, P. 2001. "Environmental impacts associated with an abandoned mine in the Witbank Coalfield, South Africa". *International Journal of Coal Geology*, vol. 45, no. 2-3, pp. 195-216.

Blowes, D.W., Ptacek, C.J. and Jurjovec, J. 2003. "Mill tailings: Hydrogeology and geochemistry", In: *Environmental Aspects of Mine Wastes*: Short Course Series 31. Jambor, J.L., Blowes, D.W. and Ritchie, A.I.M. (Eds.). Mineralogical Society of Canada, pp. 95-116.

Bosman, J.B. 2007. "Dense medium cyclones, past, present and future". Coal Processing Conference, 11-13 September 2007, Johannesburg.

Brantley, S.L., Kubicki, J.D and White, A.F. 2008. *Kinetics of Water Rock Interaction.* Springer Science Business Media LLC, New York, NY, pp. 151–210. ISBN 978 0 387 73562 7.

Bryan, C.G. 2006, "A study of the microbiological populations of mine wastes", PhD dissertation, School of Biological Sciences, University of Wales.

Buckman, C.H., White III, W. and Lapakko, K. 2009. "Standardization of mine waste characterisation methods by ADTI-MMS". Securing the Future and 8th ICARD, June 22-26, Skelleftea Sweden.

REFERENCES

Chou, C.L. 1990. "Geochemistry of sulfur in coal". In: *Geochemistry of Sulfur in Fossil Fuels*. Orr, W.L. and White, C.M. (Eds.). Chapter 2, pp. 30 -52. Amer. Chem. Soc. Symp Series, 429.

Chou, C.L. 2004. "Origins and evolution of sulfur in coals". "*Western Pacific Earth Sciences,* vol. 4, pp. 1 – 10.

Cline, J.D. 1969. "Spectrophotometric determination of hydrogen sulphide in natural waters". *American Society of Limnology and Oceanography*, vol. 14, no. 4, pp. 454-458.

Czerewko, M.A., Cripps, J.C., Reid, J.M and Duffell, C.G. 2003. "Sulfur species in geological materials – sources and quantification". *Cement & Concrete Concepts*, vol. 25, no. 7, pp 657-671.

de Korte, G.J. 2004. "Coal beneficiation in South Africa – Past, present and future". Presented at the meeting of the International Organising Committee for the XV International Coal Preparation Congress, 17th October, 2006 Beijing China.

Demchuk, T.D. 1992. "Epigenetic pyrite in a low-sulphur, sub-bituminous coal from the central Alberta Plains". *International Journal of Coal Geology*, vol. 21, no. 3, pp. 187- 196.

Devasahayam, S. 2007. "Application of particle size distribution analysis in evaluating the weathering in coal mine rejects and tailings". *Fuel process technology,* vol. 88, pp. 295 – 301.

DME. 2001. "National inventory discard and duff coal." Department of Minerals and Energy (DME), Pretoria. http://www.energy.gov.za

Du Cann, V.M. 2011. "A petrographic investigation of one bituminous coal for UCT: 500945 Middleburg sample". Petrographics SA. Test report, PSA 2011-190, April 2011, Pretoria.

Eberhard, A. 2011. "The future of South African coal: Market, Investment and Policy challenges". A working paper for the program on energy and sustainable development. Freeman Spogu Institute for International Studies.

Enviromine, 2012. (http://technology.infomine.com/enviromine/ard/home.htm). Article accessed 18 June 2012 : 15:59.

EPA and Hardrock Mining. 2003. "A Source Book for Industry in the Northwest and Alaska"., January 2003.

Eskom. 2010. "Integrated Report". Eskom Holdings Limited (Eskom), Megawatt Park, Johannesburg. http://www.eskom.co.za

Falcon, R. and Ham, A.J. 1988. "The characteristics of Southern African coals". *South African Institute of Mining and Metallurgy*, vol. 88, no. 5, pp. 145-161.

Gaffney, J.S. and Marley, N.A. 2009. "The impacts of combustion emissions on air quality and climate - From coal to biofuels and beyond". *Journal of Atmospheric Environment*, vol. 43, pp. 23-36.

Gaigher, J.L. 1980. "The mineral matter in some South African coal". MSc thesis, University of Pretoria pp 60.

REFERENCES

Galbreath, K., Zygarlicke, C., Casuccio, G., Moore, T., Gottlieb, P., Agron-Olshina, N., Huffman, G., Shah, A., Vang, N., Vleeskens, J and Hamburg, G. 1996. "Collaborative study of quantitative coal mineralanalysis using computer-controlled scanning electron microscopy". *Fuel*, vol. 75, no. 4, pp 424-430.

Gluskoter, H.J. 1975. "Inorganic sulfur in coal", Presented at the symposium on Sulfur and Nitrogen in Coal and Oil Shale, Spring, Philadelphia 20(2)

Gorbaty, M.L. and Kelemen, S.R. 2001. "Characterization and reactivity of organically bound sulphur and nitrogen fossil fuels". *Fuel processing technology*, vol. 71, pp. 71 – 78.

Gryglewicz, G., Boudou, J., Boulègue, J., Machnikowska, H. and Jasienko, S. 1995. "Sulfur characterization of Polish coals, their lithotypes and macerals". *Fuel* , vol. 74, no. 3, pp. 349-355.

Gryglewicz, G., Rutkowski, P. and Yperman, J. 2002." Characterization of sulfur compounds in supercritical coal extracts by gas chromatography-mass spectrometry". *Fuel processing technology,* vol. 77-78, pp. 167 – 172.

Guma, M. and Sofute, N. 2006. "Environmental life cycle assessment of cleaner production interventions in the South African coal industry". 4th year project, Department of Chemical Engineering, University of Cape Town.

Guney, M., 1968. "Oxidation and Spontaneous Combustion of Coal – Review of Individual Factors". Colliery Guardian, no. 216, pp 105-110 and 137-143.

Hansen, Y., Notten, P.J, and Petrie, J.G. 2002. "The environmental impact of ash management in coal-based power generation". *Journal of Applied Geochemistry*, vol. 17, no. 8, pp 1131-1141

Hansen, Y. 2004, "Environmental Impact Assessment of Solid Waste Management in the Primary Industries - A New Approach". PhD Dissertation, University of Sydney, Australia.

Harvey, R.D. and Ruch, R. 1986. "Overview of mineral matter in U.S. coals". Illinoise State Geological Survey Chanpaign, IL 61820.

Hesketh, A.H., Broadhurst, J.L., Bryan, C.G., van Hille, R.P. and Harrison, S.T.L. 2010. "Biokinetic test for the characterisation of AMD generation potential of sulfide mineral wastes". *Journal of Hydrometallurgy,* vol. 104, no. 3-4, pp. 459-464.

Hesketh, A.H. 2010. "An integrated approach to AMD mitigation through sulfide removal from tailings". MSc Dissertation, University of Cape Town.

Hornberger, R.J. and Brady, K.B.C. 1998. *Kinetic (Leaching) Tests for the Prediction of Mine Drainage Quality*. In: Coal Mine Drainage Prediction and Pollution Prevention in Pennsylvania, Brady K.B.C., Smith M.W. and Schueck, J. (eds). Department of Environmental Protection, Pennsylvania. http://www.dep.state.pa.us/dep/deputate/minres/districts/CMDP/main.htm. Accessed 19-01-2010.

REFERENCES

Huggins, F.E. 2002. "Overview of analytical methods for inorganic constituents in coal", *International Journal of Coal Geology*, vol. 50, pp. 169-214.

Hutton, A. and Mandile, A.J. 1996. "Quantitative XRD measurement of mineral matter in Gondwana coals using the Rietveld method". *Journal of African Earth Sciences,* vol. 23, no. 1, pp. 61-72.

Inter-ministerial committee. 2010. "Mine water management in the Witwatersrand Gold Fields with special emphasis on acid mine drainage". Report to the Inter-Ministerial Committee on Acid Mine Drainage, Department of Water Affairs, Pretoria.

International Committee for Coal and Organic Petrology. 2011. "Chapter 2. Organic petrology, maceral microlithotypes, lithotypes, minerals, rank". ICCP training course on dispered organic matter. Departmento de Geociencias, Ambiente e Ordenamento do Territoria, Faculdade de Ciencias da Universidade do Porto, 7 September 2011, Portugal.

International Standards Organization. 1996. BS 1016-106.5:1996. *Coal – Determination of sulphur forms*. ISBN: 0 580 26463 7.

Jambor, J.L. and Blowes, D.W, 1998. "Theory and application of mineralogy in environmental studies of sulphide-bearing mine wastes". In: *Modern Approaches to Ore and Environmental Mineralogy*. Cabri, L.J., Vaughan, D.J. (Eds.), Mineralogical Association of Canada. Chapter 12, pp. 367-401.

Jeffrey, L.S. 2005. "Characterization of coal resources of South Africa". *The Journal of The South African Institute of Mining and Metallurgy*, vol. 105, no. 2, pp. 95-102.

Jenkins, R.G. and Walker Jr, P.L. 1978. "Analysis of mineral matter in coal", In: *Analytical Methods for coal and coal products*. Karr, C. (Ed.), Academic Press, New York, NY, vol. 2. Chapter. 26, pp. 265-292.

Johnson, D.B. and Hallberg, K.B. 2005. "Acid mine drainage remediation options: a review". *Science of The Total Environment,* vol. 338, no. 1-2, pp. 3-14.

Jorjani, E., Yperman, J., Carleer, R. and Rezai, B. 2006. "Reductive pyrolysis of sulfur compounds in different Tabas coal samples (Iran)". *Fuel*, vol. 85, pp. 112 - 120.

Karadad-Nelson, M. 2010. "Mpumalanga's not –so-clean coal", Mail and Guardian online. Accessed Feb 04 2011 13:49. (http://www.mg.co.za/article/2010-11-29-mpumalangas-notsoclean-coal)

Kaymakci, E. and Didari V. 2002. "Relations between coal properties and spontaneous combustion parameters". *Turkish journal of engineering environmental sciences,* vol. 26, no.1, pp. 59.

Keating, M., Baum, E., Hennen, A. and Hill, B. 2001. "Cradle to Grave: The environmental impacts from coal", Clean Air Task force. Keaton energy holdings. Accessed: Feb 25 2011 15:11 http://www.keatonenergy.co.za/cm/why_coal.asp

REFERENCES

Kleinman, R.L.P. 2000. "Prediction of water quality at surface coal mines". *The National Mine Land Reclamation Centre*, WestVirginia University in Morgantown, West Virginia.

Komadel, P. and Stucki, J.W. 1988. "Quantitative assay of minerals for Fe^{2+} and Fe^{3+} using 1,10-phenanthroline: III. A rapid photochemical method". *Clays and Clay Minerals*. vol. 36, pp. 379-381.

Koper, E.L. 2004. "Sulphur removal from coal or from products? Is prevention better than cure - A technical review of the prevention option". MSc Dissertation, University of the Witwatersrand, Johannesburg.

Kuenzer, C., Zhang, J., Tetzlaff, A., van Dijk, P., Voigt, S., Mehl, H. and Wagner, W. 2007. "Uncontrolled coal fires and their environmental impacts: Investigating two arid mining regions in north-central China". *Journal of Applied Geography*, vol 27, pp. 42-62.

Lapakko, K., 1991. "Mine Waste Drainage Quality Prediction: A Literature Review". Draft report to the Minnesota Department of Natural Resources, pp. 50.

Lapakko, K., 1992. "Evaluation of Tests for Predicting Mine Waste Drainage pH". Draft report to the Western Governors' Association, May 1992. pp. 72.

Lasaga, A.C, 2000. "Fundamentals aspects of quantitative models for geochemical cycles", *Chemical Geology*. vol. 145, pp. 161-175.

Lefebvre, R., Hockley, D., Smolensky, J. and Gelinas, P. 2001. "Multiphase transfer processes in waste rock piles producing acid mine drainage, 1: Conceptual model and system characterization". *Journal of Contaminant Hydrology* vol. 52, pp. 137–164.

Liu, Y., Gupta, R., Sharma, A., Wall, T., Butcher, A., Miller, G., Gottlieb, P. and French, D. 2005a. "Mineral matter–organic matter association characterisation by QEMSCAN and applications in coal utilisation". *Fuel,* vol. 84, no. 10, pp. 1259-1267.

Liu, Y., Gupta, R., Wall, T., Butcher, A., Gottlieb, P. and French, D. 2005b. "Mineral-minerals associations in pulverized Australian coal". 5th Asia-Pacific Conference on Combustion, The university of Adelaide, Adelaide, Australia, 17-20 July 2005.

Loos, M.A., Cleghorn, C., and Mödinger, H. 2000. "Occurrence of bacteria causing acid mine drainage in the outer layers of coal wate dumps in relation to abiotic ecological determinants and soil covers used for dump rehabilitation". *Water Research Commission*, Report No. 454/1/2000

Lu, L., Sahajwalla, V., Kong, C. and Harris, D. 2001. "Quantitative X-ray diffraction analysis and its application to various coals". *Carbon,* vol. 39, no. 12, pp. 1821-1833.

Meek, F.A. 1981. "Development of a Procedure to accurately account for the presence of siderite during mining overburden analysis". Proc. 2nd Annual West Virginia Surface Mine Drainage Task Force Symposium, 27 April 1981, West Virginia University., Morgantown.

REFERENCES

Michalski, S.R., Winschel, L.J. and Gray, R.E. 1990. "Fires in abandoned coal mines". *Bulletin of Association of Engineering Geologists*, vol. 27, pp. 479–495.

Miller, S. 2008. "Development of ARD assessment for coal process wastes", *Environemtnal Geochemistry international PTY LTD.* ACARP PROJECT C15034.

Moitsheki, L.J., Matjie, R.H., Baran, A., Mooketsi, O.I. and Schobert, H.H. 2010. "Chemical and mineralogical characterization of a South African bituminous coal and its ash, and effect on pH of ash transport water". *Minerals Engineering,* vol. 23, no. 3, pp. 258-261.

Musapatika, E., Onyango, M. and Aoyi, O. 2010. "Cobalt(II) removal from synthetic wastewater by adsorption on South African coal fly ash". *South African Journal of Science,* vol. 106, no. 9/10.

Naiker, K., Cukrowska, E. and McCarthy, T.S. 2003. "Acid mine drainage arising from gold mining activity in Johannesburg, South Africa and environs". *Environmental Pollution*, no.122, pp. 29-44.

Napier-Munn, T and Wills, B.A. 2006. *Wills' Mineral Processing Technology, An introduction to the practical aspects of ore treatments and mineral recovery*. 7th Edition published by Butterworth-Heinemann, ISBN-13: 978-0750644501, pp. 15-16.

Nowaczyk, K. and Domka, F. 2000. "Oxidation of pyrite and marcasite by *Thiobacillus ferrooxidans* Bacteria". *Polish Journal of Environmental Studies*, vol. 9, no. 2, pp. 87 - 90.

Parker, G.K. and Robertson, A. 1999. "Acid Drainage, AMEEF Occasional paper no 11". *Australian Minerals and Energy Environment Foundation*, Melbourne, pp. 101-117

Pinetown, K.L., Ward, C.R. and vd Westhuuizen, W.A. 2007. "Quantitative evaluation of minerals in coal deposits in the Witbank and Highveld Coalfields, and the potential impact on acid mine drainage". *Coal Geology*, vol. 70, no. 1-3, pp. 166-183.

Pone, J.D.N., Hein, K.A.A., Stracher, G.B., Annegard, H.J., Finkleman, R.B., Blake, D.R., McCormack, J.K. and Schroeder, P. 2007. "The spontaneous combustion of coal and its by-products in the Witbank and Sasolburg coalfields of South Africa". *Coal Geology*, vol. 72, no. 2, pp. 124-140.

Prevost, X. 2010. Unpublished SA coal statistics. DME / XMP Consulting, Pretoria.

Querol, X., Chinenon, S., Lopez-Soler, A., 1989. "Iron sulphide precipitation sequence in Albian coals from the Maestrazgo basin, southeastern Iberian Range, northeastern Spain". *International Journal of Coal Geology.* No.11, pp 171– 189.

Querol, X., Cabrera, Ll., Pickel, W., Lopez-Soler, A., Hagemann,J.L. and Fernandez-Turiel, J.L. 1996. "Geological controls on the coal quality of the Mequinenza subbituminous coal deposit, northeast Spain". *International Journal of Coal Geology*. no.29, pp 67–91.

REFERENCES

Querol, X., Klika, Z., Weiss, Z., Finkelman, R.B., Alastuey, A.,Juan, R., Lopez-Soler, A., Plana, F., Kolker, A. and Chenery,S.R.N 2001. "Determination of element affinities by density fractionation of bulk coal samples". *Fuel* vol.80, pp 83–96.

Rao, C.P. and Gluskoter, H.J. 1973. "Occurrence and distribution of minerals in Illinois coals". Illinois State Geological Survey, Circular no. 476, pp 56.

Reddick J. 2006. "An investigation of cleaner production opportunities in the South African coal mining industry". MSc Dissertation, University of Cape Town.

Reddick, J.F., von Blottnitz, H, and Kothuis, B. 2007. "A cleaner production assessment of the ultra-fine coal waste generated in South Africa". *South African Institute of Mining and Metallurgy*, vol. 107, no. 12, pp 811.

Roberts, D.L. 1988. "The relationship between macerals and sulphur content of some South African Permian coals". *International Journal of Coal Geology,* vol. 10, no. 4, pp. 399-410.

Shelton, P.A., Ammons, J.T. and Freeman, J.R. 1984. "Neutralization Potential: A Closer Look, Green Lands". *West Virginia Mining and Reclamation Association, Charleston,* vol. 13, no. 4, pp. 35-37.

Ross, A.B., Junyapoon, S., Bartle, K.D., Jones, J.M. and Williams, A. 2001. "Development of pyrolysis-GC with selective detection: coupling of pyrolysis-GC to atomic emission detection (py-GC-AED)". *Journal of analytical and applied physics*, vol. 58-59, pp. 371-385.

South African National Standard. 1985. *Methods for the petrographic analysis of bituminous coal and anthracite. Part 2: Method of preparing coal samples*. ISBN: 978 0 626 20488 4.

South African National Standard. 1994. *Methods for the petrographic analysis of bituminous coal and anthracite. Part 3: Method of determining maceral group composition*. ISBN: 978 0 626 20489 1.

Singer, P.C and Stumm, M.W. 1968. "Kinetics of the oxidation of ferrous iron". Presented at the 2nd Symposium on coal mine drainage, 14 - 16 May 1968 Pittsburgh Pennsylvania.

Singer, P.C and Stumm, M.W. 1970. "Acid mine drainage: The rate determining step", *Journal of Science*, *Washington DC,* vol. 176, pp. 1121 - 1123.

Skousen, J., Simmons, J., McDonald, L.M. and Ziemkiewicz, P. 2002. "Acid - Base Accounting to Predict Post-Mining Drainage Quality on Surface Mines". *Journal of Environmental Quality*, vol. 31, pp. 2034-2044.

Skousen, J., Renton, J., Brown, H., Evans, P., Leavitt, B., Brady, K., Cohen, L., and Ziemkiewicz, P. 1997. "Neutralization Potential of Overburden Samples Containing Siderite". *Journal of Environmental Quality,* vol. 26, pp. 673-681.

Smart, R., Skinner, B., Levay, G., Gerson, A., Thomas, J., Sobleraj, H., Schumann, R., Welsner, C., Weber, P. 2002. "Prediction of Kinetic control of Acid Mine Drainage", AMIRA International, ARD Test Handbook Project P387A.

REFERENCES

Snyman, C.P. and Botha, W.J., 1993. "Coal in South Africa". *Journal of African Earth Sciences (and the Middle East),* vol. 16, no. 1-2, pp. 171-180.

Sobek, A.A., Schuller, W.A., Freeman, J.R. and Smith, R.M. 1978. "Field and laboratory methods applicable to overburdens and minesoils". Environmental Protection Technology Series, Morgantown, West Virginia, EPA-600/2-78-054.

Sonjica. 2010, Keynote address, "The Official launch of Optimum Coal's Water treatment plant at Optimum Colliery, Pullenshope, Mpumalanga".

Speight, J.G. 2005. *Handbook of Coal Analysis*. Wiley Interscience. vol. 166. ISBN 0-471-52273-2

Stefanova, M., Marinova, S., Yperman, J. and Carleer, R. 2005. "Reductive pyrolysis of Mioceneaged lithotypes using MS and GC/MS detection systems for analysis of organic sulfur groups". *Fuel*, vol. 84, pp. 71-79.

Stewart, W., Miller, S., Thomas, J.E., and Smart R. 2003. "Evaluation of the Effects of Organic Matter on the Net Acid Generation (NAG) Test". Proceedings of the Sixth International Conference on Acid Rock drainage I, pp. 211-222.

Stewart, W.A., Miller, S.D. and Smart, R. 2006. *Advances in acid rock drainage (ARD) characterisation of mine wastes*. In R.I. Barnhisel (ed), Proceedings of the Seventh International Conference on Acid Rock Drainage, American Society of Mining and Reclamation, Lexington, KY, pp. 2098-2119.

Stewart, W., Schuman, R., Miller, S. and Smart, R. 2009. "Development of prediction methods of ARD assessment of coal process wastes" Securing the future and 8th ICARD, June 22-26 2009, Skelleftea, Sweden.

Stracher, G.B. and Taylor, T.P. 2004. "Coal fires burning out of control around the world: thermodynamic recipe for environmental catastrophe". *Coal Geology*, vol 59, pp. 7-17.

Swaine, D.J., 1990. "Trace Elements in Coal". Butterworths, London.

van Alphen, C. 2007. "Automated mineralogical analysis of coal and ash products - Challenges and requirements.". *Minerals Engineering,* vol. 20, no. 5, pp. 496-505.

Van Alphen, C., Matjie, R.H., Rajoo, P. unkown, "Qemscan analysis of coal and fly ash formation model-New developments"

Van der Scholtz M and Trautmann, C. 2007, "Environmental life cycle assessment of fine coal use for power generation in South Africa". 4th year project, Department of Chemical Engineering, University of Cape Town.

Vassilev, S.V. and Tascon, J.M.D. 2003. "Methods for characterization of inorganic and mineral matter in coal: A critical overview", *Energy and Fuels,* vol. 17, no. 2, pp. 271-281.

Wagner, N.J. 2007. "The abnormal condition analysis used to characterize weathered discard coals". *Coal Geology,* vol. 72, pp. 177-186.

REFERENCES

Wagner, N.J. 2008, "The characterization of weathered discard coals and their behaviour during combustion", *Fuel*, vol. 87, no. 8–9, pp. 1687-1697.

Ward, C.R. 2002. "Analysis and significance of mineral matter in coal seams". *International Journal of Coal Geology,* vol. 50, no. 1-4, pp. 135-168.

Weber, P.A., Stewart, W.A., Skinner, W.M., Weisener, C.G., Thomas, J.E. and Smart, R.S.C. 2004. "Geochemical effects of oxidation products and framboidal pyrite oxidation in acid mine drainage prediction techniques". *Applied Geochemistry,* vol. 19, no. 12, pp. 1953-1974.

Whitehead, P.G., Cosby, B.J., and Prior, H. 2005. "The Wheal Jane wetlands model for bioremediation of acid mine drainage". *Science of the Total Environment*, vol. 338, pp. 125-135.

Wilkin, R.T. 2007. "Metal Attenuation Processes at Mining Sites". *United States Environmental Protection Agency, Ground Water Issue.*

APPENDICES

APPENDIX

TABLE OF CONTENTS

LIST OF TABLES AND FIGURES

A 1. Chemical Analysis methods

A 1.1. Acid digestion for ICP-OES

The concentration of the major and minor elements was determined using ICP-OES at ALS Laboratory Group in Witbank.

i. Mix two parts by mass light magnesium oxide and one part anhydrous sodium carbonate to create Eshcka mixture

ii. Weigh approx. 0.5g of sample and mix intimately with 0.8g of Eschka mixture in a crucible and level the contents of the crucible and cover with 0.2g Eshcka mixture

iii. Place the charged crucible into a the muffle furnace at ambient temperature, heat at a uniform rate to 800 °C over 2 hours and maintain at this temperature for a further 2 hours.

iv. Remove the crucible and allow to cool, transfer all the contents of crucible to a 100 mL glass beaker

v. Add 10 mL of a hydrochloric acid/ hydrofluoric acid mixture to the polypropylene bottle.

vi. Allow for low temperature acid digestion for roughly 30 minutes

vii. Add excess Boric acid (H_3BO_3)

viii. The resulting solution is analysed by ICP-OES

A 1.2. Sulphur speciation procedure according to ISO 157:1996

Acid digestion procedure

i. Weigh out the sample according to Table A.1.1

Table A.1.1: Measurement of test sample according to total sulphur content

Total sulphur content %(m/m)	Mass of sample (g)
< 0.7	8
0.7 to 2.0	5
> 2.0	2

ii. Transfer the sample to a 250 ml conical flask, add 50 ml of15% hydrochloric acid and fit a cold-finger condenser into the neck of the flask.

iii. Boil for 30 minutes, remove the condenser and filter the mixture through a medium textured, doubly acid-washed filter paper into a beaker.

iv. Wash the residue three times with the 15% hydrochloric acid and a further three times with hot distilled water, using a total volume of approximately 30 mL.

v. Retain the filtrate for the determination of sulphates sulphur and the residue for the pyritic sulphur determination.

Sulphate sulphur determination procedure (Follows step v in the acid digestion procedure)

i. Add 5mL of 30% hydrogen peroxide to the filtrate from step (v) and boil for 5 minutes.

ii. Add 2 to 3 drops of methyl red indicator and 25% ammonia solution drop by drop until the solution colour turns yellow, then add 5 additional drops as an excess amount. Filter and remove the precipitate that formed.

iii. Add 36% hydrochloric acid drop by drop until the colour of the solution turns pink, then add 1 additional drop in excess.

iv. Add 25mL of 2g/L potassium sulphate solution and cover with a watch glass and heat.

v. Add 10mL of 85g/L barium chloride solution to the heated solution and maintain heating for a further 30 minutes then filter the solution and retain the precipitate

vi. Add a small drop of 17g/L silver nitrate to the precipitate and gravimetrically determine the sulphate sulphur concentration.

vii. Prepare a blank solution by following steps i – vii but omitting the filtrate from step (i) and gravimetrically determine the sulphate sulphur concentration

Pyritic sulphur determination procedure (Follows step v in the acid digestion procedure)

i. Reflux the residue from the acid digestion procedure with 9% nitric acid and discard the un-dissolved residue.

ii. Add 5mL of 30% hydrogen peroxide to the filtrate and boil for 5 minutes

iii. Allow solution to cool and determine iron content through one of three methods:

   a. Atomic absorption spectroscopy (AAS)
   b. Tirimetry
   c. Colorimetry

iv. The iron content is then back calculated assuming a stoichiometry where 1 mole of pyrite (MW = 87.84) per mole of Fe (MW = 55.84) is used.

A 1.3. Sulphur speciation procedure according to the ACARP method

Pyritic sulphur determination procedure according to the CRS method performed in duplicate

i. Prepare a zinc acetate solution by dissolving 60g of zinc acetate in 1.5L of deionised water.

ii. Weigh out 0.545 grams of sample into a 250mL double-neck round bottom digestion flask.

iii. To the flask add the following before purging with nitrogen gas for 2 minutes:

   a. 2.0 grams of technical grade chromium powder
   b. 10mL 95% Ethanol
   c. 60mL of 6M hydrochloric acid

iv. Draw out 100mL of the zinc acetate solution into an Erlenmeyer flask and prepare the set up according to Figure A.1.1 – Section 3.3.4

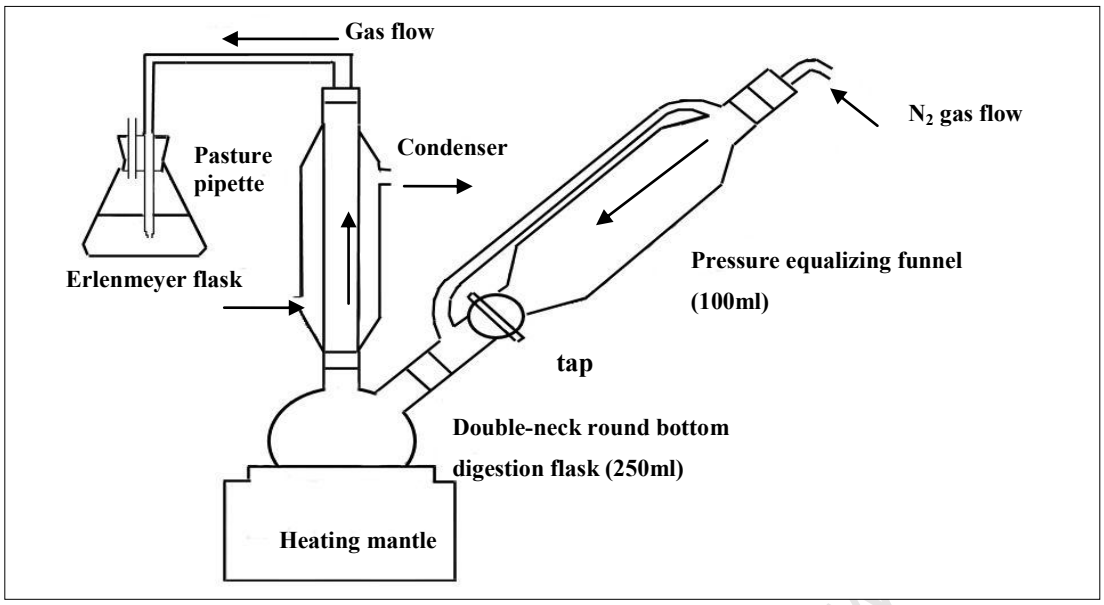

Figure A.1. 1: Schematic representation of the apparatus used in the chromium reducible sulphur test for the determination of pyritic sulphur. (Source: Ahern *et al*., 2004)

v. The zinc sulphide in the Erlenmeyer flask is then assayed for sulphide content using a UV-Vis spectrophotometer in accordance with the method developed by Cline (1969) and the dilution factors proposed in Table A.1.2 – Section 3.3.4.

   a. Pipette 200µL of Zinc Acetate
   b. Add 20µL of sample
   c. Make up the remaining volume to 5mL with deionised water
   d. Add 0.5mL of N,N-dimethyl-p-phenylene diamine dihydrochloric
   e. Add 0.5mL of ferric chloride solution
   f. Vortex and read at 670nm

Table A.1.2: Reagent concentrations and dilution factors used in the sulphide sulphur assay in the various concentration ranges as suggested by Cline (1969)

Sulphide concentration (µmole/litre)	Diamine concentration (g/500ml)	Ferric concentration (g/500ml)	Dilution factor (mL:mL)	Path length (cm)
1 – 3	0.5	0.75	1:1	10
3 – 40	2.0	3.0	1:1	1
40 – 250	8.0	12.0	2:25	1
250 - 1000	20.0	30.0	1:50	1

Sulphate sulphur determination procedure according to the KCl extraction method performed in duplicate

i. 80 mL of 1M inert KCl solution is mixed with 2 grams of sample in a sealed plastic bottle.

ii. The plastic bottle is attached to a retort stand and suspended above a vortex then agitated for 1hour.

iii. Filter the mixture using 0.45 μm filter paper. Separate the filtrate into two equal parts.

iv. One part of the liquor is assayed using ICP-OES to assess the concentration of dissolved sulphur. This provides an indication of the total soluble sulphates in the sample.

v. The second part is titrated with 0.05M sodium hydroxide to a pH of 7 to determine the soluble acid forming sulphates in the sample.

vi. The soluble non-acid forming sulphates are deduced by the difference between the total soluble sulphates and the acid forming soluble sulphates.

A.2.1. Mineralogical characterisation

A.2.1. Quantitative x-ray diffraction (QXRD)

i. Split the samples to attain statistically equal aliquots with a mass of 3.5 grams each. Reserve two of these samples for analysis

ii. Micronize the samples for 10 minutes, remove all sample for the mill and clean the mill using 90% Ethanol solution.

iii. Dry the samples under drying lamps

iv. Powder QXRD spectra is obtained by using a Bruker D8 Advance powder diffractometer with Vantec detector and fixed divergence and receiving slits with Co-Ka radiation.

v. The phases are identified using Bruker Topas 4.1 software and the relative phase (weight %) were estimated using the Rietveld method.

The samples were prepared for QXRD analysis at the centre for mineral research (CMR) laboratory and analysed at the Department of Chemical Engineering at the University of Cape Town.

A 2.2. Quantitative evaluation of minerals by scanning electron microscopy (QEMSCAN)

i. Samples were prepared in duplicate and analysed at the Eskom Research and Innovation Centre (ERIC), Rosherville, Johannesburg.

ii. Each sample is split to produce a representative 0.2 gram sample

iii. 30mm mould blocks are prepared by heating the moulds in an oven for 30 minutes at 80^{o}C with the insides of the blocks coated with oil

iv. Carnauba wax flakes are melted in a microwave for 5 minutes and poured into the prepared moulds to the ¾ level mark.

v. The weighed samples are added to the moulds and stirred in a figure of 8 pattern

vi. The moulds are then returned to the oven at 60^{o}C for 40 minutes

vii. Once cooled and free of defects, grit and deep scratches are removed by surface grinding and polishing

viii. The polished surfaces are coated with graphite and analysed using QEMSCAN (Instrument is based on a Zeiss EVO 50 SEM)

A.3. AMD prediction methods

A 3.1. Acid neutralising capacity (ANC) methods

Fizz rating

Approximately 1.0 g sample is reacted with 1-2 drops of 25% HCl. The reaction of carbonates within the sample is noted by an audible/visible fizz. The intensity of the fizzing is rated based on Table A. 1.3 – Section **Error! Reference source not found.** and the volume and concentration of the HCl used to the ANC tests is based thereon.

Table A.2.1: Fizz rating and acid-base additions for the ANC tests

Reaction	Fizz Rating	HCl molarity (M)	HCl volume (ml)	NaOH molarity (M)
None	0	0.5	4	0.1
Slight	1	0.5	8	0.1
Moderate	2	0.5	20	0.5
Strong	3	0.5	40	0.5
Very strong	4	1.0	40	0.5
Carbonate	5	1.0	60	0.5

Once the HCl has added to the sample, the solution pH is measured to ensure that it was between 0.8 and 1.5. If the pH is found to be outside of this range, the fizz rating is readjusted according to Table 13 and the ANC tests repeated.

A 3.1.2 Hydrogen peroxide for siderite correction in the ANC tests

Acid Digestion

i. Weigh duplicate samples of 2 g into 250 ml Erlenmeyer flasks.
ii. Add HCl according to fizz rating and make up to 100 ml with de-ionised water.
iii. Boil for 5 min

Back titration

iv. Allow to cool and filter solution.
v. Confirm liquor pH is between 0.8 and 1.5
vi. Using a burette, back titrate liquor to pH 4.5, recording NaOH addition.
vii. Add 5 ml 30% H_2O_2 and boil for another 5min
viii. Back titrate to pH 7
ix. Leave solution for 24 hours
x. Check pH and back titrate to pH 7.
xi. Add a further 5 ml H_2O_2, boil for 5 min.
xii. Repeat steps viii. to xi. over 72 hours.

ANC is calculated according to Equation (10) – Section **Error! Reference source not found.**:

$$ANC = \frac{[Vol_{HCl} - Vol_{NaOH} \times C] \times M_a \times 49}{W} \quad \text{Equation (10)}$$

Where:

M_a is the concentration of HCl as molarity (M)

W is the mass of the sample in grams (g),

Vol_{HCl} is the volume of HCl (in litres L) added as instructed by the fizz rating

Vol_{NaOH} is the volume (L) of NaOH titrated.

A stoichiometric conversion factor of 49 is used to give the units kg H_2SO_4/tonne of material.

A blank sample is prepared in accordance with the fizz rating obtained for the sample. Equation (11) shows the computation of C.

$$C = \frac{Vol_{HCl} inBlank}{Vol_{NaOH} inBlank} \quad \text{Equation (11)}$$

A 3.2 Net acid generation (NAG) test methods

A.3.2.1 Single addition NAG test

i. Weigh 1.25 g sample into 250ml Erlenmeyer flask.

ii. Add 125ml 15% H_2O_2, cover, and allow to react for 24h in a fume hood.

iii. Measure pre-boil pH.

iv. Heat solution until effervescence stops or for a minimum of 2 hours.

v. Allow to cool, make up volume to 125ml with de-ionised water.

vi. Record after-boil pH.

vii. Filter, retaining solids residue and liquor.

viii. Back titrate with NaOH recording volume added at pH 4.5 and pH 7.

The NAG at pH 4.5 and pH 7 respectively were calculated according to Equation 13 – Section **Error! Reference source not found.**:

$$NAG = \frac{49 \times Vol_{NaOH} \times M_b}{W} \quad \text{Equation (13)}$$

Where, Vol_{NaOH} is the volume of NaOH in litres (L), 49 is the stoichiometric conversation factor, M_b is the concentration of the base (NaOH) in molarity (M) and W is the mass of the sample is grams (g).

A.3.2.2. Sequential NAG test

i. Carry out single addition NAG test as stage 1 of sequential NAG

ii. Repeat steps ii. to viii. on solid residue until no effervescent reaction is seen and after-boil NAG pH is > pH 4.5

A 4. Kinetic tests – Microbial AMD prediction test methods

A 4.1. Draw and fill shake flask tests

All draw and fill tests were conducted in triplicate.

i. Sterilize the autotrophic basalt salt (ABS) solution in an autoclave.

ii. Separate the ABS solution into two equal parts. Adjust the pH of one part using concentrated H_2SO_4 to pH 2 and the other to pH 6 using concentrated NaOH

The same procedure is applied for the pH 2 media and the pH 6 media.

iii. Add 150ml autotrophic basal salts (ABS) solution to 250 ml Erlenmeyer flask.

iv. Weigh in 7.5 grams tailings sample into each flask.

v. Inoculate with 7.5 ml mixed culture of iron and sulphur oxidising microorganisms.

vi. Measure Redox potential and pH.

vii. Weigh each flask and place in shaking incubator at 150 rpm at 37°C.

viii. Before sampling, weigh flask. Top up with de-ionised water to account for water loss by evaporation.

ix. Every 2-4 days remove the flasks from the shaking incubator and allow the sediment to settle. Record pH, redox, ferrous and total iron concentrations before removing 90% of the supernatant.

x. Using a syringe and rubber tube, remove 135mL of supernatant and replenish with the required ABS solution (according to whether the test condition is acid fed or circum-neutral fed)

xi. After approximately two weeks, sampling instances are adjusted to 1 week

Ferrous assay is conducted following the 1-10 phenanthroline method (Komadel and Stucki 1988).

A 4.2 Batch tests

All batch tests were conducted in duplicate.

i. Steps i. to viii. are repeated for the batch tests

ii. Redox, pH, ferrous iron and total iron concentrations were recorded every 2-4 days.

A 4.3. Static AMD prediction results

A.4.3.1. Acid base accounting results

Table A.4.3.1: Acid base accounting results for the untreated size fractions

Sample	MPA (kg H2SO4/ton)	ANC	NAPP
- 75µm	63.65 ±1.27	31.90 ± 0.26	31.75 ± 1.03
+ 75 - 106µm	49.57 ±0.99	27.69 ± 0.58	21.88 ± 0.413
+ 106 - 180µm	32.74 ± 0.01	29.82 ± 0.04	2.93 ± 0.028
+180 - 212µm	30.91 ± 0.01	31.43 ± 2.58	-0.50 7± 2.57
+212 - 355µm	31.52 ± 0.01	28.21 ± 2.95	3.31 ± 2.94

A.4.3.2. Net acid generating results

Table A.4.3.2: Sequential net acid generating test results with stage 1 also indicating the single addition test

		-75µm		+75 - 106 µm		+106 - 180 µm		+180 -212 µm		+212-355 µm	
	NAG	Test (1)	Test (2)	Test (1)	Test (2)	Test (1)	Test (2)	Test (1)	Test (2)	Test (1)	Test (2)
Stage 1	NAGpH	2.48	2.52	2.89	5.69	2.84	2.82	3.12	2.88	2.92	3.01
	$NAGpH_{4.5}$	28.62	29.40	20.78	21.17	22.34	20.38	14.50	22.15	19.60	16.86
	$NAGpH_{7.0}$	57.04	29.60	26.66	1.96	29.79	31.36	29.99	49.39	24.30	40.77
Stage 2	NAGpH	2.68	2.67	3.18	2.72	2.74	2.73	2.73	2.75	2.73	2.72
	$NAGpH_{4.5}$	49.85	54.00	69.10	55.63	59.01	57.21	62.01	60.68	71.84	67.33
	$NAGpH_{7.0}$	35.13	39.60	40.06	52.77	40.09	39.30	48.76	37.34	41.05	39.97
Stage 3	NAGpH	5.72	5.301	4.94	4.66	4.97	5.11	4.6	4.76	4.76	4.76

A.5. 1. QEMSCAN modal reports

Table A.5. 1: QEMSCAN modal results for the untreated size fractions

	Sample (µm)				
	+212 -355	+180 – 212	+106 - 180	+75 - 106	-75
Min Size (µm)	212.0	180.0	106.0	75.0	0.0
Max Size (µm)	355.0	212.0	180.0	106.0	75.0
Calculated ESD Particle Size (µm)	146.0	64.1	64.8	35.8	48.8
	Sample (µm)				
Mineral Mass (%)	+212 -355	+180 – 212	+106 - 180	+75 - 106	-75
Sulphate	0.76	0.07	0.53	0.72	2.16
Muscovite	0.96	0.81	1.13	0.92	0.97
Muscovite_Illite	0.94	0.60	0.97	0.92	1.35
Albite	0.00	0.00	0.00	0.00	0.00
Ferrosilite	0.10	0.05	0.12	0.12	0.15
Microcline	2.01	0.49	2.17	3.00	2.75
Kaolinite	18.12	18.60	20.19	18.51	15.34
Quartz	19.66	17.18	21.22	23.80	16.80
Pyrite	5.06	2.62	6.91	7.95	6.73
Alunite	0.12	0.10	0.16	0.14	0.12
Siderite	2.03	1.42	1.73	1.55	5.07
Hematite	0.02	0.00	0.01	0.03	0.11
Rutile	0.14	0.09	0.16	0.16	0.20
Calcite	3.81	2.17	4.75	5.71	3.06
Dolomite	0.52	0.35	0.52	0.43	0.74
Ankerite	0.13	0.06	0.17	0.16	0.23
Gypsum	1.15	0.03	0.73	1.07	3.42
Monazite	0.00	0.00	0.00	0.00	0.00
Zircon	0.03	0.03	0.01	0.00	0.08
Barite	0.06	0.00	0.03	0.06	0.25
Spinel	0.00	0.34	0.08	0.13	0.01
Bright Coal	8.16	5.35	5.30	7.35	5.51
Dull Coal	47.24	33.34	30.09	35.16	35.74
	Sample (µm)				
ESD particle size per mineral (µm)	+212 -355	+180 – 212	+106 - 180	+75 - 106	-75
Calculated ESD Particle size	146.01	64.09	64.76	35.82	48.80
Muscovite	10.67	10.55	10.25	10.37	11.74
Muscovite_Illite	8.53	8.64	8.82	9.00	9.40
Albite	7.84	12.48	11.12	15.28	14.85
Ferrosilite	9.43	9.31	15.44	11.44	12.32
Microcline	16.84	27.46	36.70	23.25	30.44
Kaolinite	22.37	19.99	20.79	16.67	19.00

Quartz	48.08	37.50	42.08	24.61	33.62
Pyrite	51.70	40.03	45.80	25.17	30.15
Alunite	11.71	11.51	13.75	11.94	14.64
Siderite	30.37	21.79	21.34	19.79	19.51
Hematite	12.35	10.43	15.14	12.64	11.62
Rutile	16.76	15.44	17.98	16.09	22.27
Calcite	57.48	49.72	59.80	26.21	37.37
Dolomite	13.44	13.76	16.01	15.44	18.87
Ankerite	8.59	11.83	10.50	10.92	10.76
Gypsum	12.61	26.43	32.64	28.58	37.08
Monazite	8.33	7.76	7.73	7.64	8.32
Zircon	18.39	13.37	12.50	13.49	15.28
Barite	18.75	19.19	42.21	26.51	27.42
Spinel	11.25	108.04	52.50	57.59	11.25
Coal	26.49	46.19	20.93	20.60	15.93

Table A.5. 2: QEMSCAN modal results for the pH 2 biokinetic draw and fill residues

	Sample (µm)				
Name	+212 -355	+180 – 212	+106 - 180	+75 - 106	-75
Min Size	212.0	180.0	106.0	75.0	0.0
Max Size	355.0	212.0	180.0	106.0	75.0
Calculated ESD Particle Size	152.0	106.7	60.3	60.7	152.0
	Sample (µm)				
Mineral	+212 -355	+180 – 212	+106 - 180	+75 - 106	-75
Sulphate	0.07	0.06	0.07	0.04	0.07
Muscovite	0.67	0.90	0.76	0.92	0.67
Muscovite_Illite	0.58	0.76	0.76	1.13	0.58
Albite	0.00	0.00	0.00	0.00	0.00
Ferrosilite	0.00	0.00	0.00	0.00	0.00
Microcline	0.92	1.86	1.50	2.39	0.92
Kaolinite	20.85	27.50	23.06	18.53	20.85
Quartz	15.50	17.86	12.11	14.42	15.50
Pyrite	0.04	0.11	2.34	0.26	0.04
Alunite	0.14	0.14	0.16	0.09	0.14
Siderite	0.49	0.63	1.68	1.03	0.49
Hematite	0.00	0.01	0.01	0.00	0.00
Rutile	0.06	0.09	0.27	0.12	0.06
Calcite	0.00	0.01	0.00	0.00	0.00
Dolomite	0.00	0.00	0.00	0.00	0.00
Ankerite	0.00	0.00	0.00	0.00	0.00
Gypsum	0.00	0.00	0.00	0.00	0.00
Monazite	0.00	0.00	0.00	0.00	0.00
Zircon	0.00	0.00	0.01	0.06	0.00

Barite	0.00	0.00	0.02	0.10	0.00
Spinel	0.00	0.00	0.00	0.06	0.00
Bright Coal	11.79	7.79	9.84	11.05	11.79
Dull Coal	48.95	42.32	47.48	49.82	48.95
	Sample (µm)				
ESD particle size per mineral (µm)	+212 -355	+180 – 212	+106 - 180	+75 - 106	-75
Calculated ESD Particle size	151.97	106.66	60.31	60.72	151.97
Muscovite	10.28	10.01	9.60	9.64	10.28
Muscovite_Illite	9.01	8.70	8.52	8.74	9.01
Albite	9.06	16.85	17.28	10.63	9.06
Ferrosilite	8.91	9.61	10.98	10.05	8.91
Microcline	25.44	31.06	25.44	27.65	25.44
Kaolinite	24.89	23.95	19.86	17.16	24.89
Quartz	53.56	40.43	27.41	26.64	53.56
Pyrite	24.88	22.35	25.95	27.76	24.88
Alunite	13.08	13.93	10.96	14.32	13.08
Siderite	14.68	13.58	16.97	12.66	14.68
Hematite	7.50	13.55	8.86	15.58	7.50
Rutile	14.61	13.30	21.58	15.74	14.61
Calcite	11.25	8.38	9.75	7.50	11.25
Dolomite	0.00	7.50	7.50	7.50	0.00
Ankerite	0.00	0.00	7.50	7.50	0.00
Gypsum	11.93	10.74	9.37	8.63	11.93
Monazite	11.29	7.85	7.66	8.10	11.29
Zircon	11.79	7.50	10.50	12.48	11.79
Barite	12.50	0.00	16.61	32.88	12.50
Spinel	0.00	0.00	17.50	76.25	0.00
Coal	49.83	35.78	26.59	28.37	49.83

Table A.5. 3: QEMSCAN modal results for the pH 6 biokinetic draw and fill residues

	Sample (µm)				
	+212 -355	+180 – 212	+106 - 180	+75 - 106	-75
Min Size	212.0	180.0	106.0	75.0	0.0
Max Size	355.0	212.0	180.0	106.0	75.0
Calculated ESD Particle Size	63.6	120.2	139.8	58.9	103.2
	Sample (µm)				
Mineral	+212 -355	+180 – 212	+106 - 180	+75 - 106	-75
Sulphate	0.05	0.02	0.04	0.02	0.01
Muscovite	1.02	0.80	0.91	0.90	0.94
Muscovite_Illite	0.83	0.57	0.63	0.96	0.72
Microcline	2.85	0.87	0.79	3.79	2.95
Kaolinite	26.88	23.28	26.23	24.15	27.56

Quartz	23.13	18.93	17.73	22.10	22.61
Pyrite	3.72	1.42	2.49	2.05	0.12
Alunite	0.11	0.05	0.08	0.05	0.01
Siderite	1.94	1.27	0.98	1.57	0.51
Hematite	0.06	0.00	0.00	0.00	0.00
Rutile	0.16	0.18	0.08	0.17	0.13
Calcite	0.01	0.01	0.00	0.00	0.01
Dolomite	0.00	0.01	0.00	0.00	0.00
Ankerite	0.00	0.00	0.00	0.00	0.00
Gypsum	0.00	0.00	0.00	0.00	0.00
Zircon	0.01	0.01	0.01	0.04	0.03
Barite	0.11	0.01	0.01	0.04	0.08
Spinel	0.00	0.00	0.00	0.00	0.00
	Sample (µm)				
ESD particle size per mineral (µm)	+212 -355	+180 – 212	+106 - 180	+75 - 106	-75
Calculated ESD Particle size	63.60	120.20	139.79	58.91	103.24
Muscovite	10.48	10.64	10.14	9.76	10.11
Muscovite_Illite	9.03	8.56	8.55	8.45	8.49
Microcline	35.00	21.96	21.85	35.14	41.69
Kaolinite	23.31	23.22	24.19	20.15	24.71
Quartz	40.71	45.78	41.89	34.95	45.46
Pyrite	36.40	32.25	33.87	29.86	44.61
Alunite	11.44	9.20	10.14	9.62	11.89
Siderite	18.12	20.87	21.06	16.27	13.38
Hematite	15.98	8.86	10.00	9.55	10.56
Rutile	16.09	22.54	11.24	16.46	15.96
Calcite	15.20	11.10	9.64	8.75	11.05
Dolomite	8.63	11.08	7.50	9.00	8.80
Ankerite	7.50	8.44	7.50	7.50	7.50
Gypsum	9.74	10.12	8.90	8.94	14.60
Zircon	11.41	13.24	12.67	12.73	13.08
Barite	37.60	25.83	28.93	26.65	49.61
Spinel	0.00	22.50	10.50	7.50	7.50
Coal	23.22	37.88	35.83	23.94	32.77

A.5. 2.QEMSCAN association reports

Table A.5. 4: QEMSCAN mineral-mineral association results for the untreated size fractions

-75µm							
Kaolinite	Quartz	Pyrite	Siderite	Calcite	Dolomite	Coal	Other
20.82	30.83	26.47	22.45	28.45	19.95	63.96	18.96
0.00	26.46	26.36	15.15	5.24	9.04	17.91	8.50
20.37	0.00	1.58	8.15	2.42	2.92	10.31	7.56
2.37	0.19	0.00	1.40	2.12	0.31	1.11	1.66
1.63	1.14	1.67	0.00	0.63	1.80	1.49	5.86
1.01	0.61	4.54	1.13	0.00	24.73	2.20	21.60
0.39	0.16	0.15	0.73	5.56	0.00	0.57	0.69
51.69	38.63	35.50	39.97	32.93	38.01	0.00	35.18
1.72	1.98	3.73	11.03	22.65	3.23	2.46	0.00
+75 - 106µm							
Kaolinite	Quartz	Pyrite	Siderite	Calcite	Dolomite	Coal	Other
27.76	36.49	33.98	32.32	32.91	26.14	68.49	23.40
0.00	21.58	16.47	7.95	3.68	6.59	13.90	5.10
17.28	0.00	2.39	5.15	2.52	3.59	8.57	5.93
2.69	0.49	0.00	4.63	2.05	0.35	1.61	2.19
1.64	1.33	5.86	0.00	0.67	2.15	2.10	9.01
0.94	0.80	3.19	0.83	0.00	22.42	1.99	22.36
0.29	0.20	0.10	0.47	3.93	0.00	0.46	0.44
47.80	36.80	33.81	35.01	26.79	35.66	0.00	31.56
1.60	2.32	4.20	13.64	27.45	3.09	2.87	0.00
+106 - 180µm							
Kaolinite	Quartz	Pyrite	Siderite	Calcite	Dolomite	Coal	Other
17.40	27.27	25.97	17.98	26.70	16.69	60.82	18.72
0.00	33.11	24.17	23.53	8.55	10.37	21.47	12.65
23.58	0.00	2.16	10.97	3.75	6.72	10.54	9.25
2.67	0.33	0.00	1.72	5.92	0.70	1.64	2.61
1.57	1.03	1.04	0.00	0.78	2.09	1.00	3.93
1.23	0.76	7.74	1.70	0.00	20.51	2.20	15.50
0.34	0.31	0.21	1.02	4.61	0.00	0.51	1.28
51.68	35.63	35.85	35.97	36.74	38.16	0.00	36.06
1.53	1.57	2.86	7.11	12.96	4.75	1.81	0.00
+180 - 212µm							
Kaolinite	Quartz	Pyrite	Siderite	Calcite	Dolomite	Coal	Other
16.61	23.90	23.97	23.45	25.63	15.90	60.05	16.88
0.00	37.08	24.28	16.21	11.86	8.86	23.17	14.07
24.18	0.00	1.85	9.71	3.99	4.46	10.17	9.03
2.42	0.28	0.00	2.71	6.31	0.61	1.61	3.25
1.06	0.98	1.78	0.00	0.57	2.55	1.05	5.87
1.51	0.78	8.03	1.11	0.00	29.43	1.78	14.40

0.31	0.24	0.21	1.35	8.02	0.00	0.54	0.94
52.44	35.30	36.47	36.11	31.75	35.35	0.00	35.56
1.47	1.45	3.41	9.37	11.86	2.85	1.64	0.00

+212 - 355µm

Kaolinite	Quartz	Pyrite	Siderite	Calcite	Dolomite	Coal	Other
5.83	9.22	7.80	7.81	10.10	5.15	47.93	8.56
0.00	37.15	21.62	24.10	17.02	6.70	33.27	16.83
21.03	0.00	2.05	18.09	5.42	4.09	13.69	9.71
0.83	0.14	0.00	1.04	6.91	0.11	0.90	3.62
1.23	1.63	1.39	0.00	1.59	2.28	0.88	8.13
1.18	0.67	12.55	2.17	0.00	27.41	1.25	10.24
0.22	0.23	0.09	1.43	12.65	0.00	0.81	1.08
68.63	49.89	48.64	35.47	37.17	52.17	0.00	41.83
1.05	1.07	5.87	9.89	9.15	2.09	1.26	0.00

A 5.3. Sulphur speciation results

Table A.5.5: Results for the KCl extraction method for non-acid forming sulphates

Sample (µm)	Concentration (g/L)	% Non-acid sulphates
-75	1.78	0.71 ± 0.11
+ 75 - 106	1.13	0.45 ± 0.11
+ 106-180	0.64	0.25 ± 0.10
+ 180 - 212	0.45	0.18 ± 0.06
+ 212 - 355	0.31	0.12 ± 0.17

Table A.5.6: Results for the chromium reducible sulphur method for pyritic sulphur

Sample No:	Sample (µm)	S_2 (mg/L)	FeS_2 (g/L)	FeS_2 (g)	m_{sample} (g)	S^{2-} (wt%)	Standard Error
1	- 75	27.93	0.052	0.002	0.501	0.223	
2	- 75	37.34	0.070	0.003	0.501	0.298	0.038
1	- 75	94.71	0.177	0.007	0.503	0.754	
2	- 75	106.9	0.200	0.008	0.503	0.851	0.048
1	+ 75 - 106	14.87	0.028	0.001	0.523	0.114	
2	+ 75 - 106	10.32	0.019	0.001	0.523	0.079	0.017
1	+ 75 - 106	95.62	0.179	0.007	0.523	0.732	
2	+ 75 - 106	96.53	0.181	0.007	0.523	0.739	0.0035
1	+ 106 - 180	12.14	0.023	0.001	0.529	0.092	
2	+ 106 - 180	34.91	0.065	0.003	0.529	0.264	0.086
1	+ 106 - 180	104.7	0.196	0.008	0.525	0.798	
2	+ 106 - 180	95.32	0.178	0.007	0.525	0.726	0.036
1	+ 180 - 212	10.01	0.019	0.001	0.525	0.076	
2	+ 180 - 212	9.107	0.017	0.000	0.525	0.069	0.003
1	+ 180 - 212	3.946	0.007	0.000	0.525	0.030	
2	+ 180 - 212	3.946	0.007	0.000	0.525	0.030	0.000
1	+ 212 - 355	7.892	0.015	0.001	0.521	0.061	
2	+ 212 - 355	6.071	0.011	0.000	0.521	0.047	0.007

Table A.5.7: ISO 157 sulphur speciation results

	Concentration of sulphur forms (mass %)		
Sample (µm)	Pyritic sulphur	Acid sulphates	Organic S (By difference)
- 75	1.05 ± 0.05	0.52 ± 0.01	0.51 ± 0.06
+ 75- 106	0.86 ± 0.04	0.29 ± 0.01	0.33 ± 0.05
+ 106- 180	0.72 ± 0.04	0.11 ± 0.00	0.24 ± 0.04
+180- 212	0.67 ± 0.03	0.09 ± 0.00	0.25 ± 0.04
+212- 355	0.64 ± 0.03	0.05 ± 0.00	0.34 ± 0.03

A.5. 4.Petrography report

A. OBJECTIVES

The main purposes of this investigation were to assess the coal in terms of its petrographic properties (rank, organic composition and general condition).

B. BACKGROUND AND INFORMATION

A brief summary of the basic aspects of coal petrology

Coals are complex combustible sedimentary rocks formed from consolidated plant remains.

They can be ranked as lignite, sub-bituminous coal, bituminous coal or anthracite according to their degree of maturation in the continuous evolution towards a pure carbon structure.

Coal petrology involves the microscopic examination of coals together with the interpretation of the analytical data and can provide valuable information regarding organic composition, maturity and the associations of the organic matter and minerals that the coals contain.

Petrographic data should be used, together with chemical and physical parameters, for the full characterization of coals necessary to gain insight into their behaviour in technological processes.

C. Classification

Coals can be classified according to three major fundamental and independent parameters:

- **Organic composition:**

This relates to the **microscopically discernable organic components of coal that are termed "macerals"** and which are analogous to minerals in inorganic rocks.

Three maceral groups are recognized - *vitrinite, liptinite and inertinite*.

These are distinguished from one another under the petrographic microscope by differences in reflectance, morphology, colour, shape, size, polishing hardness and fluorescence. Their optical, physical, chemical and technological characteristics alter as the coal matures.

- **Rank:**

This refers to the **degree of maturation**, i.e., the stage in the evolution or coalification of the plant remains.

- **Grade:**

This relates to the impurities present, conveniently represented by the **ash yield** (incombustibles remaining after burning).

The organic composition (i.e., the relative proportions of the macerals), the rank, the grade and the "freshness" of the coal, together with the process conditions applied, are all influential factors governing the technological performance of the coal.

Presentation of results tables	**Table**
Mean maximum reflectance value	a
Maceral analysis	a
Vitrinite maximum reflectance data	b
Condition analysis	c
Summary of major characteristics	d

Table A.5.8. 1: Mean maximum reflectance value

MACERAL ANALYSIS (PERCENT BY VOLUME, MINERAL MATTER FREE BASIS)															RANK REFLECTANCE	
VITRINITE			LIPTINITE			INERTINITE								TOTAL		
VIT %	PV %	TV %	S/R/C %	ALG %	TOT L %	RSF %	ISF %	F/ SEC %	MIC %	R INT %	I INT %	TOT I %	HEAT ALTERED %	OTHER %	REACTIVES %	_ Rmax %	s
17	2	19	4	0	4	12	22	6	2	12	23	77	0	0	47	0.88	0.094
THESE RESULTS RELATE ONLY TO THE SAMPLES ANALYSED																	

Table A.5.8. 2: Vitrinite maximum reflectance data

REFLECTANCE CLASSES (%)																	STANDARD DEVIATION	MEAN MAXIMUM REFLECTANCE
V 3	V 4	V 5	V 6	V 7	V 8	V 9	V 10	V 11	V 12	V 13	V 14	V 15	V 16	V 17	V 18	V 19	V 20 and >	s	Rmax%
			2	23	45	19	9	2										0.094	0.88

Table A.5.8. 3: Condition analysis

Fresh coal particles	Pyrite		Particles with extensive cracks	Severely weathered	Particles with desiccation	Particles with oxidized/thermally	Particles displaying low temperature	Severely heat altered	Total abnormal
%	normal %	altered %	or fissures %	particles %	cracks %	affected rims or zones %	devolatilization %	(coke/char) %	particles %
63	1	0	23	11	2	0	0	0	**36**

Note: A significant proportion of the particles examined displayed extensive cracks and micro-fissures. Some cracking probably occurred during handling and preparation due to the somewhat brittle nature of coal (particularly vitrinite) of this level of maturity. Approximately 11% of organic particles displayed signs of severe weathering.

Table A.5.8. 4: Summary of major characteristics

Mean maximum reflectance %	**0.88**
Vitrinite-class distribution	**V 6 to V 11**
Standard deviation **s**	**0.094**
Evidence of heating effects	**None observed**
PETROGRAPHIC COMPOSITION % by vol.	
Maceral analysis (mineral matter-free)	
Total reactive macerals %	**47**
Vitrinite content %	19
Liptinite content %	4
Total inertinite %	77
More highly reflecting material %	0
Other %	0
Maceral analysis - Total %	**100**
Condition analysis	
"Fresh" coal particles %	64
Cracks and fissures %	25
Severely weathered %	11
Particles exhibiting oxidation rims %	0
Particles displaying low temperature devolatilization %	0
Heat altered (e.g., coke/char) %	0
Condition analysis - Total %	**100**

A 6. Biokinetic results

A 6.1.1. Draw and fill biokinetic results (biotic – inoculated experiments)

Table A.6. 1: Redox potential and standard errors for the acid fed draw and fill bioleach experiments

	Redox potentials (mV)					Standard Error Sample (± mV)				
Time (Days)	-75µm	+75-106µm	+106-180µm	+180-212µm	+212-355µm	-75µm	+75 - 106µm	+106 - 180µm	+180-212 µm	+212-355 µm
0	569.67	576.33	604.67	612.67	628.00	8.00	6.43	8.62	3.21	4.51
3	554.00	509.67	501.33	485.67	524.00	29.28	38.59	10.58	2.65	196.70
6	572.67	610.00	604.67	573.67	608.00	16.70	7.81	35.79	11.53	10.02
10	670.00	687.67	668.67	656.00	654.67	17.06	64.95	4.36	9.07	6.66
13	685.33	697.67	682.67	674.00	668.33	7.81	22.74	43.62	42.00	7.37
17	680.33	679.33	666.33	652.00	626.33	72.77	22.50	49.69	3.21	54.45
21	630.00	640.00	600.67	595.33	576.67	72.77	22.50	49.69	3.21	54.45
22	630.00	640.00	600.67	595.33	576.67	28.00	5.86	24.17	8.96	177.15
25	642.67	645.33	604.33	587.00	562.00	21.03	20.00	38.51	12.53	5.57
28	642.67	645.33	604.33	587.00	562.00	12.74	24.25	23.81	8.96	177.15
36	669.33	647.67	611.00	578.00	544.00	25.77	7.94	5.13	4.93	9.54
41	642.67	645.33	604.33	587.00	562.00	16.09	2.52	12.86	4.58	7.51
49	632.33	612.00	611.00	608.33	536.67	27.06	4.73	15.31	7.77	3.46
60	642.33	630.67	650.00	658.33	620.00	25.01	10.97	22.30	5.51	7.07
70	659.67	652.00	658.33	663.67	656.00	25.01	10.97	22.30	5.51	7.07
78	636.67	641.33	641.00	645.67	649.00	46.14	10.15	13.58	7.37	1.53
87	630.00	632.67	637.33	644.67	642.00	8.00	6.43	8.62	3.21	4.51

Table A.6. 2: Redox potential and standard errors for the circum-neutral fed draw and fill bioleach experiments

	Redox potentials (mV)					Standard Error Sample (± mV)				
Time (Days)	-75µm	+75-106µm	+106-180µm	+180-212µm	+212-355µm	-75µm	+75 - 106µm	+106 - 180µm	+180-212 µm	+212-355 µm
0	577.00	606.33	623.33	600.33	595.33	4.62	3.71	4.98	1.86	2.60
3	251.33	258.33	214.00	194.00	423.00	16.90	22.28	6.11	1.53	113.56
6	249.00	207.00	215.00	227.00	233.33	9.64	4.51	20.66	6.66	5.78
10	239.00	136.00	174.00	189.67	182.67	9.85	37.50	2.52	5.24	3.84
13	308.00	279.33	396.33	265.67	264.67	4.51	13.13	25.18	24.25	4.26
17	284.00	288.67	236.33	260.33	221.50	42.02	12.99	28.69	1.86	31.44
21	284.00	288.67	236.33	260.33	221.50	42.02	12.99	28.69	1.86	31.44
22	380.00	325.67	328.67	328.33	306.00	16.17	3.38	13.96	5.17	102.28
25	397.33	402.00	362.00	335.00	340.00	12.14	11.55	22.23	7.23	3.21
28	382.33	326.00	322.00	328.33	204.00	7.36	14.00	13.75	5.17	102.28
36	389.67	321.00	344.33	347.67	332.00	14.88	4.58	2.96	2.85	5.51
41	367.00	335.33	339.67	323.00	317.67	9.29	1.45	7.42	2.65	4.33
49	387.33	345.67	348.33	327.67	312.00	15.62	2.73	8.84	4.48	2.00
60	399.33	345.33	350.33	316.33	294.00	14.44	6.33	12.88	3.18	4.08
70	399.33	345.33	350.33	316.33	294.00	14.44	6.33	12.88	3.18	4.08
78	447.33	383.00	414.67	391.33	363.67	26.64	5.86	7.84	4.26	0.88
87	577.00	606.33	623.33	600.33	595.33	4.62	3.71	4.98	1.86	2.60

Table A.6. 3: Ferric iron generated in the draw and fill acid fed bioleach experiments

	Ferric iron concentration (grams)					Standard Error of sample (± grams)				
Time (Days)	-75µm	+75 -106µm	+106-180µm	+180-212µm	+212-355µm	-75µm	+75 -106µm	+106-180µm	+180-212µm	+212-355µm
0	0.0046	0.0047	0.0052	0.0052	0.0049	0.000	0.001	0.000	0.000	0.001
3	0.0013	0.0012	0.0016	0.0023	0.0019	0.000	0.000	0.000	0.001	0.001
6	0.0029	0.0029	0.0028	0.0020	0.0018	0.000	0.000	0.000	0.001	0.000
10	0.0161	0.0155	0.0151	0.0115	0.0108	0.001	0.000	0.000	0.003	0.002
13	0.0132	0.0158	0.0113	0.0097	0.0080	0.001	0.000	0.000	0.003	0.001
17	0.0011	0.0010	0.0008	0.0007	0.0005	0.000	0.000	0.000	0.000	0.000
21	0.0014	0.0014	0.0012	0.0007	0.0007	0.000	0.000	0.000	0.000	0.000
22	0.0019	0.0022	0.0013	0.0011	0.0007	0.000	0.000	0.000	0.001	0.000
25	0.0006	0.0015	0.0006	0.0004	0.0003	0.001	0.000	0.000	0.000	0.000
28	0.0009	0.0006	0.0006	0.0005	0.0004	0.001	0.000	0.000	0.000	0.000
36	0.0062	0.0023	0.0024	0.0012	0.0004	0.001	0.000	0.000	0.001	0.000
41	0.0009	0.0006	0.0006	0.0005	0.0004	0.001	0.000	0.000	0.000	0.000
49	0.0032	0.0020	0.0031	0.0026	0.0005	0.001	0.002	0.000	0.003	0.000
60	0.0035	0.0037	0.0033	0.0068	0.0028	0.001	0.000	0.000	0.001	0.002
70	0.0048	0.0051	0.0043	0.0072	0.0067	0.001	0.005	0.000	0.002	0.001
78	0.0020	0.0021	0.0020	0.0033	0.0034	0.000	0.000	0.000	0.001	0.000
87	0.0016	0.0015	0.0000	0.0000	0.0000	0.000	0.000	0.000	0.001	0.000

Table A.6.4: Ferric iron generated in the draw and fill circum-neutral fed bioleach experiments

	Ferric iron concentration (grams)					Standard Error of sample (± grams)				
Time (Days)	-75µm	+75 -106µm	+106-180µm	+180-212µm	+212-355µm	-75µm	+75 -106µm	+106-180µm	+180-212µm	+212-355µm
0	0.0042	0.0041	0.0044	0.0043	0.0044	0.0014	0.0001	0.0001	0.0000	0.0001
3	0.0013	0.0013	0.0014	0.0012	0.0011	0.0001	0.0003	0.0001	0.0002	0.0001
6	0.0014	0.0007	0.0009	0.0013	0.0014	0.0006	-0.0003	0.0005	0.0003	0.0005
10	0.0003	0.0000	0.0000	0.0000	0.0000	0.0002	0.0000	0.0000	-0.0001	0.0000
13	0.0004	0.0004	0.0003	0.0004	0.0003	0.0000	0.0000	0.0000	0.0001	0.0001
17	0.0001	0.0001	0.0001	0.0000	0.0001	0.0000	0.0000	0.0000	0.0000	0.0000
21	0.0004	0.0005	0.0005	0.0005	0.0006	0.0000	0.0000	0.0000	0.0001	0.0000
22	0.0007	0.0007	0.0007	0.0007	0.0006	0.0002	0.0001	0.0003	0.0001	0.0000
25	0.0007	0.0007	0.0006	0.0007	0.0007	0.0001	0.0001	0.0001	0.0002	0.0001
28	0.0002	0.0002	0.0002	0.0001	0.0002	0.0000	0.0000	0.0000	-0.0001	0.0000
36	0.0001	0.0003	0.0002	0.0003	0.0003	0.0000	0.0001	0.0000	0.0000	0.0000
41	0.0002	0.0002	0.0002	0.0001	0.0002	0.0000	0.0000	0.0000	-0.0001	0.0000
49	0.0005	0.0003	0.0003	0.0003	0.0003	0.0002	0.0000	0.0002	0.0000	0.0000
60	0.0003	0.0003	0.0003	0.0003	0.0003	0.0001	0.0001	0.0000	-0.0001	0.0000
70	0.0002	0.0002	0.0002	0.0002	0.0002	0.0002	0.0000	-0.0001	0.0001	0.0000
78	0.0006	0.0003	0.0003	0.0004	0.0004	0.0000	0.0000	0.0000	0.0000	0.0000
87	0.0004	0.0002	0.0003	0.0002	0.0003	0.0000	-0.0001	0.0000	0.0000	0.0000

Table A.6.5: Total iron generated in the draw and fill acid fed bioleach experiments

	-75 µm			+ 75 - 106 µm			+ 106 - 180 µm			+180 -212 µm			+212 - 355 µm		
Time (Days)	Fe^{total} (nm)	Fe^{Total} (g/l)	Fe^{Total} (g)	Fe^{total} (nm)	Fe^{Total} (g/l)	Fe^{Total} (g)	Fe^{total} (nm)	Fe^{Total} (g/l)	Fe^{Total} (g)	Fe^{total} (nm)	Fe^{Total} (g/l)	Fe^{Total} (g)	Fe^{total} (nm)	Fe^{Total} (g/l)	Fe^{Total} (g)
0	0.128	0.032	0.005	0.134	0.034	0.005	0.144	0.036	0.005	0.147	0.037	0.005	0.134	0.033	0.005
3	0.057	0.014	0.002	0.051	0.013	0.002	0.055	0.014	0.002	0.067	0.017	0.003	0.058	0.014	0.002
6	0.081	0.020	0.003	0.080	0.020	0.003	0.082	0.020	0.003	0.058	0.015	0.002	0.050	0.013	0.002
10	2.732	0.137	0.020	2.983	0.149	0.022	2.596	0.130	0.019	2.221	0.111	0.017	2.032	0.102	0.015
13	1.813	0.091	0.014	2.177	0.109	0.016	1.554	0.078	0.012	1.336	0.067	0.010	1.107	0.055	0.008
17	0.181	0.009	0.001	0.161	0.008	0.001	0.128	0.006	0.001	0.123	0.006	0.001	0.086	0.004	0.001
21	0.194	0.010	0.001	0.195	0.010	0.001	0.163	0.008	0.001	0.097	0.005	0.001	0.095	0.005	0.001
22	0.254	0.013	0.002	0.293	0.015	0.002	0.172	0.009	0.001	0.142	0.007	0.001	0.095	0.005	0.001
25	0.127	0.006	0.001	0.245	0.012	0.002	0.120	0.006	0.001	0.104	0.005	0.001	0.075	0.004	0.001
28	0.119	0.006	0.001	0.087	0.004	0.001	0.078	0.004	0.001	0.069	0.003	0.001	0.053	0.003	0.000
36	0.843	0.042	0.006	0.336	0.017	0.003	0.348	0.017	0.003	0.181	0.009	0.001	0.060	0.003	0.000
41	0.119	0.006	0.001	0.087	0.004	0.001	0.078	0.004	0.001	0.069	0.003	0.001	0.053	0.003	0.000
49	0.456	0.023	0.003	0.286	0.014	0.002	0.438	0.022	0.003	0.365	0.018	0.003	0.088	0.004	0.001
60	0.497	0.025	0.004	0.512	0.026	0.004	0.462	0.023	0.003	0.930	0.047	0.007	0.382	0.019	0.003
70	0.655	0.033	0.005	0.715	0.036	0.005	0.603	0.030	0.005	0.992	0.050	0.007	0.918	0.046	0.007
78	0.312	0.016	0.002	0.307	0.015	0.002	0.298	0.015	0.002	0.485	0.024	0.004	0.473	0.024	0.004
87	0.231	0.012	0.002	0.225	0.011	0.002	0.021	0.001	0.000	0.022	0.001	0.000	0.019	0.001	0.000

Table A.6.6: Errors for the total iron generated in the draw and fill acid fed bioleach experiments

	-75µm			+ 75 - 106µm			+ 106 - 180µm			+180 -212µm			+212 - 355µm		
Time (Days)	Fe^{total} (± nm)	Fe^{Total} (± g/l)	Fe^{Total} (± g)	Fe^{total} (± nm)	Fe^{Total} (± g/l)	Fe^{Total} (± g)	Fe^{total} (± nm)	Fe^{Total} (± g/l)	Fe^{Total} (± g)	Fe^{total} (± nm)	Fe^{Total} (± g/l)	Fe^{Total} (± g)	Fe^{total} (± nm)	Fe^{Total} (± g/l)	Fe^{Total} (± g)
0	0.008	0.002	0.000	0.032	0.008	0.001	0.002	0.000	0.000	0.011	0.003	0.000	0.018	0.005	0.001
3	0.022	0.006	0.001	0.015	0.004	0.001	0.030	0.008	0.001	0.019	0.005	0.001	0.018	0.005	0.001
6	0.015	0.004	0.001	0.004	0.001	0.000	0.001	0.000	0.000	0.027	0.007	0.001	0.008	0.002	0.000
10	0.151	0.008	0.001	0.004	0.000	0.000	0.001	0.000	0.000	0.384	0.019	0.003	0.223	0.011	0.002
13	0.171	0.009	0.001	0.003	0.000	0.000	0.004	0.000	0.000	0.404	0.020	0.003	0.149	0.007	0.001
17	0.015	0.001	0.000	0.030	0.002	0.000	0.011	0.001	0.000	0.035	0.002	0.000	0.016	0.001	0.000
21	0.026	0.001	0.000	0.037	0.002	0.000	0.000	0.000	0.000	0.029	0.001	0.000	0.008	0.000	0.000
22	0.052	0.003	0.000	0.050	0.003	0.000	0.000	0.000	0.000	0.072	0.004	0.001	0.029	0.001	0.000
25	0.087	0.004	0.001	0.035	0.002	0.000	0.012	0.001	0.000	0.059	0.003	0.000	0.036	0.002	0.000
28	0.080	0.004	0.001	0.018	0.001	0.000	0.001	0.000	0.000	0.005	0.000	0.000	0.001	0.000	0.000
36	0.075	0.004	0.001	0.039	0.002	0.000	0.001	0.000	0.000	0.141	0.007	0.001	0.007	0.000	0.000
41	0.080	0.004	0.001	0.018	0.001	0.000	0.001	0.000	0.000	0.005	0.000	0.000	0.001	0.000	0.000
49	0.169	0.008	0.001	0.313	0.016	0.002	0.021	0.001	0.000	0.397	0.020	0.003	0.030	0.002	0.000
60	0.137	0.007	0.001	0.032	0.002	0.000	0.005	0.000	0.000	0.195	0.010	0.001	0.242	0.012	0.002
70	0.102	0.005	0.001	0.705	0.035	0.005	0.006	0.000	0.000	0.232	0.012	0.002	0.139	0.007	0.001
78	0.019	0.001	0.000	0.001	0.000	0.000	0.003	0.000	0.000	0.171	0.009	0.001	0.016	0.001	0.000
87	0.012	0.001	0.000	0.007	0.000	0.000	0.004	0.000	0.000	0.083	0.004	0.001	0.042	0.002	0.000

Table A.6.7: Total iron generated in the draw and fill circum-neutral fed bioleach experiments

	-75 µm			+ 75 - 106 µm			+ 106 - 180 µm			+180 -212 µm			+212 - 355 µm		
Time (Days)	Fe^{total} (nm)	Fe^{Total} (g/l)	Fe^{Total} (g)	Fe^{total} (nm)	Fe^{Total} (g/l)	Fe^{Total} (g)	Fe^{total} (nm)	Fe^{Total} (g/l)	Fe^{Total} (g)	Fe^{total} (nm)	Fe^{Total} (g/l)	Fe^{Total} (g)	Fe^{total} (nm)	Fe^{Total} (g/l)	Fe^{Total} (g)
0	0.119	0.030	0.004	0.114	0.028	0.004	0.116	0.029	0.004	0.119	0.030	0.004	0.118	0.030	0.004
3	0.038	0.010	0.001	0.035	0.009	0.001	0.042	0.010	0.002	0.037	0.009	0.001	0.036	0.009	0.001
6	0.037	0.009	0.001	0.024	0.006	0.001	0.025	0.006	0.001	0.034	0.009	0.001	0.036	0.009	0.001
10	0.056	0.003	0.000	0.016	0.001	0.000	0.012	0.001	0.000	0.017	0.001	0.000	0.013	0.001	0.000
13	0.064	0.003	0.000	0.068	0.003	0.001	0.058	0.003	0.000	0.068	0.003	0.001	0.060	0.003	0.000
17	0.030	0.002	0.000	0.024	0.001	0.000	0.019	0.001	0.000	0.020	0.001	0.000	0.024	0.001	0.000
21	0.065	0.003	0.000	0.086	0.004	0.001	0.085	0.004	0.001	0.077	0.004	0.001	0.087	0.004	0.001
22	0.112	0.006	0.001	0.094	0.005	0.001	0.098	0.005	0.001	0.092	0.005	0.001	0.083	0.004	0.001
25	0.117	0.006	0.001	0.114	0.006	0.001	0.103	0.005	0.001	0.114	0.006	0.001	0.109	0.005	0.001
28	0.042	0.002	0.000	0.047	0.002	0.000	0.047	0.002	0.000	0.039	0.002	0.000	0.041	0.002	0.000
36	0.045	0.002	0.000	0.089	0.004	0.001	0.052	0.003	0.000	0.053	0.003	0.000	0.050	0.003	0.000
41	0.042	0.002	0.000	0.047	0.002	0.000	0.047	0.002	0.000	0.039	0.002	0.000	0.041	0.002	0.000
49	0.069	0.003	0.001	0.077	0.004	0.001	0.073	0.004	0.001	0.074	0.004	0.001	0.067	0.003	0.001
60	0.055	0.003	0.000	0.059	0.003	0.000	0.055	0.003	0.000	0.060	0.003	0.000	0.057	0.003	0.000
70	0.048	0.002	0.000	0.061	0.003	0.000	0.046	0.002	0.000	0.047	0.002	0.000	0.044	0.002	0.000
78	0.074	0.004	0.001	0.080	0.004	0.001	0.058	0.003	0.000	0.067	0.003	0.001	0.074	0.004	0.001
87	0.058	0.003	0.000	0.067	0.003	0.001	0.062	0.003	0.000	0.067	0.003	0.001	0.073	0.004	0.001

Table A.6.8: Errors for the total iron generated in the draw and fill circum-neutral fed bioleach experiments

	-75 µm			+ 75 - 106 µm			+ 106 - 180 µm			+180 -212 µm			+212 - 355 µm		
Time (Days)	Fe^{total} (± nm)	Fe^{Total} (± g/l)	Fe^{Total} (± g)	Fe^{total} (± nm)	Fe^{Total} (± g/l)	Fe^{Total} (± g)	Fe^{total} (± nm)	Fe^{Total} (± g/l)	Fe^{Total} (± g)	Fe^{total} (± nm)	Fe^{Total} (± g/l)	Fe^{Total} (± g)	Fe^{total} (± nm)	Fe^{Total} (± g/l)	Fe^{Total} (± g)
0	0.039	0.010	0.001	0.007	0.002	0.000	0.002	0.000	0.000	0.010	0.002	0.000	0.008	0.002	0.000
3	0.006	0.002	0.000	0.009	0.002	0.000	0.007	0.002	0.000	0.008	0.002	0.000	0.008	0.002	0.000
6	0.016	0.004	0.001	0.006	0.002	0.000	0.013	0.003	0.000	0.008	0.002	0.000	0.014	0.003	0.001
10	0.032	0.002	0.000	0.009	0.000	0.000	0.002	0.000	0.000	0.001	0.000	0.000	0.006	0.000	0.000
13	0.005	0.000	0.000	0.004	0.000	0.000	0.011	0.001	0.000	0.028	0.001	0.000	0.023	0.001	0.000
17	0.008	0.000	0.000	0.006	0.000	0.000	0.004	0.000	0.000	0.006	0.000	0.000	0.004	0.000	0.000
21	0.005	0.000	0.000	0.006	0.000	0.000	0.014	0.001	0.000	0.009	0.000	0.000	0.001	0.000	0.000
22	0.025	0.001	0.000	0.018	0.001	0.000	0.037	0.002	0.000	0.011	0.001	0.000	0.004	0.000	0.000
25	0.017	0.001	0.000	0.015	0.001	0.000	0.015	0.001	0.000	0.033	0.002	0.000	0.109	0.005	0.001
28	0.004	0.000	0.000	0.003	0.000	0.000	0.004	0.000	0.000	0.001	0.000	0.000	0.041	0.002	0.000
36	0.014	0.001	0.000	0.034	0.002	0.000	0.006	0.000	0.000	0.011	0.001	0.000	0.050	0.003	0.000
41	0.004	0.000	0.000	0.003	0.000	0.000	0.004	0.000	0.000	0.001	0.000	0.000	0.041	0.002	0.000
49	0.040	0.002	0.000	0.013	0.001	0.000	0.059	0.003	0.000	0.001	0.000	0.000	0.067	0.003	0.001
60	0.009	0.000	0.000	0.009	0.000	0.000	0.002	0.000	0.000	0.011	0.001	0.000	0.057	0.003	0.000
70	0.028	0.001	0.000	0.008	0.000	0.000	0.021	0.001	0.000	0.009	0.000	0.000	0.044	0.002	0.000
78	0.023	0.001	0.000	0.001	0.000	0.000	0.006	0.000	0.000	0.004	0.000	0.000	0.074	0.004	0.001
87	0.005	0.003	0.000	0.007	0.003	0.001	0.062	0.003	0.000	0.067	0.003	0.001	0.073	0.004	0.001

Table A.6.9: Measured pH in the draw and fill acid fed bioleach experiments

	Measured pH of sample					Standard Error (± pH)				
Days	-75µm	+ 75 - 106µm	+ 106 - 180µm	+ 180 - 212µm	+ 212 - 355µm	-75µm	+ 75 - 106µm	+ 106 - 180µm	+ 180 - 212µm	+ 212 - 355µm
0	2.426	2.365	2.219	2.177	2.174	0.040	0.014	0.012	0.009	0.029
3	2.846	3.181	3.242	3.326	2.974	0.024	0.317	0.244	0.390	0.097
6	2.420	2.417	2.418	2.465	2.377	0.003	0.005	0.056	0.043	0.020
10	2.242	2.175	2.148	2.210	2.160	0.013	0.049	0.009	0.032	0.012
13	2.111	2.070	2.077	2.108	2.066	0.007	0.018	0.002	0.012	0.023
17	2.040	2.264	2.388	2.417	2.465	0.005	0.131	0.015	0.012	0.015
21	2.479	2.570	2.659	2.717	2.752	0.003	0.075	0.014	0.034	0.022
22	2.479	2.570	2.659	2.717	2.752	0.003	0.075	0.014	0.034	0.022
25	2.650	2.681	2.748	2.795	2.852	0.007	0.066	0.018	0.037	0.025
28	2.714	2.737	2.787	2.851	2.893	0.002	0.067	0.010	0.032	0.019
36	2.518	2.614	2.645	2.686	2.828	0.020	0.028	0.014	0.040	0.022
41	2.714	2.737	2.787	2.851	2.893	0.002	0.067	0.010	0.032	0.019
49	2.662	2.702	2.694	2.671	2.832	0.029	0.043	0.030	0.064	0.016
60	2.360	2.370	2.311	2.279	2.418	0.020	0.025	0.006	0.012	0.121
70	2.069	2.061	2.049	2.026	2.034	0.008	0.004	0.003	0.004	0.010
78	2.178	2.167	2.186	2.154	2.149	0.005	0.006	0.001	0.006	0.001
87	2.168	2.159	2.159	2.143	2.136	0.006	0.005	0.001	0.005	0.003

Table A.6.10: Measured pH in the draw and fill circum-neutral fed bioleach experiments

	Measured pH of sample					Standard Error (± pH)				
Days	-75µm	+ 75 - 106µm	+ 106 - 180µm	+ 180 - 212µm	+ 212 - 355µm	-75µm	+ 75 - 106µm	+ 106 - 180µm	+ 180 - 212µm	+ 212 - 355µm
0	2.856	2.828	2.819	2.844	2.823	0.011	0.009	0.011	0.018	0.007
3	6.306	6.624	7.248	7.616	4.736	0.303	0.428	0.090	0.023	1.418
6	7.620	7.940	7.980	8.023	7.560	0.055	0.040	0.021	0.011	0.217
10	7.442	7.906	7.898	7.798	7.872	0.113	0.011	0.004	0.148	0.038
13	6.311	7.173	6.600	7.095	7.605	0.078	0.231	0.132	0.458	0.008
17	6.450	6.520	6.479	6.127	7.313	0.125	0.090	0.036	0.103	0.439
21	5.980	6.320	6.353	6.133	7.117	0.366	0.023	0.038	0.212	0.394
22	5.847	6.297	6.333	6.130	7.047	0.371	0.046	0.039	0.176	0.550
25	5.773	6.360	5.982	6.310	3.886	0.327	0.010	0.249	0.234	0.344
28	5.650	6.030	5.964	5.590	5.593	0.437	0.038	0.119	0.199	0.148
36	5.022	5.762	5.629	5.500	5.640	0.136	0.135	0.111	0.082	0.106
41	5.650	6.030	5.964	5.590	5.593	0.437	0.038	0.119	0.199	0.148
49	4.928	5.379	5.009	5.313	5.535	0.252	0.036	0.177	0.029	0.035
60	4.614	5.126	4.657	5.040	5.153	0.242	0.069	0.182	0.035	0.024
70	4.247	4.977	4.364	4.848	5.271	0.254	0.158	0.154	0.090	0.029
78	3.877	4.723	4.141	4.510	5.053	0.165	0.152	0.117	0.104	0.038
87	3.520	4.374	4.001	4.200	4.854	0.088	0.160	0.063	0.115	0.051

A 6.1.2. Draw and fill biokinetic results (abiotic – un-inoculated experiments)

Table A.6.11: Measured pH in the abiotic draw and fill experiments

	-75µm				+212 -355µm			
	Acid fed		Circum- neutral fed		Acid fed		Circum-neutral fed	
Time (Days)	pH	STD Error (±)	pH	STD Error (±)	pH	STD Error (±)	pH	STD Error (±)
0	2.394	0.0055	6.275	0.005	2.152	0.010	6.430	0.032
2	6.704	0.003	7.195	0.055	5.806	0.022	7.159	0.006
6	4.175	0.015	7.280	0.010	2.940	0.005	7.415	0.010
8	2.255	0.005	7.320	0.000	2.178	0.025	7.275	0.000
13	2.224	0.002	6.195	0.005	2.083	0.005	6.425	0.003
22	2.102	0.008	0.000	0.000	2.089	0.001	6.034	0.000
29	2.021	0.001	5.000	0.010	2.013	0.025	5.845	0.010
38	2.112	0.007	4.790	0.000	2.095	0.020	4.840	0.007
46	2.347	0.000	4.765	0.015	2.355	0.015	4.965	0.002
60	2.050	0.000	4.940	0.010	2.043	0.025	4.985	0.003
67	2.086	0.004	5.290	0.000	2.087	0.005	5.105	0.002
74	2.057	0.002	5.140	0.020	2.057	0.000	5.110	0.003

Table A.6.12: Measured redox potentials in mV for the abiotic draw and fill experiments

	Acid Fed		Circum-neutral fed		Acid fed		Circum-neutral fed	
Time (Days)	Redox (mV)	STD Error (±)	Redox (mV)	STD Error (±)	Redox (mV)	STD Error (±)	Redox (mV)	STD Error (±)
0	413.5	0.500	275.5	0.500	432.5	0.500	253.0	0.500
2	271.5	3.500	210.5	0.500	231.0	1.000	194.0	0.500
6	299.5	2.500	130.5	0.000	414.0	0.000	175.0	0.000
8	299.5	2.500	130.5	0.000	414.0	0.000	175.0	0.000
13	529.0	0.000	180.5	1.500	554.0	0.000	174.5	1.500
15		0.500		0.500	561.50	0.500	266.0	0.500
22	537.5	0.500	298.0	0.500	577.5	1.500	276.0	0.500
29	568.5	0.500	296.0	1.500	587.5	1.500	255.5	1.500
38	567.0	0.000	312.0	1.000	578.0	0.000	312.5	1.000
46	591.5	0.500	336.0	1.000	591.0	0.000	314.5	1.000
60	583.0	0.000	406.5	0.500	596.5	0.500	406.5	0.500
67	576.0	6.000	293.5	1.000	548.5	8.500	302.5	1.000
74	579.5	1.500	318.0	1.500	552.5	10.500	315.5	1.500

A 6.1.3. Batch biokinetic results

Table A.6.13: Measured pH of the batch acid fed bioleach experiments

	Measured pH in the abiotic samples			Standard error in the abiotic samples (± pH)			Measured pH in the biotic samples			Standard error in the biotic samples (± pH)		
Time (Days)	-75	+106 - 180	+212 - 355	-75	+106 - 180	+212 - 355	-75	+106 - 180	+212 - 355	-75	+106 - 180	+212 - 355
0	2.323	2.084	2.070	0.019	0.005	0.004	2.266	2.110	2.093	0.0305	0.007	0.008
2	6.778	6.760	6.007	0.008	0.018	0.0315	4.194	7.288	5.929	0.007	0.0015	0.030
6	7.065	6.900	6.375	0.005	0.01	0.005	5.305	7.425	6.845	0.005	0.005	0.005
8	7.095	6.950	6.405	0.005	0.000	0.005	5.225	7.395	7.065	0.015	0.005	0.005
13	7.185	7.350	7.020	0.005	0.010	0.000	5.075	6.945	0.000	0.015	0.005	0.020
15	6.155	7.220	6.930	0.015	0.000	0.000	4.900	6.890	5.990	0.020	0.030	0.030
22	6.635	6.085	5.810	0.015	0.025	0.010	4.600	6.105	5.335	0.010	0.035	0.045
29	6.750	5.605	5.570	0.030	0.015	0.030	4.530	5.325	4.930	0.020	0.015	0.010
38	6.665	6.720	5.735	0.025	0.000	0.055	4.380	5.285	4.675	0.020	0.035	0.025
46	6.795	6.880	6.560	0.005	0.020	0.020	4.176	4.871	4.486	0.012	0.006	0.010
60	6.895	6.955	6.780	0.045	0.065	0.060	3.841	4.250	4.245	0.005	0.005	0.005
67	6.400	7.350	7.205	0.020	0.010	0.005	3.337	4.187	4.184	0.002	0.064	0.006
74	6.055	7.450	7.310	0.015	0.020	0.000	2.988	3.908	3.935	0.015	0.003	0.005

Table A.6.14: Measured pH of the batch circum-neutral fed bioleach experiments

	Measured pH in the abiotic samples			Standard error in the abiotic samples (± pH)			Measured pH in the biotic samples			Standard error in the biotic samples (± pH)		
Time (Days)	-75	+106 - 180	+212 - 355	-75	+106 - 180	+212 - 355	-75	+106 - 180	+212 - 355	-75	+106 - 180	+212 - 355
0	6.520	6.435	6.430	0.01	0.005	0.005	2.705	2.715	2.800	0.010	0.005	0.000
2	7.425	7.297	7.244	0.025	0.0015	0.004	7.583	7.514	7.582	0.008	0.176	0.0025
6	7.590	7.615	7.275	0.01	0.005	0.005	7.645	7.710	7.745	0.005	0.000	0.005
8	7.605	7.640	7.295	0.005	0.01	0.005	7.590	7.725	7.750	0.020	0.005	0.000
13	7.430	7.375	7.080	0.01	0.015	0.020	6.485	7.190	0.000	0.015	0.000	0.010
15	7.260	7.330	7.010	0	0.02	0.010	6.095	6.045	7.550	0.015	0.025	0.010
22	7.335	7.405	7.030	0.005	0.015	0.020	6.455	7.360	7.615	0.005	0.010	0.005
29	7.380	7.450	7.155	0.04	0.01	0.035	6.905	7.475	5.625	0.025	0.065	0.045
38	6.140	7.595	7.375	1.32	0.045	0.005	7.270	7.505	6.470	0.020	0.085	0.080
46	7.760	7.815	7.420	0	0.005	0.100	7.335	7.580	7.175	0.005	0.010	0.005
60	7.720	7.870	7.355	0.02	0.02	0.075	6.955	7.650	7.430	0.015	0.010	0.060
67	7.615	7.775	7.760	0.005	0.005	0.010	6.960	7.640	7.710	0.010	0.010	0.010
74	7.730	7.860	7.840	0.01	0.01	0.010	6.865	7.620	7.770	0.015	0.010	0.010

Table A.6.15: Measured redox potentials in mV of the batch acid fed experiments

	Measured redox potential in the abiotic samples (mV)			Standard error in the abiotic samples (± mV)			Measured redox potential in the abiotic samples (mV)			Standard error in the biotic samples (± mV)		
Time (Days)	-75	+106 - 180	+212 - 355	-75	+106 - 180	+212 - 355	-75	+106 - 180	+212 - 355	-75	+106 - 180	+212 - 355
0	429.5	431.5	439.0	1.500	3.50	0.000	541.0	561.0	555.5	1.000	1.000	3.500
2	198.5	185.5	238.0	0.500	0.50	4.000	348.0	170.0	228.5	3.000	6.000	0.500
6	221.5	239.5	220.0	0.500	0.50	0.000	302.5	167.5	163.5	0.500	0.500	0.500
8	221.5	239.5	220.0	0.500	0.50	0.000	302.5	167.5	163.5	0.500	0.500	0.500
13	151.0	147.5	165.5	0.000	0.50	0.500	263.5	158.5	0.0	0.500	0.500	2.500
15	171.5	140.5	168.5	0.500	0.50	0.500	264.5	201.5	229.5	0.500	0.500	0.500
22	250.5	249.5	222.5	0.500	0.50	1.500	309.5	261.0	291.5	0.500	1.000	0.500
29	239.0	287.5	290.5	2.000	0.50	0.500	332.0	307.5	326.5	1.000	0.500	0.500
38	254.5	261.5	310.0	0.500	6.50	5.000	351.5	302.0	308.5	2.500	4.000	0.500
46	255.0	251.5	254.0	0.000	0.50	0.000	381.0	354.5	334.0	2.000	1.500	0.000
60	248.5	261.0	254.5	0.500	1.00	0.500	467.0	392.5	392.0	0.000	0.500	1.000
67	280.5	216.0	208.0	0.500	0.00	0.000	515.5	341.0	333.0	1.500	1.000	1.000
74	329.5	242.5	231.5	0.500	0.50	0.500	570.5	359.0	350.5	1.500	0.000	0.500

Table A.6.16: Measured redox potentials in mV of the batch circum-neutral fed experiments

	Measured redox potential in the abiotic samples (mV)			Standard error in the abiotic samples (± mV)			Measured redox potential in the abiotic samples (mV)			Standard error in the biotic samples (± mV)		
Time (Days)	-75	+106 - 180	+212 - 355	-75	+106 - 180	+212 - 355	-75	+106 - 180	+212 - 355	-75	+106 - 180	+212 - 355
0	227.5	227.5	231.5	0.500	0.500	0.500	541.5	556.5	569.5	2.500	1.500	1.500
2	179.5	154.0	213.5	0.500	0.500	0.500	182.5	168.5	169.5	0.500	0.500	0.500
6	185.0	195.5	199.5	0.000	0.000	0.000	170.5	146.0	126.0	0.000	0.000	0.000
8	185.0	195.5	199.5	0.000	0.000	0.000	170.5	146.0	126.0	0.000	0.000	0.000
13	147.0	147.5	175.0	1.500	1.500	1.500	177.0	161.5	0.0	1.500	1.500	1.500
15	130.5	135.5	186.5	0.500	0.500	0.500	214.0	224.0	179.5	0.500	0.500	0.500
22	215.5	197.0	189.5	0.500	0.500	0.500	212.0	189.5	257.0	0.500	0.500	0.500
29	198.5	189.0	196.0	1.500	1.500	1.500	207.0	216.5	327.0	1.500	1.500	1.500
38	216.5	200.0	204.5	1.000	1.000	1.000	223.0	211.5	237.0	1.000	1.000	1.000
46	249.0	227.0	220.5	1.000	1.000	1.000	386.5	232.5	255.0	1.000	1.000	1.000
60	207.5	192.5	197.0	0.500	0.500	0.500	255.5	223.0	216.0	0.500	0.500	0.500
67	193.0	184.5	171.0	1.000	1.000	1.000	224.0	213.0	196.0	1.000	1.000	1.000
74	223.5	204.5	196.0	1.500	1.500	1.500	259.0	220.5	200.0	1.500	1.500	1.500